ADAR1 Regulation of Innate RNA Sensing in Immune Disease

Megan Maurano

A dissertation

Submitted in partial fulfillment of the

Requirements for the degree of

Doctor of Philosophy

University of Washington

2021

Reading Committee:

Daniel Stetson, Chair

Julie Overbaugh

Michael Emerman

Program Authorized to Offer Degree:

Molecular and Cellular Biology

University of Washington

Abstract

ADAR1 Regulation of Innate RNA Sensing in Immune Disease

Megan Maurano

Chair of the Supervisory Committee:

Daniel B. Stetson

Department of Immunology

Detection of nucleic acids and production of type I interferons (IFNs) are principal elements of antiviral defense, but can cause autoimmune disease if dysregulated. Loss of function mutations in the human ADAR gene cause Aicardi-Goutières Syndrome (AGS), a rare and severe autoimmune disease that resembles congenitally acquired viral infection. Our lab and others defined ADAR1 as an essential negative regulator of an RNA-sensing pathway. Specifically, accumulation of endogenous ADAR1 RNA substrates within cells triggers type I IFN production through the anti-viral MDA5/MAVS pathway, highlighting the connection between innate antiviral responses and autoimmunity, with important implications for the treatment of AGS and related diseases. However, the mechanisms of MDA5-dependent disease pathogenesis *in vivo* remain unknown. Here, we introduce a knockin mouse that models the most common *ADAR* AGS mutation in humans. In defining this model we confirm that the unique z-alpha domain of ADAR1 is required, along with the deaminase domain, for MDA5 regulation. We establish that it is haploinsufficiency paired with an otherwise non-deleterious allele that drives disease, and may explain the dominance of this allele amongst the broader population. We used this new *Adar*-mutant mouse model to confirm several putative effectors of disease that results from ADAR1 loss of function. These mice develop lethal disease that

requires MDA5, the RIG-I-like receptor LGP2, type I interferons, and the eIF2α kinase PKR. We additionally show that a small molecule inhibitor of the integrated stress response (ISR) that acts downstream of eIF2α phosphorylation prevents immunopathology, and rescues the mice from mortality. We also determined that haploinsufficiency is essential to the progression of disease, and demonstrate increased MDA5 signaling in *p150* and *Adar1* heterozygous mice. We describe a new set of mice that will allow *in vitro* and *in vivo* interrogation of the RNAs that activate MDA5 in the absence of sufficient ADAR1 editing. Our findings place PKR and the ISR as central components of immunopathology *in vivo* and identify new therapeutic targets for treatment of human diseases associated with the ADAR1-MDA5 axis, and shed light on how decreased ADAR1 activity may be leveraged for cancer treatments.

Table of Contents

Figure List

Acknowledgements:
Thank you, Dan, for your enthusiasm and seemingly bottomless memory for the minutiae that made this project sing.

To Iris Gratz, for taking me on fresh out of college, and teaching me everything I know about how to be a good scientist, in lab and out. Thank you for being a model of the kind of scientist, collaborator, and mentor that I can only hope to be. Whatever I might accomplish scientifically is due to your mentorship and willingness to take me under your wing. Dankeshon.

To Barbara Mantovani: For giving a random American student her first shot at research, and for supporting me after. Also, for planting an abiding interest in endogenous retroelements and appreciation for what the littlest and most reviled creatures can teach us. Grazie mille per tutto.

Thank you to each of the members of my thesis committee: Julie Overbaugh, Michael Emerman, Jesse Bloom, and David Rawlings. I would like to especially thank Julie and Michel for being my reading committee.

Thank you to every member of the Stetson Lab. In particular to Steph for tolerating my muttering and being the sounding board for all things lab and life. Hannah, for knowing everything, and sharing that with us. To both of them together fpr being the dynamic duo that luring me into the lab and keeps the rest of us on track. Joanna, for being the heart of the lab that keeps us all sane. Emily for her editing expertise, coffee shop hours and going all east coast at the most unexpected and most delightful of times.

Thank you to our collaborators: Jorge Henao Pineda, for making the mice, and being unfailing supportive of this project, and kind to me. Jess Snyder, for being a real partner, treating me with respect, and reteaching me all I forgot, and more, about histology. Your contributions made this project so much stronger. To Carmela for her expertise, support, patience, and generous collaboration. To Brenda Bass for discovering ADAR, and for always being kind while asking spectacularly perceptive questions that I mulled over for months afterward. And for being 100% right about needing to look at the RNA.

To the Immunology Class of 2016, for adopting me into your TAship and year. Particularly to Nick Hubbard, for seeing me in this hole and jumping in to explore. To my MCB cohort for being

brilliant and inspiring me to do better. To my MSTP cohort, for all the fun, feedback, and growing up together.

Finally, Thank you to my family. To my parents, for supporting me even when you didn't understand what I was doing or why. To my brothers, for teaching me to fight. Thank you to the Bakers, for so readily adopting me.

Thank you, most of all, to Rachel, for riding along for the ups and downs of grad school, and your ceaseless support and belief in me throughout.

For Marie Rita Sherin Maurano (March 25, 1919 - November 26, 2018)

Chapter 1: Introduction

Innate Immunity in Host Defense

The major function of the immune system is protection from infection. From bacteria combatting phages to humans clearing an infection with SARS-CoV-2, the detection and elimination of pathogens are essential to the persistence of life. In order to succeed in this, all organisms must have a means of recognition of "non-self" as different from "self". The different strategies for recognizing pathogen must be highly specific and tightly regulated since they are coupled to pathways that could otherwise damage the cell or organism if activated inappropriately.

One example of pathogen recognition and elimination that evolved in prokaryotes is restriction enzymes which cleave specific DNA sequences contained in invading phage. These sequences are absent in host DNA or hidden by host modification of these specific sequence motifs [1]. A major limitation of this approach as a defense against infection is that it is exquisitely sequence-specific: it relies on recognition of a very specific short set of nucleotides, rather than a more broadly shared characteristic of phage, so any given restriction enzyme can only target a subset of phage. In contrast, some of the viral recognition pathways in vertebrates detect broader pathogen-specific molecular patterns that share the characteristics of being *distinct* from mammalian cellular components and *essential* to the pathogen such that mutation cannot easily result in immune evasion.

Pathogen recognition receptor (PRR) specificities are encoded by the innate immune system which is germline encoded and thus will not change in an organism over its lifetime. This is in contrast to the evolving recognition capacity of the adaptive arm of the vertebrate immune system, in which reassortment of lymphocyte antigen receptor gene fragments creates almost limitless recognition potential. Instead, to make the innate immune system an effective early system for the detection of the world of potential pathogens, PRR recognize common elements of pathogens: from bacterial cell wall components and toxins, to damage induced

during infection. Bacterial and fungal cell wall lipopolysaccharides, peptidoglycans, and sugars are clearly distinct from any element of human biology. However, since viruses rely on the host for many of their functions, there are fewer ways to recognize them as foreign and it is far more difficult to specifically and reliably detect them without also constantly responding to parts of a healthy host. Nonetheless, one component all viruses must contain is a nucleic acid genome. Accordingly, nearly all the patten recognition receptors of the innate immune system recognize viruses by detecting DNA or RNA of viral genomes, either by unique locations of these nucleic acids, unique modifications, or unique structures in the nucleic acids.

After recognition of viral nucleic acids, the pattern recognition receptors alert the immune system, induce inflammation, and limit or clear infection via an antiviral defense mediated by the cytokine interferon. There are over a dozen interferon genes encoded in the human genome, with overlapping functions. IFN beta[2] is the first type I IFN produced during an antiviral response, under the most direct regulation from PRR activation, and will be referred to here as simply, IFN.

IFN-Beta, the focus of this thesis, acts in both autocrine and paracrine manners, inducing hundreds of interferon-stimulated genes, called ISGs. The ISGs establish an antiviral state in both the infected cells and those nearby through wide-ranging functions, from antagonizing the virus in myriad ways at almost every step of the viral replication cycle, to promoting cell survival through the stress of infection, and recruiting immune cells to the site of infection through chemokine and cytokine production. Nearly all nucleated cells express the heterodimeric type I IFN receptor (IFNAR), and thus can respond to IFN by induction of ISGS. Therefore, an IFN response can have systemic effects.

The initial steps of induction of ISGs involves IFNAR engagement by IFN which results in activation of JAK kinases which phosphorylate Signal Transducers and Activators of Transcription 1 and 2 (STAT1 and STAT2). A complex of STAT1 and 2 phosphorylates Interferon regulatory Factor 9 (IRF9), and this is the transcription factor that drives transcription

of interferon stimulated genes (ISGs) with Interferon-Sensitive Response Elements (ISREs) in their promoters[3]. Many of the nucleic acid sensors, which initiate the IFN response, including MDA5, are themselves IFN-inducible[3], so that cells near to those in which infection is first detected are primed to be more sensitive to any encroaching pathogen.

The importance of the IFN response is evident in mouse models that lack interferon signaling – IFN receptor knock out mice are highly susceptible to most viral infections, and viral infections are more often lethal in the absence of IFN[4]. Deficiencies in any of the PRRs also leaves knock out mice for any of the PRRs extremely susceptible to infection by viruses of classes that are typically recognized by the missing PRR[5,6]. In humans, children with mutations in IFN signaling components (mutations in both components of IFNAR1, IRF9, STAT1 and STAT2 have all been identified) are associated with developing disease from vaccination with live attenuated measles virus[7], and to developing severe disease from viral infections that are typically mild[8,9]. The importance of the IFN pathway is further underlined by the many viruses that antagonize each of these steps in IFN signalling to combat the antiviral effects[10]. Moreover, the IFN response is so effective that often viruses will antagonize more than one step of the IFN signaling cascade to try to prevent this potent antiviral response.

Interferon Induction by Nucleic Acid Sensors

One family of PRRs for viruses is the Toll Like Receptor (TLR) family. This family of proteins surveys the environment external to the cell, by sensing directly on the cell surface and surveying endosome contents for pathogens**.** In humans, TLRs 7, 8, 9, and 3 (in mice, TLRs 7, 9, and 3) specifically detect phagocytosed nucleic acids.[11] This is effective for virus detection since viral nucleic acids are often targeted to internal vesicles during viral entry or as a consequence of non-specific uptake of extracellular material by cells. When activated, the TLRs drive the production of cytokines and antiviral programming. All the nucleic acid sensing TLRs induce IFN to activate the antiviral response, as well as NFKB-dependent inflammatory genes, optimized for recruitment of immune cells.[12] For maximal recognition potential in endosomal

compartments, the TLRs are most highly expressed in phagocytic immune cells, like plasmacytoid dendritic cells.

In contrast to the cells that express the TLRs most strongly, nearly every cell type in vertebrates express the intracellular sensors Cyclic GMP-AMP Synthase (cGAS) and the RIG-I-Like Receptor (RLR) family of proteins. These proteins function predominantly to detect nucleic acids (DNA for cGAS and RNA for the RLR family) within the intracellular space subsequent to the induction of type I Interferon (IFN). Upon recognition of viral DNA, cGAS generates cyclic GMP-AMP (cGAMP)[13–15], which signals through STimulator of Interferon Genes (STING) to induce phosphorylation of TBK1[16,17]. TBK1 then phosphorylates IRF3 and 7, triggering IFN transcription. In an analogous manner, Retinoic acid inducible gene I (RIG-I) and Melanoma Differentiation Associated protein 5 (MDA5) recognize their respective RNA ligands[18,19,20].

RIG-I responds to RNA with 5' triphosphate moieties and MDA5 to long double stranded (ds)RNA structures. Both MDA5 and RIG-I form oligomers on viral RNA, which allows oligomerization of their CAspase Recruitment Domains (CARDs) and subsequent oligomerization and activation of Mitochondrial AntiViral Signaling protein (MAVS)[18,21]. Intriguingly, MDA5 must form cooperative filaments to activate, and this is long ds RNA – which are MDA5 ligands – are distinguished from shorter RNAs[22]. The RLR/MAVS pathway converges with the cGAS/STING DNA sensing pathway on the phosphorylation of TBK1, IRF3, and IRF7, causing induction of the IFN response. MAVS, like TLRs 3, 7, 8, and 9, also activates Nuclear Factor Kappa-B (NFKB), and inflammatory cytokine transcription[23].

Though activation of cGAS or the RLRs results in a common outcome, each sensor responds to a unique structure of nucleic acids. cGAS, for example, recognizes double-stranded DNA (dsDNA), the RLRs recognize RNA. Previously, cGAS was thought to avoid encountering and therefore responding to cellular DNA by physical separation of cGAS in the cytosol from DNA in the nucleus. This model has recently been revised, however, as multiple studies established that cGAS is also present in the nucleus[24–26]. The exact mechanisms that prevent

chronic cGAS activation are still under investigation, though binding to nucleosomes appears to be important[27–32].

The RLRs recognize RNA structures that normally exist within the cell cytoplasm. For example, RIG-I recognizes tri-phosphates on the 5' ends of RNAs, which[33], under normal conditions, are removed from most host mRNAs before entering the cytosol and encountering RIG-I. MDA5, which is also exclusively cytosolic, recognizes long (approximately one kilobase) double stranded RNA (dsRNA) structures. These are not common structures amongst host RNAs as they predominantly only occur in introns and are therefore spliced out before MDA5 might encounter them. Interestingly, the final RLR family member, Laboratory of Genetics and Physiology 2 (LGP2), can recognize both RIG-I and MDA5 substrates. However, it lacks the CARD domain required for downstream signaling and induction of the IFN response, so is thought to instead modulate MDA5 and RIG-I activity, generally boosting MDA5 signaling and decreasing RIG-I signaling[34]. Together, these three signaling-competent sensors – cGAS, MDA5, and RIG-I - provide a basic level of near-ubiquitous surveillance for nucleic acids of pathogens. Simultaneously, their recognition of viral-specific nucleic acid structures and/or restricted access to certain subcellular compartments help differentiate between host and viral RNAs.

Negative Regulators of Nucleic Acid Sensing

Since inappropriate activation of the PRRs would be detrimental, there are multiple negative regulators of these pathways to prevent activation of PRRs by host nucleic acids. For example, secreted DNase enzymes degrade extracellular and endosomal DNA before TLRs can be triggered. Loss-of function-mutations in DNases have been found in Systemic Lupus Erythematosus (SLE), a heterogeneous autoimmune disease associated with elevated IFN[35]. Mice without DNAse1 develop antibodies to nuclear components, and resultant autoimmunity, presumably from chronic stimulation of TLRs[36]. The nucleic acid sensing TLRs, which may be exposed to self nucleic acids taken up into endosomes after cell death, must undergo extensive

post-translational processing[37,36] which limits their activity until they are safely in the endosome, where they start to surveil the endosomal compartments for nucleic acids taken up by the host cells.

The cytosolic sensors also have negative regulators that modify or degrade potential self-ligands, depicted in Figure 1. Mutations in all have been identified in human diseases associated with chronic IFN responses

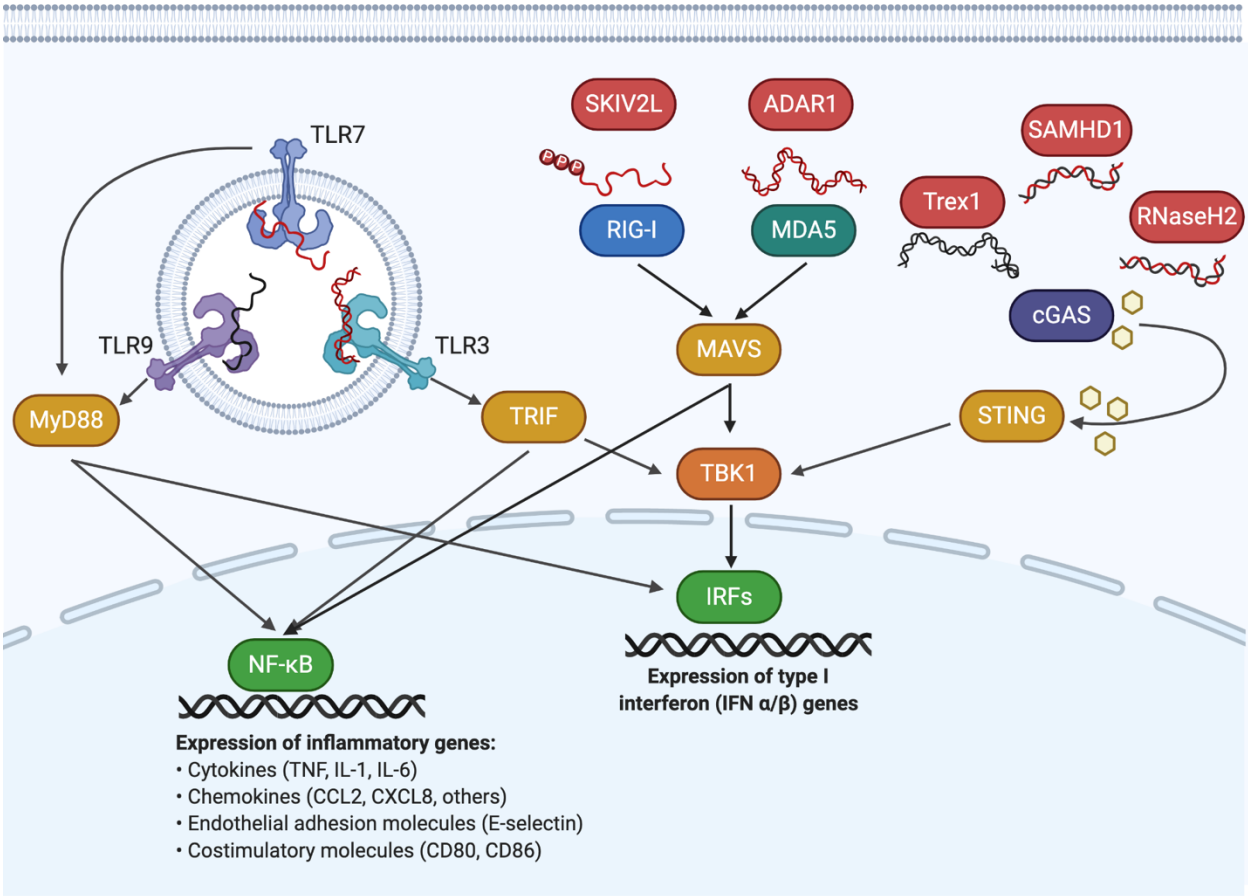

Figure 1: Nucleic acid sensing and negative regulators of cytosolic sensors. Endosomal Toll-like receptors and sensors of cytosolic nucleic acids are depicted, together with key negative regulators, downstream signaling components, and transcriptional outcomes.

Three different enzymes contribute to the prevention of cGAS/STING activation by self-DNA. Three prime Repair Exonuclease 1 (TREX1) is a DNA exonuclease, anchored to the endoplasmic reticulum in the cytosol[38]. Mouse models lacking TREX1 have severe and lethal

inflammation that is entirely cGAS/STING dependent[39], confirming that TREX1 is preventing recognition of self-DNA. Though the source of the DNA that activates cGAS in the absence of TREX1 is unknown, TREX1 can degrade both cDNA of active retrotransposons and byproducts of DNA repair and replication[40]. The role of RNAseH2 has similarly been established by studying the aberrant chronic IFN response that arises in knock-in mutant mice carrying a mutation associated with human autoinflammatory disease[41]. Spontaneous IFN production in RNAseH2B mutant mice is also cGAS-STING dependent, suggesting that RNAseH2 is degrading dsDNA under normal conditions[41]. RNaseH2 can incise the RNA strand of an RNA-DNA hybrid, and cleave the phosphodiester backbone adjacent to a single ribonucleotide in double-stranded DNA, degrading potential nucleic acid ligands before cGAS encounters them[42]. SAMHD1, a dNTP triphosphohydrolase, was also identified as a negative regulator of cGAS/STING signaling when *Samhd1-/-* mice were shown to have a cGAS-STING-dependent spontaneous IFN response[43]. In the setting of viral infection, SAMHD1 degrades dNTPs, and in cells at baseline, SAMHD1-/- cells have higher rate of DNA damage suggesting this as the source of endogenous ligand. [45]

As with the DNA sensors, the RLRs also have dedicated negative regulators, which are essential to prevent chronic responses to self RNA. SKIV2L is a component of the cytosolic RNA exosome, which helps eliminate damaged RNAs[46]. Patients and cells with SKIV2L mutations also have a spontaneous IFN response, though it is dependent on RIG-I, placing SKIV2L as a negative regulator of the recognition of damaged self-RNA by RIG-I[47]. Adenosine Deaminase Acting on dsRNA (ADAR1), the focus of this thesis, is a double stranded RNA deaminase that converts adenosines in double stranded regions of RNA to inosines through hydrolytic cleavage[48,49]. Base conversion disrupts the base pairing and therefore double stranded structure of the RNA, which MDA5 requires for activation. As with mouse models of many of the other negative regulators, *Adar-/-* mice have a spontaneous IFN response[50]. This

IFN response is dependent entirely on MDA5 and MAVS, confirming that ADAR1 regulates endogenous RNA sensing[51–53].

Autoimmunity from recognition of self-nucleic acids

The existence of negative regulators of all known nucleic acid sensors suggests the importance of tightly controlling the activity of these sensors. Indeed, almost all of the sensors, and mutations in their negative regulators (Figure 1), which prevent chronic antiviral signaling by degrading or modifying self nucleic acids, have been implicated in autoimmune disease. In fact, the association of mutations in these genes human autoimmune disease is often how their role in regulating self-nucleic acid sensing was first discovered.

Aicardi-Goutières Syndrome

The best example of the link between faulty regulation of antiviral nucleic acid sensing and disease is Aicardi Goutières Syndrome (AGS). AGS was only recognized in the mid 1980s, since it was long mistaken for *in utero* acquired viral infection. The close clinical resemblance highlights that AGS is an antiviral response run amok. AGS is a leukodystrophy defined by characteristic clinical and neuroimaging features, including cerebral atrophy, white matter disease, intracranial calcifications, and a chronic IFN signature[54]. Onset is typically in infancy or early childhood, often signaled by developmental regression. Presentation is variable, but almost all patients have motor dysfunction. AGS patients can also exhibit a constellation of other signs and symptoms, including seizures, microcephaly, liver dysfunction, chilblains, and a predisposition to diabetes insipidus and hypothyroidism. 19% of patients die prematurely, and 74% are profoundly disabled[55].

AGS can be caused by mutations in a variety of enzymes, all of which regulate the response to endogenous DNA and RNA[56,57]. Loss of function mutations in TREX1, RNAseH2, SAMHD1, and ADAR1, as well as hyperactivating mutations in MDA5 all cause AGS[58]. Most recently, mutations in LSM11 and RNU7-1, which contribute to histone mRNA processing, have also been identified as causes of AGS, through untethering and thereby derepression of cGAS

signaling in response to chromosomal DNA[59]. Though there are many mutations in many genes, all AGS presents similarly: AGS patients have increased production of type-I IFN alpha in the cerebral spinal fluid, and chronic upregulation of ISGs in the blood.

The standard of treatment for AGS is symptomatic and preventative – screening for diabetes onset and the like - rather than curative. Recent trials have focused on reverse transcription inhibitors (RTIs)[60], after they were demonstrated to rescue a *Trex1-/-* mouse model of AGS[61]. RTIs are thought to work in this setting by preventing replication of endogenous retroelements (ERV). By inhibiting ERV replication, even in the absence of negative regulators to eliminate the stimulatory capacity of self nucleic acids, the chronic IFN response can be abrogated. A clinical trial with RTIs in AGS patients did show a reduction in ISG expression, and some functional improvement, as well as some genotype-specific responsiveness to treatment: patients with RNaseH2B mutations showed more improvement of symptoms in response to RTI treatment [60]. More recent trials have focused on JAK/STAT inhibitors, to inhibit IFN signaling in AGS patients. One such trial with baricitinib, an oral JAK1/2 inhibitor, demonstrated effective blockade of IFNAR signaling in patient cells *ex vivo*, a reduction in ISG score measured in patient blood, and resolution of some patient skin findings[62]. Most promisingly, they found, by way of symptom diaries, some indication for neurological functional improvement[63]. However, another trial using ruxolitinib, also a JAK1/2 inhibitor, failed to prevent progression to disease of an infant identified presymptomatically as carrying RNASEH2B mutations associated with AGS[62], illustrating that IFN inhibition alone will not be a cure all for interferonopathies such as AGS.

RNA editing by ADAR enzymes

ADAR1 was first identified in 1987 as “dsRAD”, in xenopus extracts[48,71]. ADAR1 was identified for its ability to deaminate and cause unwinding of dsRNA. Since then, two other ADAR proteins have been described in mammals - ADAR2 and ADAR3[72]. All are modular proteins, comprised of different numbers and combinations of dsRNA binding domains,

deaminase domains, and “z-alpha” domains. However, only ADAR1 and ADAR2 have demonstrated deaminase activity; ADAR3 lacks a functional deaminase domain (Fig. 4). ADAR1 and ADAR2 catalyze the conversion of adenosine to inosine within double-stranded regions of cellular RNAs, disrupting A-U base pairing. Inosine pairs better with cytosine than uracil, and thus ribosomes will decode former adenosines as guanosine.

While ADAR proteins are found throughout metazoans, and their deaminase activity is conserved, their physiological functions vary. Cephalopods seem to exhibit a particular reliance on the recoding capacity of the ADAR enzymes. Squid have more than 57,000 editing sites which result in sequence change, affecting most transcripts in the nervous system, and many thousands of editing sites have also been identified in the octopus[73]. Adaptation to different water temperatures through nonsynonymous changes introduced through RNA editing has been characterized in the octopus[74]. High editing levels destabilize the open state of a potassium voltage-gated channel, and octopuses living in cooler water temperatures have higher editing levels at this site, while those in warmer water temperatures have lower editing levels because more stable channels that do not open as easily are advantageous in warmer conditions. Similarly, ADARs heavily edit and recode neuronal receptors and ion channel components in Drosophila[75].

As expected, based on the role of ADAR editing in cephalopods and drosophila, ADAR1 and ADAR2 are most highly expressed in the neurological systems of humans and in mice, though both are expressed in most tissues. Full knock outs of either ADAR1 or ADAR2 result in spontaneous lethality. ADAR2 knock out in mice is lethal shortly after birth because, in a parallel to its function in cephalopods and drosophila, ADAR2 is required to edit the neuronal glutamate receptor *Gria.* Only edited *Gria2* pre-mRNA is spliced efficiently, and unedited pre-mRNA is retained in the nucleus. In the absence of edited Gria2, mice have uncontrolled seizures and die shortly after birth. If a recoded *Gria2* is knocked in, the mice are rescued, confirming *Gria2* editing is the major survival function of ADAR2[76]. ADAR1 has also been shown to mediate

recoding events with putative physiological effects. ADAR1 edits the 5HT2C serotonin receptor, which results in modulation of serotonin signaling [77–79]. Though not essential for life in mice, changed serotonin signaling, such as that which results from editing of 5HT2C has been linked to metabolic regulation, alcohol and drug dependency, anxiety, and depression[79]. ADAR editing has also been shown to increase miRNA generation[80,81] and suppress circular RNA generation[77,78], both of which can result in dramatic RNA expression changes.

However, recoding has not been demonstrated to be the major role of ADAR1 in mammals. Despite the significance of particular recoding events introduced by ADARs, editing in protein-coding regions of transcripts is relatively rare in mammals, and only about 40 such sites are conserved between mice and humans[82]. Studies of the editing patterns of ADAR1 have shown that, surprisingly, editing in both humans and mice falls predominantly in noncoding RNA regions in introns and 3′ untranslated regions[83]. Within those noncoding regions, ADAR1 editing concentrates in regions with the potential to form double-stranded RNA structures. This potential arises from the repeated insertion on endogenous retroelements. Because the same sequence is repeatedly inserted into the genome, if the repeats are near enough to one another in an inverted orientation, they can adhere to one another and form a nearly perfect long dsRNA when transcribed. This makes them an ideal substrate for ADAR modification and/or MDA5 activation.

One family of particular interest for ADAR1 biology is Short Interspersed Nuclear Elements (SINEs). A subset of these SINEs are derived from and ancestral 7SL signal recognition particle. In mice, the 7SL descendent SINE B1s are approximately 120 base pairs long and constitute about 8% of the mouse genome[84]. In humans, the same element is duplicated to form the Alu element, which is approximately 300 base pairs long and comprises about ten percent of the human genome[85]. As expected with regions that form dsRNAs, the majority of genes with Alus in their 3′ UTRs transcripts undergo at least partial editing by ADAR[86,87], and SINEs and Alus are where the majority of ADAR1 editing is found in mice and

humans, respectively. Both the increased length of Alus compared to SINEs in mice, and their larger relative percentage of the genome likely explain the higher frequency of editing overall in humans compared to mice[88]. Rates of A-to-I editing have increased dramatically throughout vertebrate, mammalian, and especially primate evolution, such that RNA editing in humans is several fold more common than in mice[89]. Alus are unique to primates[86], and their introduction may explain the different localization of ADAR1 edits in humans vs mice.

Despite most editing falling in repeated sequences, an examination of ADAR1 editing patterns across tissue types in humans confirmed that editing frequency is variable by tissue. Editing is highest in the brain, particularly in the cerebellum, perhaps a hint as to why disease in ADAR1 mutation patients often effects cerebellar function[90]. A similar survey in mice confirmed that the brain is also the most highly edited organ[91].

A survey of editing comparing different ADAR mutant mice also revealed tissue variability in editing, and allowed differentiation between ADAR1 and ADAR2 activity. Comparison of tissues from *Adar-/-* day 12 embryos, adult *Adar1 E861A/E861A Ifih1−/−* (catalytically inactive ADAR1) mice, and adult *Adar2−/− Gria2R/R* mice (Adar2 knock out mice, with edited glutamate receptor knocked in to rescue lethality) showed where ADAR1 and ADAR2 introduce edits in mice. 1,457 and 976 sites were identified as edited by ADAR1 or ADAR2, respectively, and 698 sites as edited by both[90]. Which ADAR enzyme was responsible for most editing depended on the tissue. In the brain, editing activity was about equally divided between ADAR1 and ADAR2, whereas in the liver, spleen and thymus, ADAR1 is the dominant editing enzyme, which may explain the dramatic impact of ADAR1 loss on hematopoiesis in the liver of mice. This, along with the human editing survey results, suggest that some of the tissue-specificity of the response to ADAR1 loss is explained by ADAR1 expression levels, which are known to correlate with editing frequencies.

ADAR1 Mutations in Disease

As noted above, ADAR1 plays a central role in regulating the response endogenous RNA by MDA5. Thus it is perhaps not surprising that a variety of ADAR1 mutations (Shown in Figure 2) are associated with AGS. Most are found in the catalytic deaminase domain (Fig. 2) and decrease editing efficacy *in vitro*, though expression of ADAR1 protein is maintained[64]. It is thought that decreased editing *in vivo* allows persistence of contiguous dsRNA stretches in 3' UTRs of mRNAs, which trigger MDA5 activation. Two more unusual mutations are found in non-catalytic Z-DNA binding domain (ZBD) of ADAR1. Interestingly, these mutations also decrease editing *in vitro*[64] even though the function of the ZBD in ADAR1 function is unclear. All patients except those with G1007R, which is dominant negative, are compound heterozygotes[65].

In addition to AGS, ADAR1 mutations have been linked to other diseases that demonstrate the essentiality of ADAR1. Many of these are motor diseases, with overlapping clinical signs but differing imaging findings. Bilateral Striatal Necrosis (BSN) is defined by dystonic movement in the presence of bilateral striatal MRI changes with or without swelling. Progressive spastic paraparesis and spastic dystonia with normal intellect are similar motor diseases, in the presence of either normal neuroimaging or mild nonspecific changes sometimes including calcification of the basal ganglia, reminiscent of AGS[66]. More rarely, ADAR1 mutations have been tied to adult-onset psychological difficulties with intracranial calcifications[67,68].

The most common disease caused by ADAR1 mutations is Dyschromatosis Symmetrica Hereditaria (DSH), an autosomal dominant, childhood-onset dermatological disease defined by the presence of hyperpigmented and hypopigmented macules on the dorsal aspects of the extremities. DSH is unique amongst diseases driven by ADAR1 mutations because it is autosomal dominant, caused by a single mutated copy of *ADAR*, while, excepting one particular mutation found rarely in AGS, all the neurological diseases above require biallelic loss of function mutations of *Adar1*[64]. More than 130 different *ADAR1* mutations – stop, frameshift, or

missense – have been documented in individuals with DSH. Some of those mutations are the same as those found in AGS (Fig. 2). Interestingly, despite the overlap of mutations, skin lesions typical of DSH have not been described in AGS patients, who can have other unrelated skin findings. Patients with each of these diseases – BSN, progressive tetraparesis, and DSH – have all been found to have elevated ISG signatures in the blood, solidifying loss of regulation of the IFN response as likely to play a key role in all known ADAR1-associated diseases[69,70]. Interestingly, mutations in other AGS-linked genes have not been tied to DSH, BSN, or progressive tetraparesis, suggesting that these diseases are unique to mutation of ADAR1.

Figure 2: Mutations in ADAR1 found in AGS A schematic of the domains of ADAR1, with all known ADAR1 mutations found in AGS patients *Adapted from Rice et al, 2012*

ADAR1 regulation of antiviral sensing

Our understanding of how ADAR1 mutations cause disease associated with chronic IFN responses has been developed using mouse models. *Adar-/-* mice demonstrated that ADAR1 was responsible for preventing chronic IFN production in the absence of viral infection[92]. Loss of ADAR1 in mice causes embryonic lethality, at approximately embryonic day 12, associated with a strong spontaneous IFN response, defective hematopoiesis and widespread apoptosis[93–95]. Both the embryonic lethality and IFN response in ADAR1 knock out mice are dependent on MDA5 and MAVS, which established that ADAR1 is an essential negative regulator of MDA5. In contrast, neither STING knockout nor RIG-I knockout affected lethality of *Adar-/-* mice, or the IFN response, confirming the specificity of ADAR1 regulation of MDA5 as opposed to any other PRR [53].

Similar to mouse studies, human cells also exhibit a dependency on ADAR1 to prevent chronic innate sensing of self-RNA by MDA5. Tests in a number of human cell lines have all identified MDA5 as essential for the IFN response after ADAR1 loss, demonstrating that this relationship is conserved in humans[53,96,97]. However, the ligands that activate MDA5 after ADAR1 have not been incontrovertibly proven. Nonetheless, two studies have identified MDA5 as binding to IR-Alus in RNA isolated from ADAR1 null human cells[98,99]. Most likely, it is the set of transcripts containing IR SINEs expressed in a given cell at a given time which cause MDA5 activation. Confirmation of this, as opposed to, for example, one ubiquitous transcript causing MDA5 activation, is an area of active research.

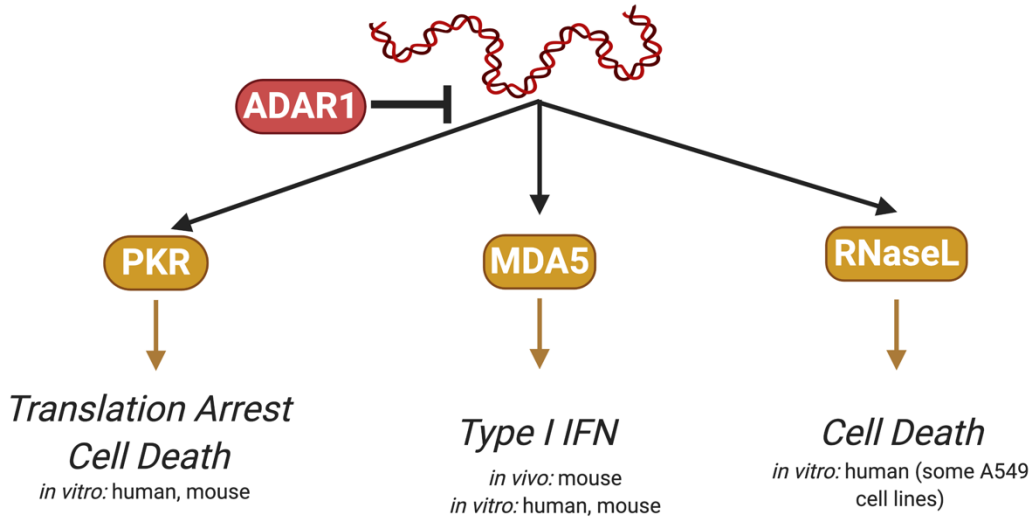

Figure 3: Summary of current knowledge of ADAR1 regulation of RNA-sensing PRRs that have been shown to be regulated by ADAR1 *in vitro* or *in vivo*, and whether it is was in live mice, mouse cells, or human cells.

Like MDA5, Protein kinase R (PKR), is an IFN-inducible double-stranded RNA sensor[100]. It is often categorized as both a viral RNA receptor and an antiviral effector molecule due to its ability to sense the presence of viral RNAs and also to directly suppress viral replication by arresting translation. PKR contains a dsRNA binding domain composed of two tandem repeats of a dsRNA-binding motif that closely resembles the dsRNA-binding domains of ADAR1, so it has long been hypothesized to recognize overlapping species of RNA[101]. PKR has also been

shown to be able to bind, like MDA5, to inverted repeats of *Alus*, though it is unclear if the same is true after ADAR1 loss[102]. The only known requirement for activation of PKR is that dsRNA be approximately 30 bp or longer, giving it considerable overlap with any MDA5 recognition capacity.

PKR has been identified in multiple *in vitro* studies as essential to cell death after ADAR1 knock out, in both human and mouse cells[96,103]. Interestingly, PKR knock out rescue of *Adar-/-* mice has previously been tested, and did not prevent embryonic lethality[104]. However, *Ifnar-/-* also does not rescue *Adar-/-* mice[51], despite the central role of IFN downstream of MDA5. Thus. the lack of rescue of *Adar-/-* mice by PKR knock out may be a reflection of other dysfunctions in the mice and/or the overwhelming nature of the response to total ADAR1 loss rather than evidence that PKR and IFNAR do not play a role *in vivo*. Instead, a more accurate model of disease mutations that occur in disease is needed to be able to test these candidates.

In the absence of viral infection or other stimuli, PKR exists in the inactive monomeric form. Upon dsRNA binding, PKR phosphorylates itself and dimerizes to form an active kinase[105,106]. Activated PKR then phosphorylates the alpha subunit of the translational elongation initiation factor 2 (eIF2). During the normal course of translation, eIF2 is essential for delivery of the initiating methionine-charged tRNA, and recognition of the start AUG to initiate translation of the mRNA. Once translation is initiated, eIF2 dissociates and the B subunit catalyzes the exchange of GDP to GTP, preparing eIF2 for initiation of the next round of translation. Only GTP-bound eIF2 has a high affinity for methionine-charged tRNAs so this recycling is required for initiation on a new mRNA and continued translation within the cell. eIF2α phosphorylation, which happens downstream of PKR activation, or downstream of activation of three other kinases that detect diverse stimuli[107], blocks recycling of GDP to GTP by eIF2B, thereby halting cap-dependent translation. This leads to global arrest of protein synthesis, both host and virus. There is a subset of transcripts that can still be translated under these conditions – those that contain an internal ribosomal entry site, so do not require the

ribosome to associate first with the cap for translation to begin. These transcripts comprise the "Integrated Stress Response", which bridge the cells through the stressor, though chronic translation inhibition may result in apoptosis.

Understanding PKR's role in immunity has been complicated by two different mouse models which show divergent effects of PKR loss in a variety of settings. One has a deletion in the N terminus, the other in the C terminus. Both still express truncated versions of PKR, which retain partial functionality. The kinase catalytic domain, which is lost in the C terminal knock out mice, is necessary for suppression of mRNA translation, and induction of inflammation in response to excessive consumption of nutrients and energy. These are the mice used in Chapter 3 in this thesis. The dsRNA binding domain, which is lost in N terminal KO mice, is required for the activation of PKR under conditions of metabolic stress[108], and is intact in the *Eif2ak2-/-* mice used here.

An additional twist in the relationship between MDA5, PKR, and ADAR1, is that PKR has been suggested to be essential for the function of MDA5 and induction of IFN, though the mechanisms are unclear[109]. Currently, in the setting of ADAR1 loss, it is thought that MDA5 is responsible for the IFN response and parallel PKR activation in responsible for death through chronic translation inhibition and induction of apoptosis[97].

The final RNA sensing pathway that ADAR1 has been linked to in the literature is the 2'5' Oligoadenylate synthetase/RNaseL pathway. As with MDA5 and PKR, OAS proteins recognize cytosolic dsRNA species[110]. In a parallel to cGAS/STING signaling, recognition of RNA by OAS triggers production of 2-5 oligoadenlyate, which signals downstream to activate RNAseL. Activated RNaseL cleaves single-stranded RNA, degrading viral and cellular RNAs[111]. The cleavage products have also been suggested to be ligands for RIG-I-dependent IFN in some systems[112], tying RNaseL activation back to IFN production, and ligands for PKR in others[113]. Two papers have shown that a line of ADAR null adenocarcinomic alveolar basal epithelial cells can be rescued from cell death by either knocking out or chemically inhibiting

RNaseL[114]. However, these results have not been replicated in a the same cell line in a different lab[115], and RNaseL has not emerged in screens for effectors of cell death after ADAR1 loss in either human or mouse cells, so the generalizability of this finding is unclear. RNaseL loss has not, to our knowledge, been tested for its ability to rescue *Adar-/-* mice, so any role of regulation *in vivo* remains unresolved.

Functions of isoforms of ADAR1

ADAR1 has a number of features that make it unique amongst the ADAR proteins. Most significantly, ADAR1 has two isoforms[116], named p150 and p110 for their molecular weights. While ADAR2 and ADAR3 are exclusively nuclear, p110 can traffic between the nucleus and cytosol, and p150 preferentially localizes to the cytosol[117]. Additionally, p150 is uniquely IFN-inducible and contains a "z-alpha domain," aka a Z-DNA binding domain (ZBD), named for its ability to bind to z-form DNA *in vitro*[118]. The function of the ZBD in ADAR1 function is as yet unclear.

Much of what we know about the unique roles of the two isoforms of ADAR1 was established by comparing *Adar p150-/-* mice, which lack only p150, and *Adar-/-* mice, which lack both p110 and p150. Functions that are lost in *Adar-/-* mice compared to *Adar +/+,* and restored in A*dar p150-/-* mice are specific to p110. *Adar p150-/-* mice grossly phenocopy *Adar-/-* mice, exhibiting embryonic lethality and spontaneous IFN upregulation that is rescued by knocking out MDA5 or MAVS, demonstrating that the p150 isoform is responsible for MDA5 regulation, while p110 is dispensable. p110 instead plays roles in the more homeostatic, non-immune functions of ADAR1 by regulating kidney development and editing 5HT2CR[53].

In addition to establishing the dependence of embryonic lethality and IFN response on MDA5, *Adar-/-* and *p150-/-* mice demonstrated that there are other critical MDA5-independent functions of Adar1 and p150. The persistence of severe runting and spontaneous death in both *Adar-/- Ifih1-/-* and *Adar p150-/- Ifih1-/-* mice[119] suggests there are other essential functions of ADAR1, beyond MDA5 regulation. Further supporting this, *Adar-/- Mavs-/-* mice have residual

transcriptional dysregulation despite abrogation of the IFN/ISG response. The transcripts that remain upregulated in *Adar-/- Mavs-/-* mice include genes involved in lipid metabolism and transport, and cell fate specification during development. In addition to transcriptional abnormalities, *Adar-/- Mavs-/-* also have disrupted kidney architecture, extramedullary hematopoiesis, and a depletion of B cells. Thus, ADAR1 controls expression of two classes of genes: innate immune response genes driven by MAVS signaling, and MAVS-independent and implicated in development and metabolism. None of these MDA5/MAVS-independent problems have been documented in patients with ADAR1 mutations, suggesting it is MDA5 regulation that plays a critical role in human disease

Two pieces of evidence suggest that the MDA5-independent functions of ADAR1 are not mediated by the deaminase activity of ADAR1. Firstly, *Adar E861A/E861A mice*, which have a deaminase dead mutation, are fully rescued by MAVS knock out[120]. This is in direct contrast to the persistent mouse death in *Adar-/- Ifih1-/-* and *Adar p150-/- Ifih1-/-* mice, and demonstrates that while editing regulates MDA5, and it is the other domains of ADAR1 that mediate MDA5-independent functions. Secondly, none of the mutations in ADAR1 associated with AGS are found in the RBDs, but rather in either deaminase domain or the ZBD, suggesting these are the domains most important for regulating MDA5 and IFN production. In direct contrast to the mouse models, in which all protein expression is lost, patients with ADAR1 mutations maintain ADAR1 protein expression[65], so it is likely that these MDA5-independent functions of ADAR1 are not compromised in AGS patients, and the current null mouse models therefore do not represent the ADAR1 dysfunction that causes human disease. The most notable difference between p150 and p110, which are both transcribed from the same locus, is the inclusion of the Z-DNA-binding domain in the p150 isoform of ADAR1. Only two mammalian proteins, ADAR1 and ZBP1, contain Z-DNA-binding domains (ZBD), a subfamily of winged helix-turn-helix domains with the unique property of binding to DNA in the left-handed helical conformation known as Z-DNA, which forms during supercoiling of the helix, as during replication while RNA

Pol II moves along the DNA[121]. The ZBD of p150 has been hypothesized to be responsible for localizing p150 to actively transcribing genes in the nucleus[122], in order to immediately neutralize any potential MDA5-activating sequences as they are generated. The ZBD is well-conserved across all known proteins that contain one, including the ZBDs of viral antagonist proteins, such as E3L of vaccinia[123].

ZBDs have also been shown to have the ability to bind to Z-form dsRNA as well, though it is less clear where and when this would form in a cell[124]. Z-RNAs have been suggested to form in stress granules during influenza viral infection, but the actual structure of the RNA in that setting is still to be confirmed[125]. Alus contain sequences – stretches of purine pyrimidine repeats – that make them prone to forming z-nucleic acid structures[126], another suggestive link between ADAR1 editing and z-form nucleic acids.

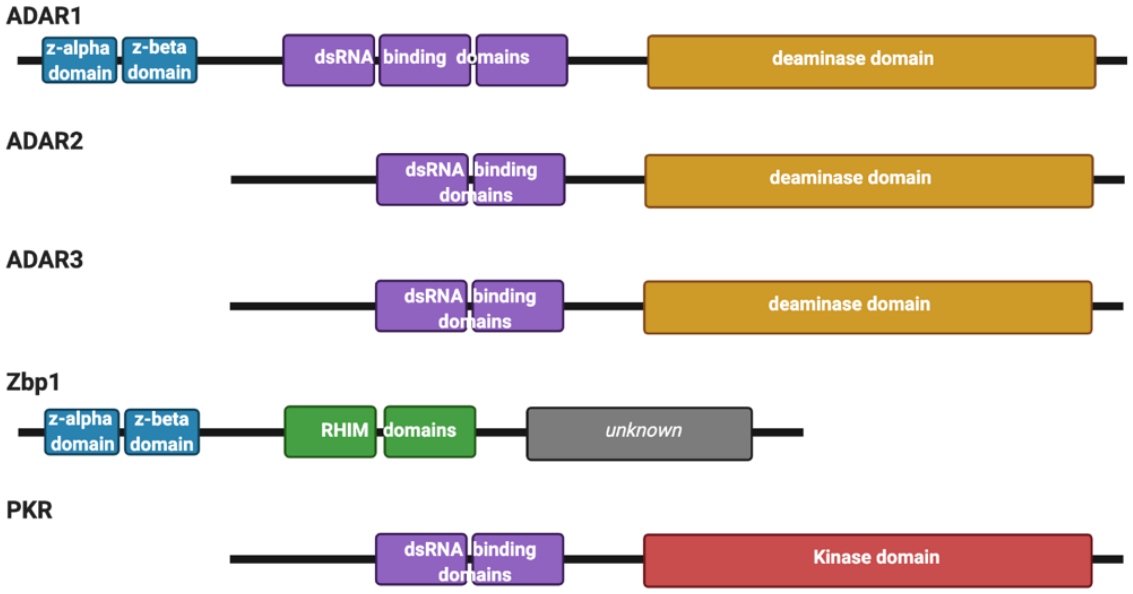

Figure 4: Domain structures of mammalian ADAR1, 3, and 3, ZBP1, and PKR. Demonstrating which shared domains retain homology between the various proteins

The ADAR1 ZBD-DNA cocrystal structure and several structures of ZBDs from other proteins have established key features necessary to bind to nucleic acids: a tyrosine, an asparagine, and a tryptophan (Tyr177, Asn173, and Trp195 in ADAR1 ZBD) form a conserved

structural motif in all known ZBDs. A mutation of any of these three residues results in the loss of Z-form DNA binding[127]. Interestingly, the Pro193 (in the ADAR1 ZBD) residue, which falls in the region of the ZBD that contacts the nucleic acid backbone (Fig. 2), is conserved in all known ZBDs, except for that of ZBP1. In the equivalent site of the ZBP1 ZBD, the wild type form has an alanine[127], which mimics the most common ADAR1 mutation associated with AGS - P193A. The ZBDs of ADAR1 and ZBP1 are otherwise interchangeable, and are responsible for the localization of p150 and ZBP1 to stress granules[128].

As part of its role in arresting translation, PKR drives the formation of stress granules upon viral infection[129], sites of translationally stalled mRNAs. Formation of stress granules provides eukaryotic cells with a protocol for survival during stress, including after detection of viral RNA by PKR[130]. Sequestration of the set of translationally arrested mRNAs allows selective synthesis of proteins required for cell survival[130,131]. When stress conditions are removed, sequestered mRNAs reassemble on polysomes and resume translation[130]. In ADAR1 knockdown cells, stress granules form after exposure to IFN in a PKR-dependent manner. The p150 isoform of ADAR1 localizes to SGs in a ZBD-dependent-manner, as does ZBP1, described below. MDA5 has also been found localizing to stress granules[132], suggesting p150 may be playing a role in regulating protein-RNA interactions in stress granules.

ADAR1 as a therapeutic target in tumors

In addition to its role in fundamental biology, interest in the links between dysregulated editing and the development of cancer, and whether editing drives tumorigenesis or persistence of tumors has been a subject of much investigation in recent years. A-to-I RNA editing has been found to be dysregulated in 17 different cancer types relative to normal tissues[133]. Editing levels correlate with the expression levels of ADAR1, and the majority of cancer types evaluated showed tumor-specific hyperediting, and only a small fraction of tumors showed hypoediting, suggesting that ADAR1 overexpression may be playing a role pro-tumor role. Whether

misregulation of A-to-I editing in a particular disease is a cause or a consequence remains unclear, however.

Several studies have queried whether ADAR1 is essential in cancer cells and tumors, and which pathways are triggered after ADAR1 deletion. All of them identified an MDA5-mediated IFN response and simultaneous activation of PKR as essential to tumor cell lethality[96,134,135]. Not all tumor lines were found to die after ADAR targeting; instead, the susceptibility of tumor cells to death after ADAR1 knock down correlates with their baseline expression of ISGs, like MDA5[96], offering a way to screen for efficacy of any ADAR-targeting intervention. Intriguingly, ADAR1 knockdown can also synergize with checkpoint blockade to increase tumor clearance, and overcome blockade of PD-1 inhibitors[134]. A recent study also demonstrated that depletion of ADAR1 in patient-derived cancer cells potentiated therapy with 5-azacytidine, restraining tumor growth and reducing cancer initiation while upregulating transcripts that contain IR-Alus[99], which presumably trigger MDA5. Thus, in addition to understanding what pathways are activated in the setting of loss of function mutations in autoimmune disease like AGS, a better understanding of all the effectors of the response to ADAR1 loss can help guide ADAR1 targeting as a tool for cancer therapy.

Goals of this thesis

The goals of this thesis are, most broadly, to better understand the elements of ADAR1 biology that are essential for its regulation of MDA5 in order to . In Chapters 2 and 3, I describe a new mouse model in which we could test the contributions of the numerous effectors described above in a setting of ADAR1 mutation *in vivo*. We sought to thereby identify new potential therapeutic targets in AGS and other diseases caused by ADAR1 dysfunction, and to understand those required for effective tumor treatment using ADAR1 targeting. Additionally, we wished to shed light on whether and how the ZBD of ADAR1 contributes to regulation of MDA5. Finally, in Chapter 4, we developed a system to identify which RNAs cause MDA5 activation in

the absence of ADAR1 editing in greater detail than ever before, in the hope of better understanding how disease occurs and why it manifests when and where it does in patients.

Chapter 2: PKR and the Integrated Stress Response drive immunopathology caused by ADAR1 mutation

Sections of text in this chapter have been modified slightly from the following manuscript: **Maurano M**, Snyder JM, Connelly C, Henao-Mejia J, Sidrauski C, Stetson DB. 2020. PKR and the integrated stress response drive immunopathology caused by ADAR1 mutation. *In revision. Immunity.*

Introduction

Over 200 distinct mutations in the *ADAR* gene have been identified that cause numerous human diseases associated with a type I IFN response, including Aicardi-Goutières syndrome (AGS), Bilateral Striatal Necrosis (BSN), and Dyschromatosis Symmetrica Herediteria (DSH) [65,69,136]. Despite considerable progress in understanding the molecular mechanisms of AGS and related diseases, these conditions remain untreatable and incurable, underscoring the need to identify new therapeutic targets for intervention. Three mouse models of ADAR1 mutation have been instrumental in defining the relationship between ADAR1 RNA editing and the MDA5-MAVS pathway: *Adar*-null mice that lack both ADAR1 isoforms[93,94,104], an *Adar p150* knockout mouse that lacks ADAR1 p150 but retains ADAR1 p110[137], and a knockin *Adar* point mutation that disrupts deaminase activity but retains ADAR1 protein expression.[120] Moreover, CRISPR targeting of the *ADAR* gene in human cells has been used to further explore consequences of ADAR1 loss[53,97,138], and ADAR1 blockade was recently identified as a potential strategy to enhance innate immune responses in tumor cells. However, characterization of the ADAR1-MDA5 regulatory axis *in vivo* has been hampered by the embryonic lethality caused by the null alleles of *Adar* in mice, which can only be rescued by simultaneous disruption of the genes that encode MDA5 or MAVS. Thus, study of the relationship between ADAR1 and MDA5 in live mice has been impossible using current models.

To address these limitations and to enable the identification of AGS disease mechanisms *in vivo*, we generated a knockin mouse that models the most common *ADAR* allele found in AGS: a nonsynonymous point mutation that converts a proline to an alanine at position 193 in the human ADAR1 protein (P193A; P195A in mice). This mutation is located within the

Za domain that is unique to the p150 isoform, and it is present at a remarkably high allele frequency of ~1/360 in humans of northern European ancestry[139,140]. Using these mice, we show that *Adar P195A* paired with a null allele of *Adar* causes complete, postnatal, MDA5-dependent mortality. We further define essential requirements for the RLR LGP2, type I IFNs, and the eIF2α kinase PKR in disease progression. Finally, we show that therapeutic inhibition of the integrated stress response (ISR) downstream of PKR is sufficient to completely prevent disease. Together, these data reveal effector mechanisms downstream of MDA5 activation that contribute to immunopathology *in vivo*, with implications for treatment of human diseases caused by *ADAR* mutation.

Results

Over 60% of AGS patients with *ADAR* mutations carry the P193A allele as a compound heterozygote with either a frameshift mutation or a mutation in the deaminase domain of ADAR1[58,65]. Interestingly, no AGS patients have been identified who are homozygous for *ADAR P193A*. We hypothesized that this was because homozygosity of P193A mutation would be incompatible with life, similar to the phenotype of total ADAR1 loss in mice[93,104]. To determine how this mutation impacts ADAR1 function and self-RNA detection, we used CRISPR targeting of fertilized mouse oocytes to generate mice carrying the orthologous P195A mutation in the endogenous *Adar* locus (Fig. 5A). We intercrossed *Adar P195A/+* mice and identified live births of *Adar+/+*, *Adar P195A/+*, and *Adar P195A/P195A* mice at the expected Mendelian ratios (Fig. 5B). We tracked the survival and weights of *Adar P195A/+* and *Adar P195A/P195A* mice and found them to be indistinguishable from wild type controls (Fig. 5C, D). This suggests that the absence of known *ADAR P193A/P193A* AGS patients might be due to a lack of disease.

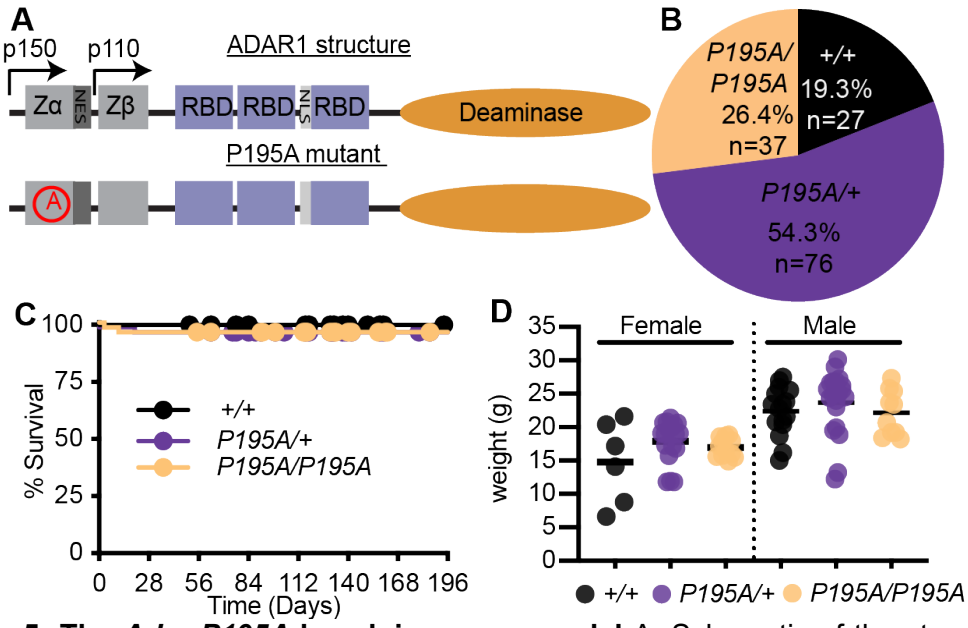

Figure 5: The *Adar P195A* knock-in mouse model A. Schematic of the structure of ADAR1, and the location of the P195A mutation. Zα, Zβ, = Z-DNA binding domains, NES = Nuclear export signal, NLS = nuclear localization signal. B. Percentage of mice of the indicated genotype from intercrosses of *Adar P195A/+* mice. C. Survival of *Adar* +/+ (n=23), *Adar P195A/+* (n=47), *Adar P195A/P195A* (n=48) mice. D. Weights of mice of the indicated *Adar* genotypes at 23 days of age. Bar represents the mean.

We then measured expression of *Adar* mRNA in cerebellum and in bone marrow-derived macrophages (BMDMs) and found that the *Adar P195A* mutation did not impact *Adar* mRNA levels in resting cells or after treatment with recombinant IFN beta (IFNb; Fig. 6). Moreover, the protein expression levels, inducibility, and nuclear and cytosolic distribution of the ADAR1 p110 and p150 isoforms were unaffected by the *Adar P195A* mutation (Fig 6). Because the *ADAR P193A* mutation in AGS is invariably found as a compound heterozygote with a more severe *ADAR* allele[58,65], we intercrossed *Adar P195A/P195A* mice with either *Adar+/-* or *Adar p150+/-* mice to model the combinations of *ADAR* alleles found in AGS patients. We found that both *Adar P195A/-* mice and *Adar P195A/p150-* mice were born at frequencies that matched the recovery of heterozygous mice from crosses of the parental *Adar*-null and *Adar p150*-null alleles (Fig. 6A, B). However, and in stark contrast to the *Adar P195A/P195A* mice (Fig. 5C), we noted

complete postnatal mortality when the P195A mutation was paired with either the full *Adar* null allele or the *Adar p150*-null allele (Fig. 7A, B).

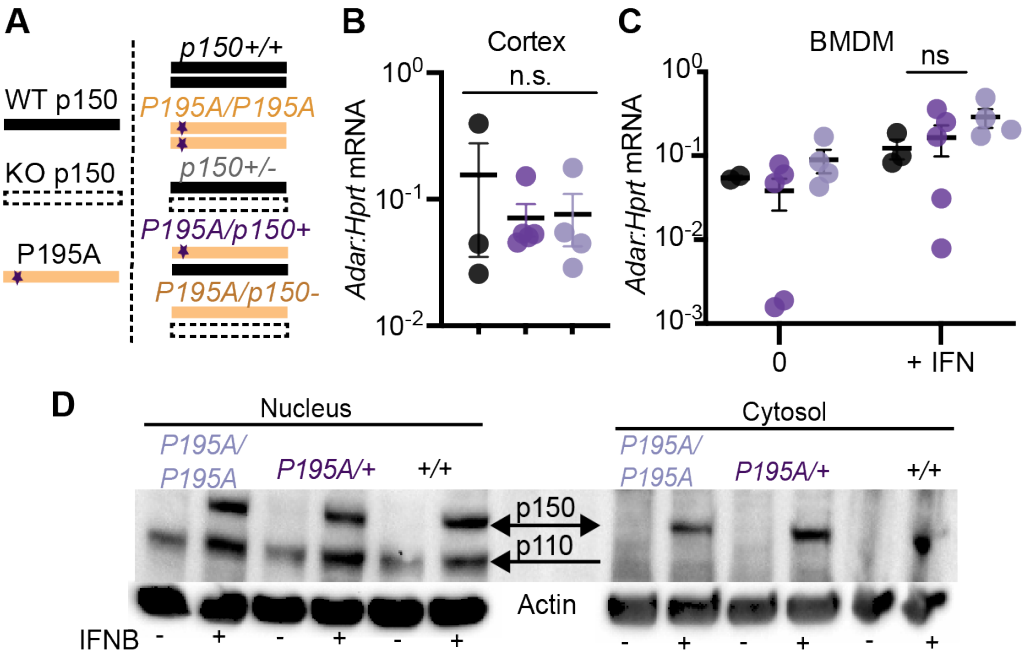

Figure 6: A. Schematics representing the different *Adar p150* alleles, and different *Adar P195A/p150* genotypes. B. Expression of *Adar* mRNAs in the cortex of *Adar P195A/P195A*, *Adar P195A/+* and *Adar+/+* mice. C. Expression of *Adar* mRNAs in BMDM from *Adar P195A/P195A*, *Adar P195A/+* and *Adar+/+* mice, with and without 24 hour treatment with recombinant IFNb. Bars represent mean and SEM. D. Western blot for ADAR1 in the cytosol and nucleus of primary MEFs of the indicated genotypes with and without 24 hour treatment with recombinant IFNb.

Mortality in the *Adar P195A/-* mice (median survival 21 days) progressed more rapidly than in the *Adar P195A/p150-* mice (median survival 40 days; Fig. 7A, B). Next, we performed these same intercrosses of the *Adar P195A* mutation with the *Adar*-null and *Adar p150*-null alleles on an *Ifih1-/-* (MDA5 KO) background and observed complete rescue from mortality of both *Adar P195A/-Ifih1-/-* and *Adar P195A/p150-Ifih1-/-* mice (Fig. 7C, D). Consistent with the essential contribution of MDA5 to disease, we found that the *Adar P195A/-* and *Adar P195A/p150-* mice were severely runted at weaning compared to littermate controls, and that this runting was entirely MDA5-dependent (Fig. 7E, F). We also noted that heterozygosity for *Ifih1* delayed mortality, revealing a gene dosage-specific effect of MDA5 expression on disease

(Fig. 8C, D). Taken together, these data demonstrate that the *Adar P195A* mice recapitulate the human *ADAR* genotypes found in AGS and develop severe disease that is driven by MDA5. More broadly, they represent the first *Adar*-mutant mice that are born with intact MDA5 signaling, allowing the dissection of disease mechanisms *in vivo*.

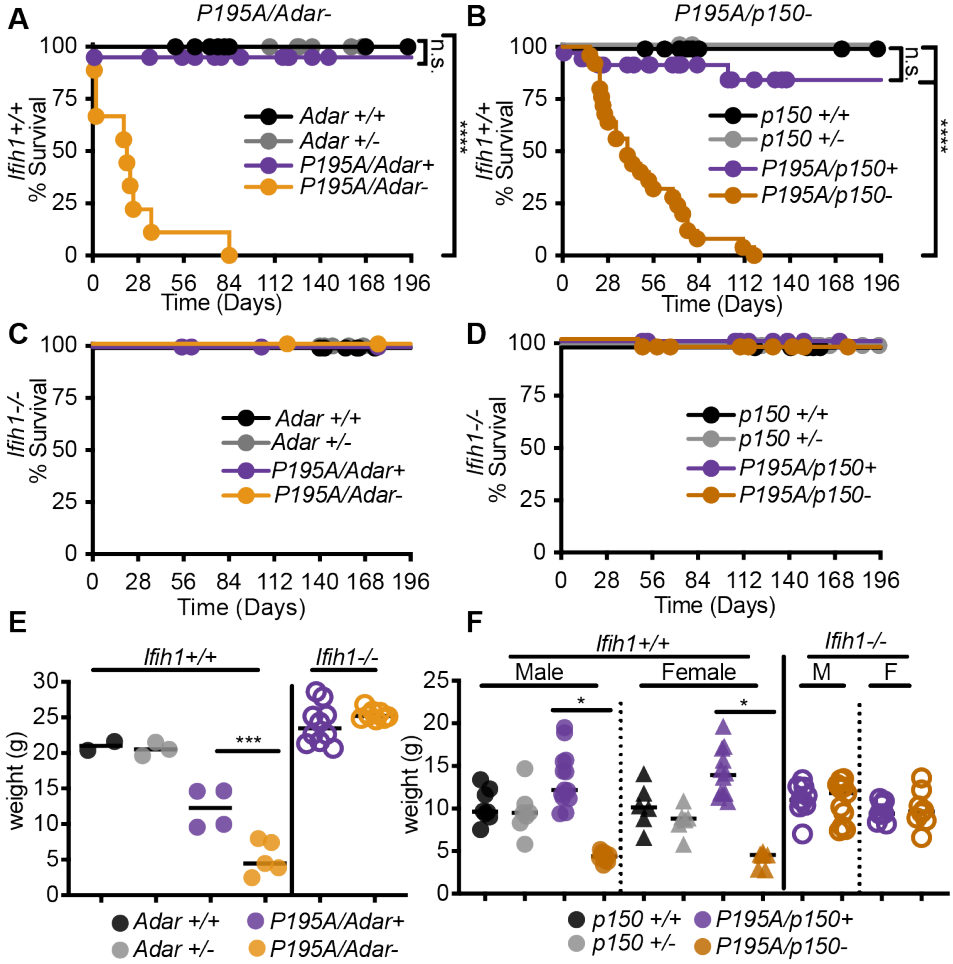

Figure 7: Recapitulation of AGS patient genotypes causes severe disease in *Adar P195A* mice A-B. Survival of *Ifihi1*+/+ mice of the indicated genotypes: *Adar*+/+ (n=14), *Adar*+/- (n=21), *Adar P195A/Adar*+ (n=41), *Adar P195A/Adar*- (n=9); *Adar p150*+/+ (n=15), *Adar p150*+/- (n=6), *Adar P195A/p150*+ (n=34), *Adar P195A/p150*- (n=25). C-D. Survival of *Ifihi1-/-* mice of the indicated genotypes: *Adar*+/+ (n=18), *Adar*+/- (n=22), *Adar P195A/Adar*+ (n=14), *Adar P195A/Adar*- (n=19); *Adar p150*+/+ (n=17), *Adar p150*+/- (n=24), *Adar P195A/p150*+ (n=25), *Adar P195A/p150*- (n=28). E-F. Weights of mice of the indicated genotypes, measured at 23 days. Bars represent mean. Male and female mice are pooled in (E) because there was no significant difference by sex.

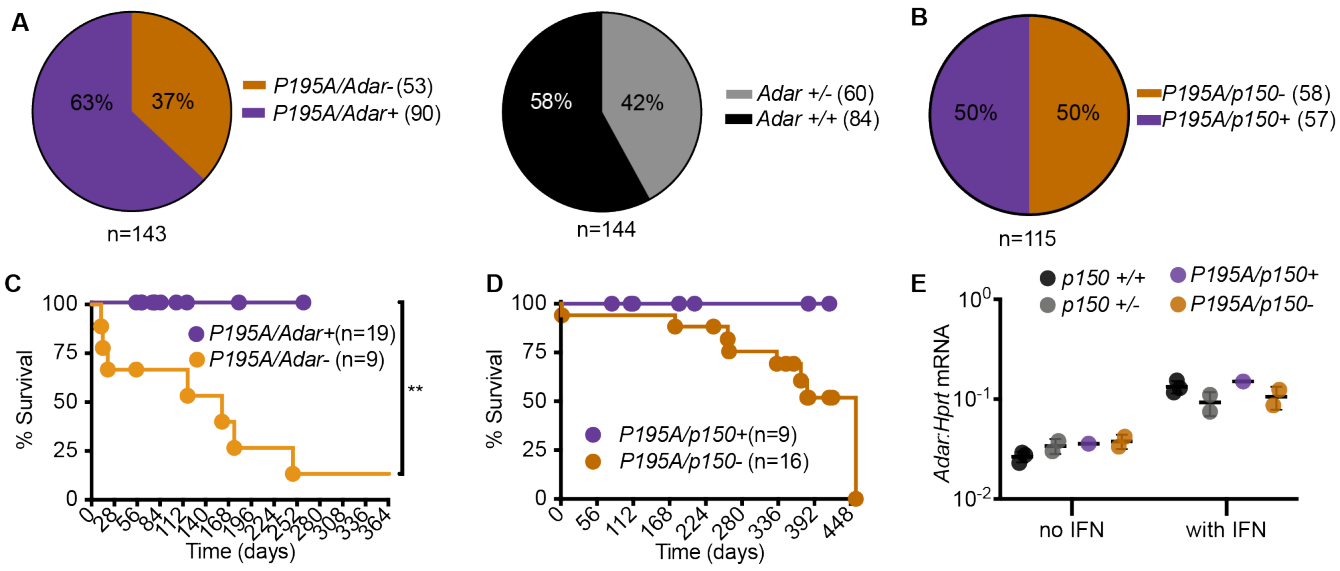

Figure 8: Features of *Adar P195A* mice crossed to *Adar* null alleles
A. Percentage of mice of the indicated genotype born from crosses of *Adar P195A/P195A* and *Adar+/-* mice (left panel), and *Adar+/+* and *Adar+/-* mice (right panel). Number of each genotype is indicated in parentheses. *Adar+/-* mice are born at a lower than Mendelian frequency, as has been previously observed. B. Percentage of mice of the indicated genotype born from crosses of *Adar P195A/P195A* and *Adar p150+/-* mice (right panel). C. Survival of mice of the indicated *Adar* genotype on an *Ifih1+/-* background, revealing partial rescue from mortality. D. Survival of mice of the indicated *Adar p150* genotype on an *Ifih1+/-* background, revealing partial rescue from mortality. E. Expression of *Adar* mRNA transcript in independently derived primary MEFs of the indicated genotypes, with and without 24 hours of treatment with recombinant mouse IFNb. Bars represent mean and SEM.

To better understand the causes of runting and mortality in this model, we performed necropsies on sex-matched *Adar P195A/p150-* and *Adar P195A/p150+* littermates to evaluate the pathologies associated with disease. We focused these and all additional analyses on the *Adar P195A/p150-* mice because they survived longer than *Adar P195A/-* mice (Fig. 7A, B). In our initial assessment, the clearest histological defects were found in the kidney and liver. The kidney exhibited glomerular mesangial matrix expansion, and the liver exhibited extensive microvesicular cytoplasmic vacuolation that increased with age (Fig. 9A-C). Strikingly, and in contrast to the *Trex1-/-* mouse model of AGS that is driven by the cGAS-STING DNA sensing pathway rather than by MDA5-MAVS, we found no evidence of inflammatory immune cell infiltrates in these tissues (Fig. 9A-C). We additionally identified dysregulated architecture of the

spleens in *Adar P195A/p150-* mice (Fig. 9C). We developed a histological scoring approach to quantitate these pathologies across several mice per genotype. *Adar P195A/p150-* mice had significantly higher pathological scores in all three organs, and these scores were normalized to control levels in *Adar P195A/p150-Ifih1-/-* mice (Fig. 9D-F). As an independent measure of liver function, we found that serum alkaline phosphatase (ALP) levels were elevated, and serum albumin levels were reduced in *Adar P195A/p150-* mice compared to controls (Fig. 9G). We next grew primary BMDMs from *Adar P195A/p150-* mice on *Ifih1+/+* and *Ifih1-/-* backgrounds. The *Adar P195A/p150-* BMDMs did not spontaneously express elevated levels of *Ifnb* mRNA, but treatment of these cells with recombinant IFNb instigated robust, MDA5-dependent *Ifnb* transcription (Fig. 9H), as has been previously observed in *ADAR*-null human cell lines. Together, these data demonstrate severe, MDA5-dependent pathologies and MDA5-mediated aberrant type I IFN expression in *Adar P195A/p150-* mice.

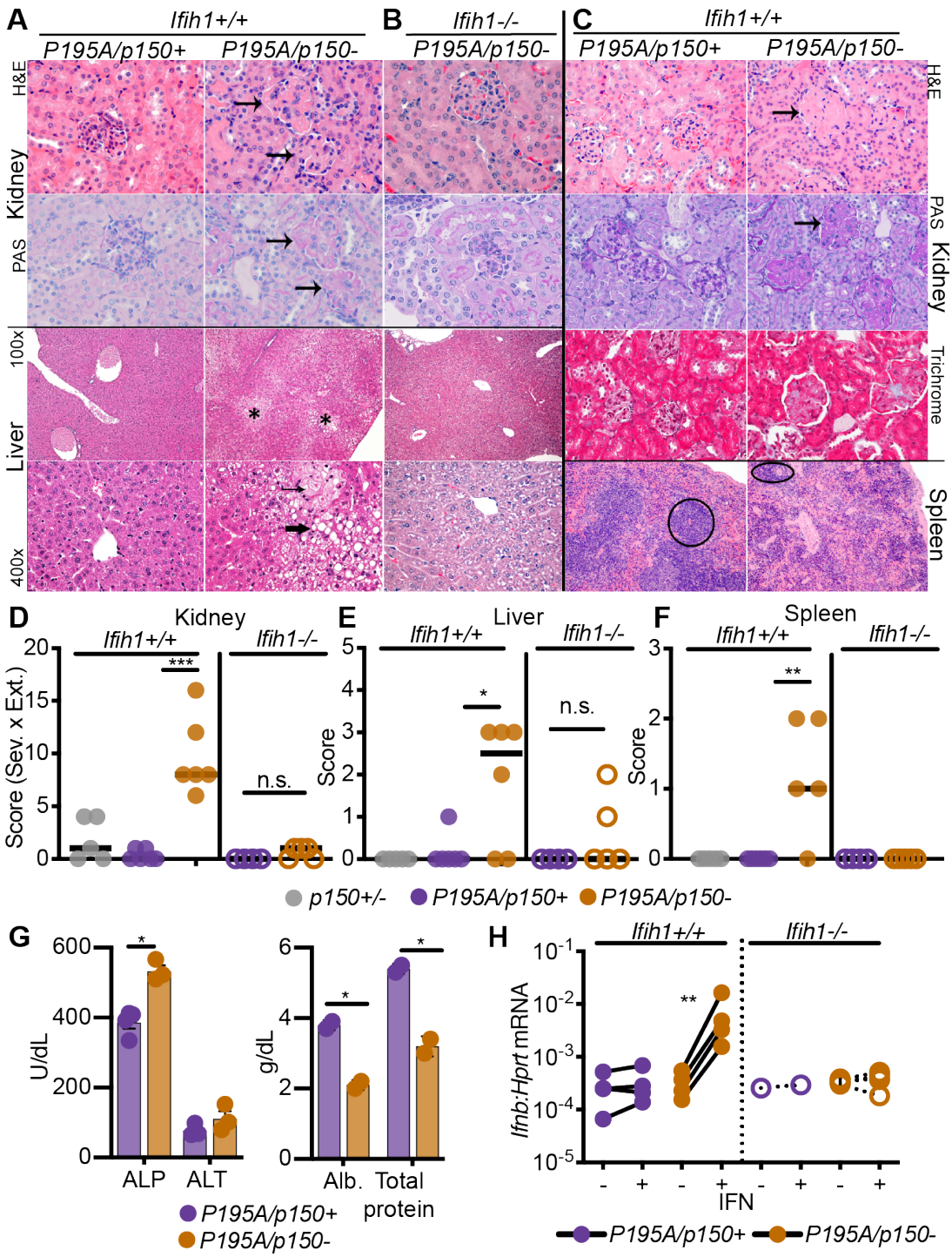

Figure 9: Organ-specific pathology in *Adar P195A/p150-* mice A. Representative histology of kidney and liver from *Adar P195A/p150-* mice measured at 23 days of age. B. Representative histology of kidney and liver from *Adar P195A/p150-Ifih1-/-* mice measured at 23 days of age. C. Representative histology of kidney, liver, and spleen from *Adar P195A/p150-* mice measured at 147 days of age. D-F. Histological scores in the kidney, liver, and spleen, measured at 23 days of age. G. ALP, ALT, Albumin, and protein measured in the serum of 23 day old mice. Bars represent mean and SEM. H. *Ifnb* transcript measured by qRT-PCR in BMDMs of the indicated genotypes, with and without 24 hours of treatment with recombinant mouse IFNb.

We performed mRNA-Seq analyses comparing age-matched *Adar P195A/p150-* mice and *Adar P195A/p150+* controls to quantitate global changes in gene expression caused by the *Adar P195A* mutation. We analyzed liver and kidney because of the specific pathologies we uncovered in these tissues (Fig. 9), and we additionally included cerebellum to compare changes in gene expression in the brains of these mice. Focusing on well-curated interferon-stimulated genes (ISGs), specifically genes in the GO term 'response to type I interferon', we carried out a gene set enrichment analysis and found significant up-regulation of this gene set in all three tissues (Fig. 10A-C). The extent of the ISG signatures varied among tissues, with cerebellum showing the most significant increases in ISG expression (adjusted p=0.007), followed by kidney (adjusted p=0.003) and then liver (adjusted p=0.01; Fig. 10A-C). We then performed quantitative RT-PCR of selected ISGs in all three of these tissues, comparing additional *Adar P195A/p150-* mice and *Adar P195A/p150+* controls, on both *Ifih1+/+* and *Ifih1-/-* backgrounds. Consistent with the complete rescue from mortality and pathology in *Adar P195A/p150-Ifih1-/-* mice (Fig. 7 and 9), we found that the significantly elevated ISG expression was also entirely MDA5-dependent (Fig. 10D-F). Thus, the *Adar P195A/p150-* mice recapitulate the MDA5-dependent ISG signatures found in the blood and cells of AGS patients[141].

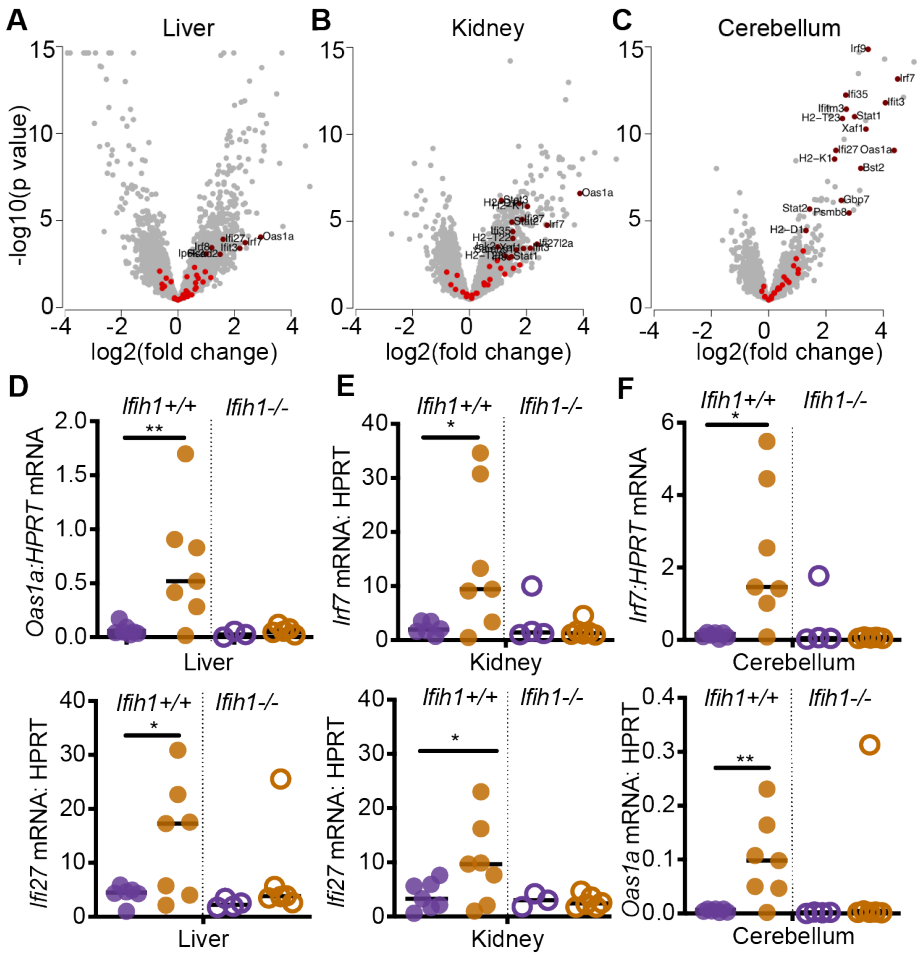

Figure 10. MDA5-dependent interferon signature in *Adar P195A/p150-* mice
A-C. Expression data for ISGs, defined by the GO term 'response to type I interferon,' were evaluated in the liver, kidney, and cerebellum of 23 day old *Adar P195A/p150-* mice, plotting the $\log_2$ fold change over matched *Adar P195A/p150+* control mice. ISGs that were not significantly changed are shown in bright red; significant expression changes are shown in dark red.
D-F. Expression of ISGs identified in A-C, measured by TaqMan qPCR, in 23 day old mice of the indicated genotypes.

The development of postnatal, lethal, MDA5-dependent disease in *Adar P195A/p150-* mice allowed us to further characterize how aberrant MDA5 signaling results in pathology *in vivo*. To do this, we performed a series of crosses to test stringently the contributions of additional signaling pathways, monitoring survival, weights, and ISG signatures. We started these analyses by examining the contribution of the third RIG-I-like receptor, LGP2, which is encoded by the *Dhx58* gene. The role of LGP2 in antiviral immunity is less well understood than that of MDA5 and RIG-I, in part because LGP2 lacks the Caspase Activation and Recruitment domain

(CARD) that is essential for RIG-I and MDA5 signaling through MAVS. Moreover, a role for LGP2 in any immune pathology has not been previously reported. However, numerous studies have demonstrated that LGP2 interacts with MDA5[142], modulates the formation of MDA5 filaments on dsRNAs[143,144], and is important for antiviral responses to RNA viruses that specifically activate MDA5[145]. We intercrossed *Adar P195A/P195A* mice with *Adar p150+/-* mice on a *Dhx58-/-* background, analyzing *Adar P195A/p150-* mice and comparing them to *Adar P195A/p150+* littermate controls. We found that LGP2 deficiency completely rescued the *Adar P195A/p150-* mice from mortality, restored their weights to normal, and prevented the ISG signature in cerebellum, liver, and kidney (Fig. 11A-C). These findings place LGP2, together with MDA5, at the apex of the signaling pathway that links ADAR1 dysfunction to disease.

Next, we tested the importance of the ISG signatures in *Adar P195A/p150-* mice by crossing them to *Ifnar1-/-* mice that lack the type I interferon signature. We found that IFNAR1 deficiency also completely rescued all aspects of disease (Fig. 11D-F), similar to the rescue of *Trex1-/-* mice on an *Ifnar1-/-* background[38]. We evaluated the *in vivo* contribution of the dsRNA-activated eIF2α kinase PKR (encoded by the *Eif2ak2* gene) to disease in *Adar P195A/p150-* mice. PKR is activated by similar dsRNA structures as those that activate MDA5/LGP2, and the activation of PKR in ADAR1-deficient cells has been clearly demonstrated in both mouse and human cell lines[97,103,146,147]. Additionally, prior studies have identified an important role for PKR upstream of the activation of type I IFNs by MDA5[148,149]. However, a specific contribution of PKR to *in vivo* immunopathology has not been described. We found that *Adar P195A/p150-Eif2ak2-/-* mice were completely protected from mortality and weight loss (Fig. 11G-H). However, the ISG signature remained significantly elevated in cerebellum and liver from these mice (Fig. 11I). These findings directly implicate PKR in the disease caused by ADAR1 dysfunction *in vivo*, and they place PKR as an essential downstream effector, rather than an activator, of the MDA5/LGP2-dependent IFN response in this model.

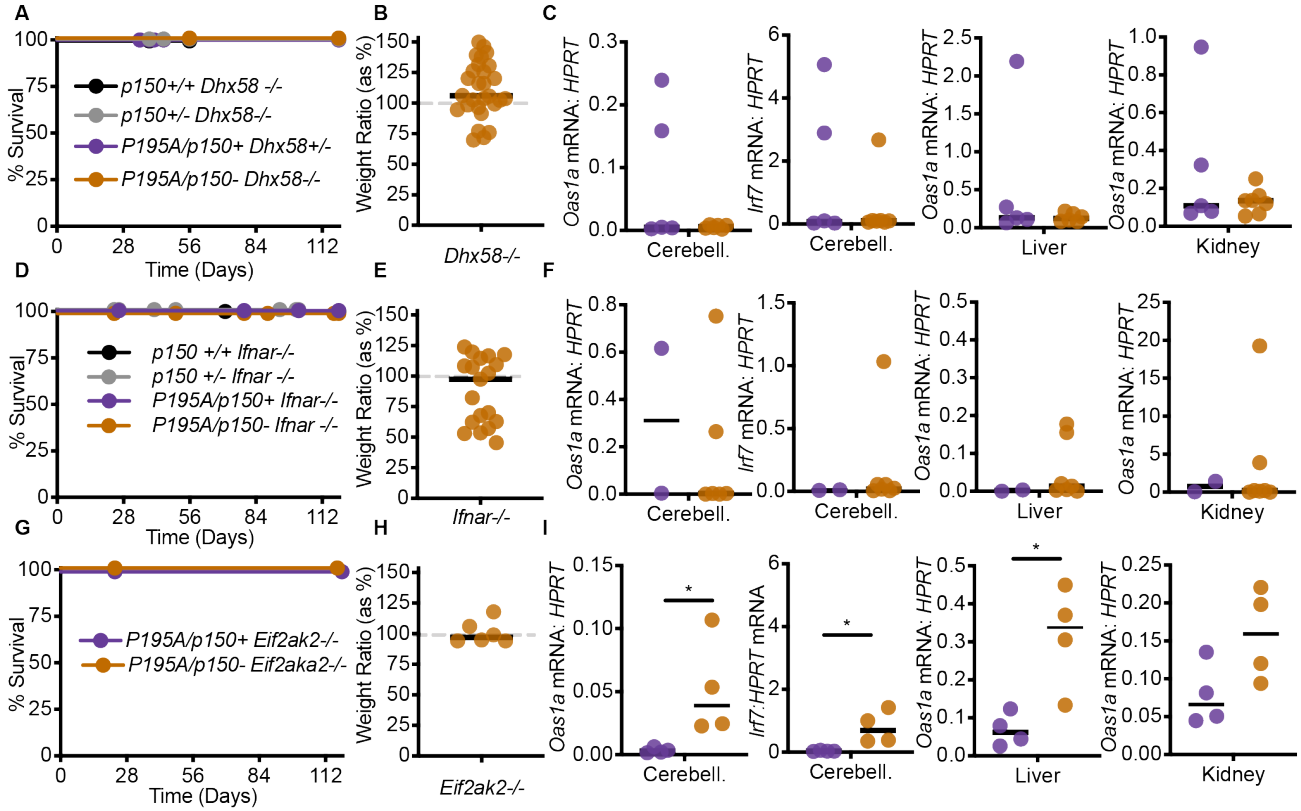

Figure 11: Genetic dissection of the *Adar P195A/p150-* phenotype *in vivo*
A. Survival of *Dhx58-/-* mice of the indicated genotype: *Adar p150+/+* (n=3), Adar *p150+/-* (n=8), *Adar P195A/p150+* (n=5), *Adar P195A/p150-* (n=12). B. Weights, measured at 23 days, of *Adar P195A/p150-Dhx58-/-* mice, as a percentage of the average weight of age- and sex-matched *Adar P195A/p150+Dhx58-/-* control mice. C. Expression of the indicated ISGs measured by TaqMan qRT-PCR, normalized to HPRT, in the cerebellum, liver, or kidney, comparing *Adar P195A/p150-Dhx58-/-* mice to *Adar P195A/p150+Dhx58-/-* controls. D. Survival of *Ifnar-/-* mice of the indicated genotype: *Adar p150+/+* (n=3), *Adar p150+/-* (n=7), *Adar P195A/p150+* (n=4), *Adar P195A/p150-* (n=16). E. Weights, measured at 23 days, of *Adar P195A/p150-Ifnar1-/-* mice, as a percentage of the average weight of age- and sex-matched *Adar P195A/p150+Ifnar1-/-* control mice. F. Expression of the indicated ISGs measured by TaqMan qRT-PCR, normalized to HPRT, in the cerebellum, liver, or kidney, comparing *Adar P195A/p150-Ifnar1-/-* mice to *Adar P195A/p150+Ifnar1-/-* controls.

We examined the contribution of the endonuclease RNase L to disease in the *Adar P195A/p150-* mouse model. RNase L is activated by the 2'-5' oligoadenylate (2-5A) products of the dsRNA-activated OAS enzymes[150,151], which are IFN-inducible nucleotidyltransferases that resemble cGAS in overall structure and catalytic mechanism[152]. Once activated by 2-5A, RNase L cleaves cellular and viral RNAs, which limits viral replication and restricts mRNA translation[153]. RNase L has been previously implicated as a key effector that mediates cell death downstream

of *ADAR* disruption in a line of human A549 cells[114,154]. We found that RNase L deficiency had no impact on the mortality or weight loss in *Adar P195A/p150-* mice (Fig. 12) suggesting that the contribution of RNaseL to disease in this model might be more subtle or cell type specific.

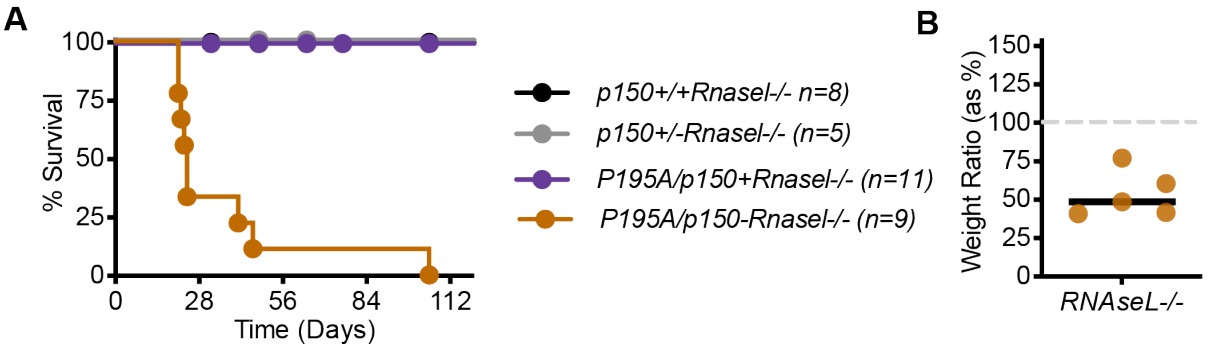

Figure 12: RNase L deficiency does not rescue Adar P195A/p150- mice A. Survival of *Rnasel-/-* mice of the indicated genotype: *Adar p150+/+* (n=8), Adar *p150+/-* (n=5), *Adar P195A/p150+* (n=11), *Adar P195A/p150-* (n=9). B. Weights, measured at 23 days, of *Adar P195A/p150-Rnasel-/-* mice, as a percentage of the average weight of age- and sex-matched *Adar P195A/p150+Rnasel-/-* control mice.

Together, this genetic dissection of the *Adar P195A/p150-* mouse model reveals new and essential contributors to *in vivo* immunopathology and places them in a hierarchy that links MDA5- and LGP2-dependent IFN responses to PKR-dependent effector mechanisms that drive disease.

Based on the striking and complete rescue of PKR-deficient *Adar P195A/p150-* mice, we explored the contribution of PKR-dependent effector mechanisms to disease in more detail. PKR is one of four metazoan eIF2α kinases that couple diverse perturbations in cellular homeostasis to a program called the integrated stress response (ISR), which restricts new protein synthesis and results in the transcriptional induction of genes that can either restore homeostasis or cause cell death, depending on the strength and duration of the insult[107,155]. The eIF2 GTPase is responsible for the delivery of the initiator methionyl tRNA to the ribosome that initiates mRNA translation at the AUG start codon. GTP hydrolysis releases eIF2 from the ribosome-mRNA complex, after which the eIF2 must be recycled from its GDP-bound inactive form into its GTP-bound active form in order to initiate a new round of mRNA translation[156].

Phosphorylation of the a subunit of eIF2 on serine 51 prevents this recycling of the eIF2 complex by the guanine nucleotide exchange factor (GEF) eIF2B, and results in a reduction of most canonical mRNA translation initiation[157]. However, certain mRNAs that contain unusual arrangements of AUG start codons in their 5' untranslated regions become selectively translated in the context of eIF2α phosphorylation[158]. These include the transcription factor ATF4, which induces the expression of ISR-activated genes[159].

The ISR gene expression program has been extensively defined in cell lines, and *in vivo* in mice that harbor hypomorphic mutations in *Eif2b5*, one of the genes that encodes the 5-subunit eIF2B complex[160]. *EIF2B* gene mutations in humans cause a lethal leukoencephalopathy called Vanishing White Matter disease (VWM) that is driven by a chronic ISR[161,162]. Using a curated ISR gene expression signature defined in the *Eif2b5*-mutant mouse model of VWM, we examined our mRNA-Seq data and found significant up-regulation of the ISR gene set in *Adar P195A/p150-* mice (Fig. 13A-C). The ISR gene set was significantly elevated in liver (adjusted p=0.02) and kidney (adjusted p=0.07) but was not significantly increased in cerebellum (adjusted p=0.57; Fig. 13A-6C). Taken together with the ISG analyses (Fig. 10), the liver and kidney exhibited elevation of both ISG and ISR gene sets, but the cerebellum exhibited only the ISG signature (Fig. 10A-C).

We selected three of the most robustly induced ISR genes in the livers of *Adar P195A/p150-* mice (*Asns*, *Cdkn1a*, and *Hmox1*), and evaluated their expression by quantitative RT-PCR, comparing the affected mutant mice to all of the rescued genotypes that we identified in figures 7 and 11. We found that induction of ISR gene expression required MDA5, LGP2, IFNAR1, and PKR (Fig. 11D-F), which precisely mirrored the rescue from mortality and pathology in all of these genotypes, even more specifically than the ISG signature that remained elevated in PKR-deficient *Adar P195A/p150-* mice (Fig. 10I).

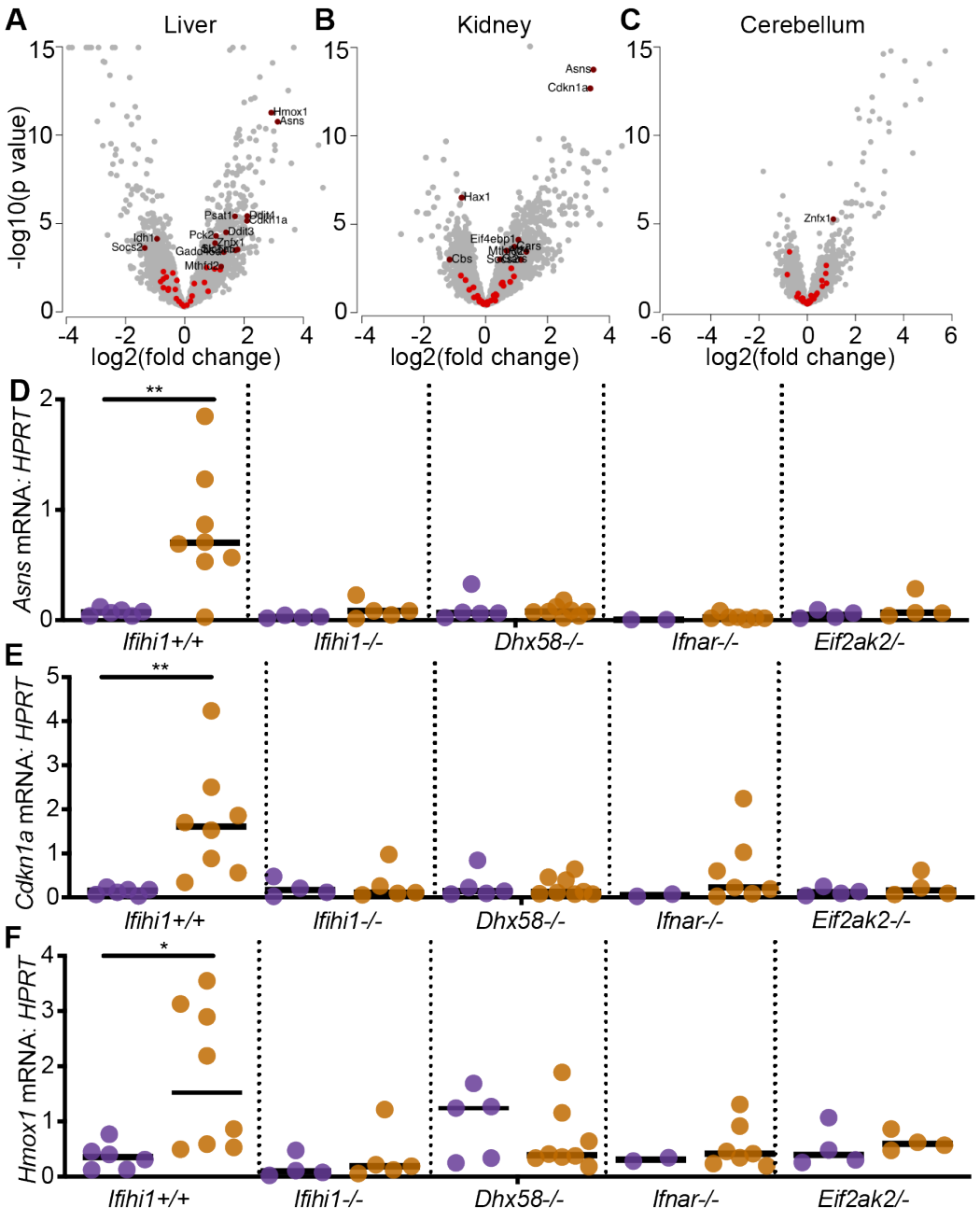

Figure 13. An ISR gene expression signature in *Adar P195A/p150-* mice
A-C. Expression data for ISR gene set genes in the liver, kidney, and cerebellum of 23 day old *Adar P195A/p150-* mice, plotting the log2 fold change over control *Adar P195A/p150+* mice. ISR genes that are not significantly changed are shown in bright red; significant expression changes are shown in dark red. D-F. Expression of ISR transcripts identified in the livers of rescued mice, measured by TaqMan qRT-PCR, and compared among the indicated genotypes. Each data point represents an individual mouse.

A small molecule called Integrated Stress Response Inhibitor (ISRIB) stabilizes the eIF2B complex and activates its GEF function, rendering eIF2B less sensitive to the inhibitory effects of eIF2α phosphorylation[163]. More recently, a similarly potent and brain-penetrant analog of ISRIB with improved *in vivo* pharmacokinetics and pharmacodynamics called 2BAct was shown to prevent all aspects of VWM in a mouse model of *Eif2b5* mutation, including brain pathology and induction of ISR genes. We tested whether the ISR inhibitor 2BAct could impact disease in the *Adar P195A/p150-* mouse model. To do this, we formulated 2BAct into mouse chow, and we placed breeders on 2BAct-containing or control chow two days after timed matings. We maintained the mice on this regimen through birth and nursing of pups, and then continued treatment of the mice following weaning. We tracked survival and disease phenotypes for 125 days after birth, which is three times the median survival of unmanipulated *Adar P195A/p150-* mice (Fig. 7). We found that dietary introduction of 2BAct nearly completely rescued the *Adar P195A/p150-* mice from mortality, and it restored the mice to normal weights (Fig. 14A-B). Moreover, 2BAct-treated *Adar P195A/p150-* mice were indistinguishable from controls when examined by tissue pathology in liver, kidney, and spleen, both at weaning and at the end of the 125-day treatment (Fig.14C-D). Interestingly, the ISGs remained significantly elevated in 2BAct-treated *Adar P195A/p150-* mice (Fig. 14E), but expression levels of the three ISR genes were restored to control levels (Fig. 14F). Thus, we have shown that therapeutic amelioration of the ISR is sufficient to prevent mortality and pathology in this *Adar*-mutant mouse model, revealing an essential IFN-dependent effector mechanism that contributes to disease *in vivo*.

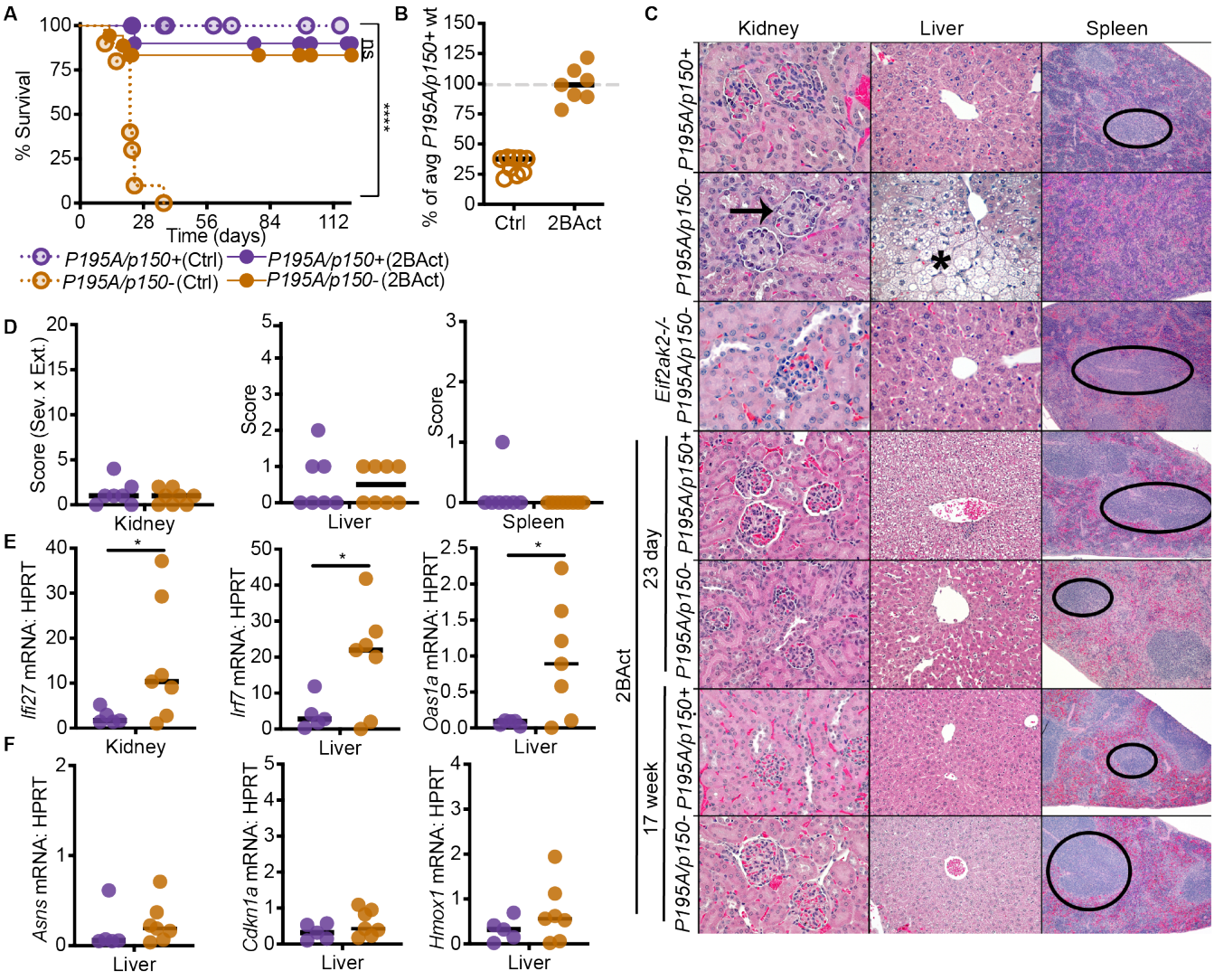

Figure 14. Pharmacological Inhibition of the ISR rescues *Adar P195A/p150-* mice
A. Survival of mice on control chow: *Adar P195A/p150+* (n=23), *Adar P195A/p150-* (n=10); versus survival of mice on 2BAct chow: *Adar P195A/p150+* (n=17), *Adar P195A/p150-* (n=17). B. Weights of *Adar P195A/p150-* mice on control chow or 2BAct chow, as a percentage of average weight of age- and sex-matched *Adar P195A/p150+* mice on control chow. C. Representative histology of kidney, liver, and spleen of untreated, *Eif2ak2-/-,* and 2BAct-treated mice of the indicated genotypes. D. Histological scores of the kidneys, livers, and spleens of 2BAct-treated mice at day 23. E. ISG expression in the kidneys and livers of *Adar P195A/p150+* and *Adar P195A/p150-* mice treated with 2BAct.

Discussion

We introduce a new mouse model of an AGS *Adar* mutation that develops postnatal, MDA5-dependent mortality. We use this model to delineate the genetic pathways responsible for pathology and we reveal a therapeutic approach that completely prevents disease, with

implications for our understanding of disease mechanisms and targets for intervention in the human immune disorders caused by *ADAR* mutation.

Our studies of the *Adar P195A/p150-* mice offer new insights into the links between ADAR1 dysfunction, MDA5, and disease manifestations. First, we show that the RLR LGP2 is essential for the MDA5-mediated antiviral response in this model, revealing a new target for therapeutic intervention. Prior *in vitro* studies of the biochemical mechanisms of MDA5 filament formation on dsRNAs in the context of ADAR1 editing have focused exclusively on interactions between synthesized dsRNAs and purified recombinant MDA5[98]. Because LGP2 can modulate the size of MDA5 filaments and stabilize smaller MDA5-dsRNA complexes[144,164], the size and composition of dsRNAs that are competent to trigger LGP2/MDA5 *in vivo* in the context of ADAR1 dysfunction might be distinct from those defined *in vitro*. Second, our findings reveal essential contributors to disease that were not appreciated in prior studies of the *Adar*-null alleles in mouse models. Specifically, neither IFNAR1 deficiency nor PKR deficiency rescued *Adar*-null mice to birth[104,165]. However, we have now found that both IFNAR1 and PKR are essential for disease in the *Adar P195A/p150-* mouse model (Fig. 11). This likely reflects the severity of the null alleles of *Adar* compared to the *Adar P195A* point mutation, together with the essential function of ADAR1 that is independent of its role in regulating MDA5. Unlike the *Adar*-null alleles, which eliminate both functions of ADAR1, the *Adar P195A* mouse model isolates the specific MDA5 regulatory roles of the p150 isoform of ADAR1.

By modeling the disposition of human *ADAR* AGS mutations in mice, we have established a genetic pathway that links ADAR1 dysfunction to disease. This pathway places MDA5 and now LGP2 as the initiating sensors that are required for detecting the self-RNAs that fail to be edited in *Adar P195A/p150-* mice. Next, the MDA5- and LGP2-dependent type I interferon response drives all aspects of disease pathology. Finally, we define PKR as an essential IFN-dependent effector that mediates the disease manifestations and mortality. Whereas PKR is clearly important for antiviral defense and it is targeted by virus-encoded

antagonists[166], PKR has not previously been implicated in self RNA-mediated immune pathology *in vivo*.

We have found that the ISR inhibitor 2BAct, administered in food, prevents mortality and all aspects of disease pathology in *Adar P195A/p150-* mice. Moreover, we identify an ISR gene expression signature in affected mice that is more specific than the ISG signature in its correlation with genetic and therapeutic rescue. Specifically, the ISGs remain significantly elevated in PKR-deficient *Adar P195A/p150-* mice and in 2BAct-treated *Adar P195A/p150-* mice, but the loss of the ISR signature correlates perfectly with all of the genetic and therapeutic rescues that we have defined. These findings have a number of important implications. First, we reveal a new therapeutic path to treat human diseases caused by ADAR1 dysfunction that targets a specific effector mechanism while leaving other antiviral responses intact. Second, we directly implicate the ISR as the cause of immune pathology. Third, we identify a gene expression signature that could be harnessed to explore the contributions of the ADAR1-MDA5/LGP2-PKR axis to additional immune diseases in which IFNs and MDA5 have been implicated, including type I diabetes and systemic lupus erythematosus[167,168].

In summary, we have developed and characterized a mouse model of ADAR1 dysfunction that recapitulates human AGS genotypes, we have revealed new contributors to disease, and we have provided proof-of-concept for a therapeutic approach targeting the ISR as an essential contributor to immune pathology *in vivo*.

Chapter 3: The ADAR1 heterozygote advantage

Introduction

One theory for why autoimmunity persists in the population is that the mutations that cause or predispose to autoimmunity also provide some protective benefit to carriers in the setting of infection. Sickle-cell anemia is one famous example of how carriers of sickle cell trait have a survival advantage in malaria infection, though the risk is that any of their children born homozygous may die young from sickle cell crises. Similarly, G6PD deficiency[169] is thought to persist because of protection conferred to carriers from lethal malaria infection. However, predominantly men (because it is X-linked) risk hemolytic anemia as a result of stressors that others tolerate without issue. Though neither sickle cell anemia nor G6PD anemia is thought to be an immune mediated mechanism, they highlight the strength of the pressure that infectious diseases exert on the human genome, and illustrate how mutations that provide survival advantage in infection can result in other disease. Innate immune genes are also some of the most rapidly evolving genes in the genome[170], underscoring the strength of the pressure exerted on proteins involved in host protection against infection, and making them likely candidates for new mutants to arise that come with some deleterious consequences but are retained for their beneficial effects in other settings.

This concept of heterozygote advantage has also been suggested for autoimmune diseases. AGS and other autoimmune diseases caused by ADAR1 mutations arise from a number of different mutations in ADAR1, all of which may have slightly different effects, but all of which decrease ADAR1 editing *in vitro*. Because the vast majority of ADAR1 mutations associated with disease are recessive, a similar balance of selection may be at play in ADAR1 mutation carriers as in G6PD and sickle cell disease.

Essential to this model is that carriers of ADAR1 mutations associated with autoimmune disease have evidence of haploinsufficiency. There is evidence in the ADAR1 literature that this is true of ADAR1. Firstly, Dyschromatosis Symmetrica Hereditaria (DSH) patients carry only one

loss of function mutation of ADAR1, some of which are the same mutations found in AGS, albeit paired with a frameshift or deaminase mutation on their second allele. DSH patients have skin pigmentation changes associated with an intermediate IFN signature suggesting that haploinsufficency of ADAR1 editing is sufficient to cause spontaneous activation of MDA5[56]. Secondly, there is evidence from mouse models where key components of the response to ADAR1 loss are ablated. For example, though the most striking outcome of MAVS knock out on *Adar+/-* x *Adar+/-* breeding is the rescue of *Adar-/-* mice from embryonic lethality to birth, there is also a rescue of the expected Mendelian ratio of *Adar+/-* mice. In *Mavs+/+* mice, *Adar+/-* mice are born below the expected Mendelian frequency – they should represent 67%, yet are only 55%[119]. In *Mavs-/-* cross mice, however, *Adar+/-* are the expected 50% of pups,[119,165] implying that some of the Mavs-dependent lethality observed in *Adar-/-* embryos occurs to a lesser degree in *Adar+/-* mice. Our own work described in chapter 2 also suggests there is some evidence of haploinsufficiency – *Adar P195A/+* and *Adar P195A/P195A* mice are entirely protected from the disease we described. However, as soon as P195A is paired with and Adar or p150 null allele, 100% of mice die, suggesting there is an effect of losing one allele.

Therefore, we hypothesized that ADAR1 mutations may also confer some protective advantage to infections by viruses sensed by MDA5. We found that

Results:

To study the role of ADAR1 in viral infection, we established a model of infection of *Adar p150+/-* and *Adar+/-* mice and cells, which are at baseline have no phenotype, with the enteric picornavirus Encephalomyocarditis Virus (EMCV), a natural pathogen of mice. We chose EMCV because it is IFN-sensitive, and provokes a strong IFN response that is entirely dependent on MDA5[171]. Indeed, MDA5 hyperactive mutant mice are protected from infection with EMCV[172]. We hypothesized that ADAR1 heterozygosity would also confer resistance to EMCV infection by loosening ADAR1 regulation of MDA5, creating MDA5 hyperactivity by other means.

We infected 8-12 week old sex-matched *Adar p150+/-, Adar p150+/+* mice with and without MDA5. We found that *Adar+/-* and *Adar p150+/-* mice both have increased survival compared to wild type littermates in oral infection with EMCV, and that this protection was eliminated in the absence of MDA5, implying there is not an MDA5-independent effect, such as from direct editing of the virus. (Fig. 15 A-B)

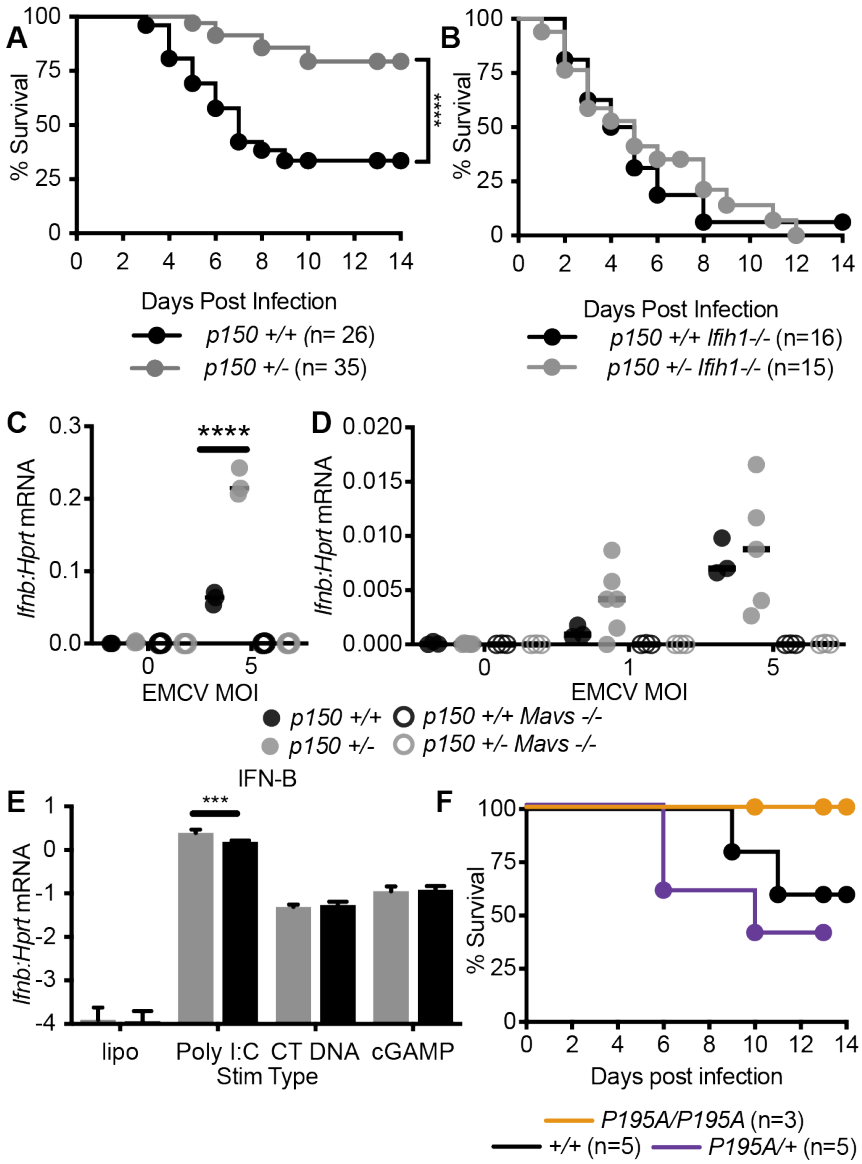

Figure 15: **Protection of ADAR1 heterozygous mice in EMCV** infection A and B. Survival of 8-12 week old mice infected 2x, 24 hours apart, by oral gavage with 10^6 PFU EMCV. C and D. *Ifnb* transcript measured in BMDM (C) and MEF (D) of the indicated genotype after 6 hours of infection with EMCV. E. *Ifnb* transcript measured by qRT-PCR 6 hours after transfection of lipofectamine alone, Poly I:C, CT-DNA, or cGAMP. F. As in A and B, with P195A mice.

To determine whether this protection was likely to be true in carriers of less dramatic mutations affecting ADAR1 function, we infected *Adar P195A/+* and *Adar P195A/P195A* mice in the same manner as above and tracked survival. Somewhat surprisingly, we found that *Adar P195A/+* mice do not demonstrate any protection. However, *Adar P195A/P195A* mice do have increased survival, though low numbers of mice have precluded statistical analysis. (Fig. 15F)

To better understand how this might be happening, we infected *Adar p150+/-* and *Adar p150+/+* BMDM and Mouse Embryonic Fibroblasts (MEF) of the same genotypes and measured IFN production in response to EMCV. We found that *Adar p150+/-* BMDM (Fig. 15C) and MEF (Fig. 15D) generate more *Ifnb* transcript in response to infection, suggesting MDA5 is responding more strongly in ADAR1 heterozygous cells, and perhaps explaining the protection from infection. With this model of ADAR1 heterozygosity, we expect only the MDA5 pathway to be more responsive to stimulation. To test whether the increased IFN in response to stimulation was pathway-specific, as opposed to a broad increase in *Ifnb* transcription, we transfected *Adar p150+/-* and *Adar p150+/+* MEF with ligands that cause IFN transcription by activating different receptors than MDA5. Calf Thymus DNA (CT DNA), and cGAMP, recognized by cGAS and STING, both work on the DNA Sensing pathway, while the IFN response to Poly I:C is dominated by MDA5. We found that only the ligands that act on MDA5 provoked a heighted IFN response in *Adar p150+/-* cells. (Fig. 15E) In agreement with our data, Mannion et al[51] found that *Adar+/-* MEFS, when stimulated with Poly I:C, have elevated IFN-a and IL-6 production relative to *Adar+/+* MEFs. They also found this elevation was entirely MAVS dependent.

Discussion:

Here we define a heterozygous advantage phenotype for *Adar+/-* and *Adar p150+/-* mice. Additionally, we suggest that homozygous P195A/P195A mice may have a similar protection. We propose that this is the result of a loosening of the regulation on MDA5, such that the threshold for MDA5 activation is, in effect, lowered in these mice because of either an increased pool of potential endogenous RNAs to activate MDA5, or because of a decrease in

the editing of EMCV replication intermediates and thus neutralization of MDA5 stimulatory capacity of EMCV RNAs. We think it is likely that, as in the cells, mice with less ADAR1 activity have an elevated IFN response to EMCV, which restricts spread of the virus and limits lethality. Also, it is possible that this more robust defense may come at the price of a predisposition of autoimmunity not just to which may have the misfortune of inheriting two mutant *Adar* alleles, but in the setting of diabetogenic infections. The strain of EMCV we used to infect the mice is known to induce pancreatic islet damage and result in diabetes in mice. It would be interesting to see if, in addition to being more likely to survive infection with EMCV, *Adar p150+/-, Adar+/-* and *Adar P195A/P195A* mice are more likely to develop severe glucose intolerance after infection

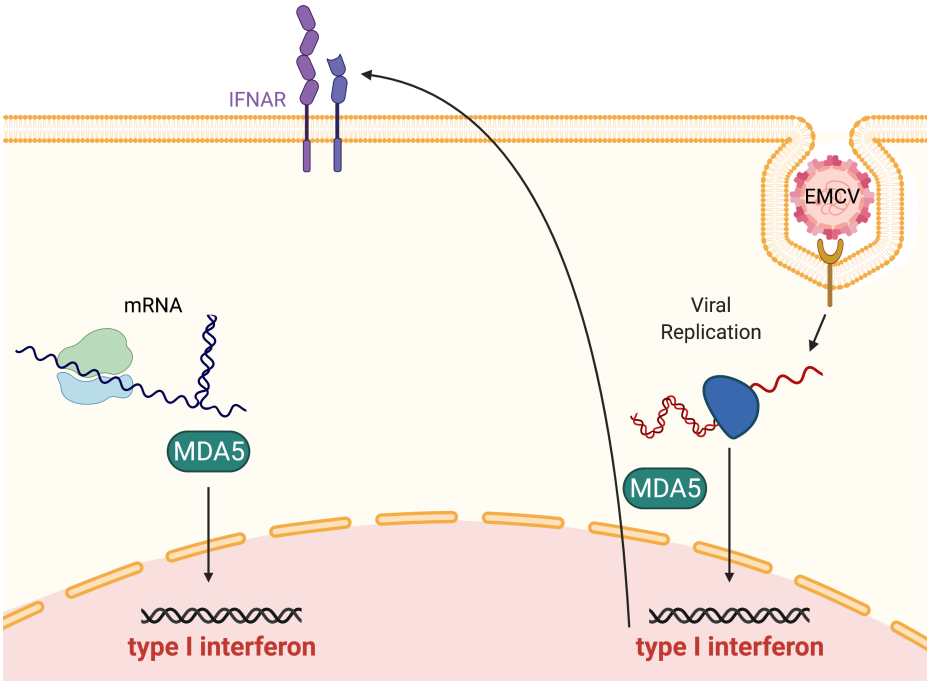

Figure 16: Possible Sources of elevated IFN in EMCV infection with decreased ADAR1 editing. On the right, unedited replication intermediates are recognized by MDA5. On the left, unedited stretches of dsRNA in mRNAs are recognized by MDA5 after upregulation by IFN produced during EMCV infection.

Though we see suggestions of pathway-specificity when ligands are transfected into cells, it remains to be seen if *Adar+/-, Adar p150+/-,* or *Adar P195A/P195A* mice would be similarly protected against viruses, like HSV or VSV, which trigger IFN through cGAS and RIG-I. Since none of these mice, or cells derived from them, have a spontaneous elevation of IFN at

baseline, we expect the protection to be narrow, and restricted only to pathogens which MDA5 plays a large role in recognizing and defending against. Measuring the IFN generated during infection with EMCV and other viruses *in vivo*, and correlating them with viral titers in the feces, blood, or other infection-appropriate site would be informative both for determining the mechanism and the breadth of the protection.

Finally, performing these experiments in the same Adar genotype mice, crossed to the MDA5-HA mice described below, would present the opportunity to identify whether the extent to which MDA5 binds EMCV RNA changes when ADAR1 status changes. In tandem with that binding assessment, it would be informative to determine whether ADAR1 edits EMCV as ADAR1 has been suggested to do to a number of viruses[173–175]; if it does, is that editing activity consistent with a pro-viral role of ADAR1?; and does it change in *Adar+/-, Adar p150+/-* and *Adar P195A/P195A* mice?

Chapter 4: A new system for identification of ADAR1/MDA5 ligands

Introduction:

Although much progress has been made in understanding the relationship between ADAR1 RNA editing and MDA5, there are no examples of a specific ADAR1 RNA substrate that, when unedited, becomes an MDA5 ligand. Some ADAR editing sites have been defined (although the specificity of ADAR1 p150 for these sites remains unknown), some MDA5-bound self-dsRNAs have been identified, but the connections between the two are inferred and remain untested. The use of ADAR1-null cells and mice precludes testing for such a mechanistic connection because not all ADAR1 editing substrates are MDA5 ligands, and the MDA5-independent roles for ADAR1 also complicate analysis of such cells. What is required is a system in which ADAR1 can be abruptly disrupted in cells, and then endogenous RNAs upon which MDA5 assembles can be identified from the same cells, together with high-resolution RNA editing analysis before and after ADAR1 disruption.

To this end, we built on our previously published model of abrupt deletion of ADAR1 *in vivo*[53], and developed an *in vitro* system from cells harvested from the same mice, allowing us to tightly control the timing of ADAR1 deletion and create a pure population of cells from which to isolate ligands.

Results:

We generated primary bone marrow derived macrophages (BMDM) from *Adar fl/fl Cre-Ert2 Tg/+* mice, together with controls that lack the Cre transgene or express the Cre transgene without the LoxP-flanked Adar allele. Treatment of these cells, as well as MEF of the same genotypes with 4-OHT for 72 hours to delete the floxed alleles results in a massive upregulation of MDA5-dependent *Ifnb* transcription (Fig. 16A and B). The *Ifnb* response after deletion *in vitro* closely parallels that which we see *in vivo* after tamoxifen injection to delete ADAR1 in adult mice (Fig. 16C) Thus, we have established two primary cell systems in which RNA editing and

innate immune responses can be compared before and after abrupt deletion of ADAR1, and from which findings can hopefully be extended to *in vivo* contexts. Additionally, we verified that we could do the same deletion experiment in *Adar fl/P195A Cre-Ert2 Tg/+ mice* (16D), abruptly recapitulating the genotypes of the mice described in Chapter 2. While the scale of the IFN response is much smaller in this setting than after biallelic deletion of ADAR1, it is clear that there is disruption of ADAR1 editing in these mice and resultant MDA5 activation. The success of this deletion will allow us to compare results from *Adar fl/fl* and *Adar fl/P195A* mice and cells to determine what editing events the ZBD is required for.

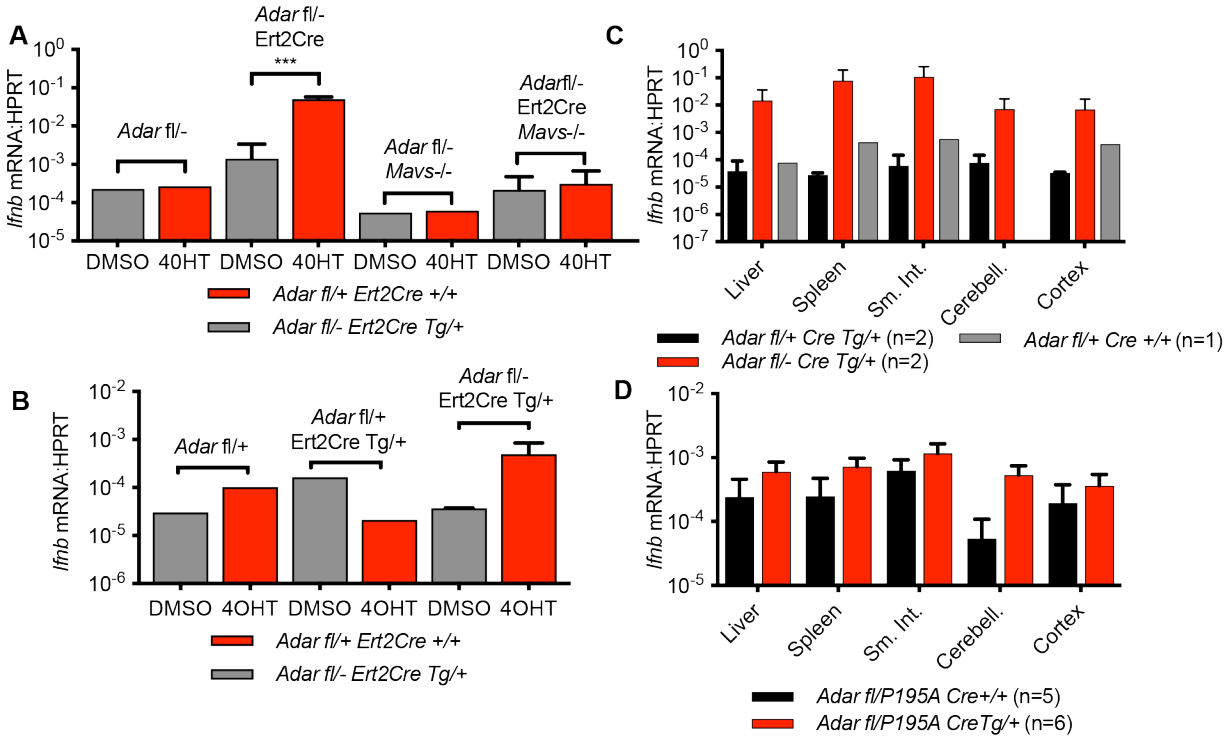

Figure 17: **A system for abrupt deletion of *Adar in vitro* and *in vivo***
A-B. *Ifnb* mRNA expression in BMDM (MEF, in B) of the indicated genotype 72 hours after inducible deletion of ADAR1 by addition of 4OHT. C-D. *Ifnb* mRNA expression in the indicated organ, in *Adar fl/fl* (C) and *Adarfl/P195A* (D) mice 72 hours after intraperitoneal injection of tamoxifen to delete Adar.

We next sought to determine if we could detect a decrease in ADAR editing after 4-OHT administration *in vitro*. We treated BMDMs from *Adar fl/fl Cre-Ert2 Tg/+* mice and *Adar fl/fl Cre-Ert2 +/+* control mice with 4-OHT for 72 hours, and then extracted RNAs. We chose to perform longer reads to enable more thorough RNA editing analysis, and we sequenced to a depth that

was 37-52 times more than required for standard gene expression analysis to increase our ability to identify rare editing events with confidence.

We performed an initial analysis of differential gene expression in these samples, revealing the expected dramatic upregulation of ISGs in the Adar-deleted cells relative to the undeleted control cells. (Fig. 17A) To analyze RNA editing, which is represented as A to G transitions in RNA-Seq data, we applied a published editing analysis pipeline[176]. We identified many sites of extensive editing, most of which were, as expected, in repetitive SINE-B1 elements embedded in 3' UTRs. We selected seven of the most highly edited sites in control samples and compared the extent of editing in these control samples to the extent of editing in the Adar-deleted samples. We found a robust reduction in the percent editing of these specific sites after abrupt *Adar* disruption, confirming our ability to identify RNA edits in mouse mRNAs, in our *in vitro* Adar disruption system. (Fig 17B)

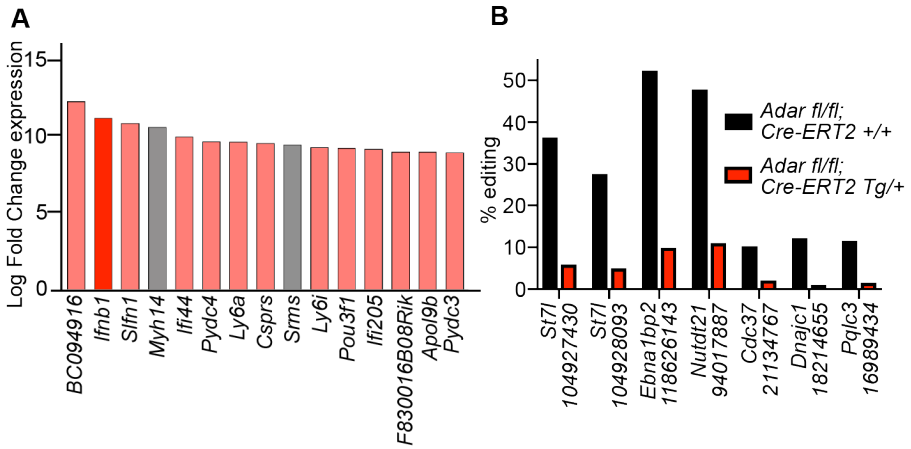

Figure 18: **mRNA-Seq analysis of gene expression and RNA editing in primary BMDM with after abrupt *Adar* deletion** A. The 15 top genes with differential expression in *Adar fl/fl; Cre-ERT2Tg/+* BMDM relative to *Adar fl/fl Cre-ERT2+/+* controls with no deletion. Interferon stimulated genes are colored in light red. B. RNA editing analysis of the transcripts with the highest percentage of editing at a particular site in the *Adar fl/fl Cre-ERT2+/+* controls, and the percent editing at the same sites after Adar deletion in the *Adar fl/fl; Cre-ERT2 Tg/+* BMDM. Gene names and nucleotide positions are indicated.

We next turned to identifying which of those lost editing events is relevant to MDA5 activation on endogenous RNAs. To facilitate the identification of RNAs upon which MDA5 has assembled in live cells, we used CRISPR targeting in fertilized mouse oocytes to generate a knockin allele of MDA5 in which we added a hemagluttinin (HA) epitope tag to the C-terminus of MDA5. We achieved germline transmission of the targeted allele, and we found that BMDM from the targeted mice had comparable levels of MDA5-HA expression when compared to WT MDA5. (Fig 18A)

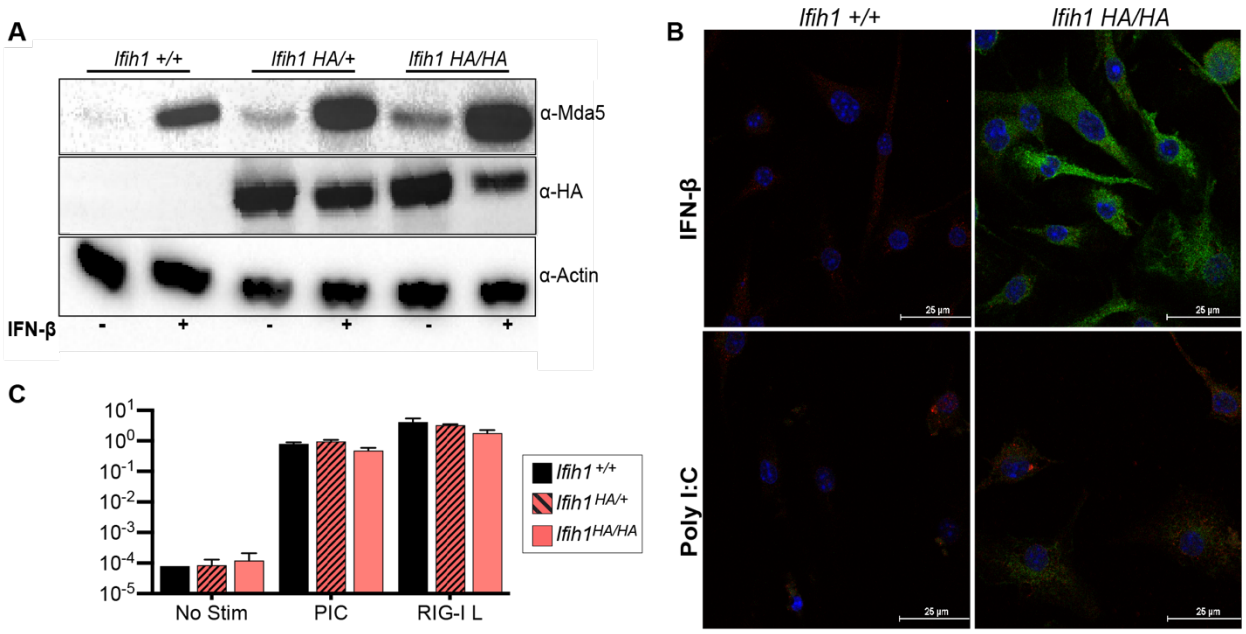

Figure 19: A system for enrichment of MDA5 ligands A. Western blot for MDA5, HA, and Actin, in *Ifih1*+/+ or *Ifih1 HA/HA* BMDM 24 hrs after 100U/mL rIFNB B. Immunofluorescence for HA (green), and dRNA (red) 12 hrs after rIFN stimulation or Poly I:C transfection into *Ifih1*+/+ or *Ifih1 HA/HA* BMDM, demonstrating the normal reactivity of MDA5. C. *Ifnb* and *Isg15* mRNA expression in BMDM of the indicated genotype 6 hrs after poly I:C transfection

First, we verified that adding the HA tag had not compromised MDA5 functionality, and that it accurately reflected MDA5 location and activity. The MDA5-HA protein is fully functional and mediates a potent antiviral response to the synthetic MDA5 ligand Poly I:C (Fig. 18C), and it can be tracked by microscopy (Fig. 18B). Unlike prior studies of MDA5 assembly on RNAs, which entailed incubating extracted, purified RNAs with recombinant MDA5 followed by RNase-protection,[98] these novel mice will allow us to prepare extracts from cells, treat them with

RNase, and then directly immunoprecipitate MDA5-HA and its bound, RNase-protected RNAs. We are crossing these mice to the conditional Adar mice; this will create a new and sensitive system in which RNA editing, antiviral responses, and endogenous MDA5 ligands can all be monitored together in primary cells.

Discussion

Using these tools, we can map MDA5-protected RNAs before and after acute Adar disruption, which will allow us to address numerous important questions with unprecedented resolution. Of the RNAs that are protected by MDA5 after Adar disruption, how many of them have evidence for editing prior to Adar depletion? What is the extent of editing of these RNAs, both within individual molecules and among all the reads that map to a particular RNA? Are the MDA5-protected RNAs completely unedited, partially edited, or edited in a manner that is indistinguishable before and after Adar disruption? Are there RNAs other than mRNAs that are protected by MDA5 after Adar disruption?

We do expect to see that *Adar P195A/-* cells have a disruption of editing, though to a lesser degree than in *Adar fl/fl* cells, as have been observed in comparisons of *Adar p150-/-* to *Adar -/-* cells, and was observed in two recently-published models of ZBD-mutated Adar1[177,178]. It will be interesting to determine not just which RNAs fail to be edited, but which activate MDA5, if there is any particular class of RNAs activating MDA5, and how it varies by cell type and organism. It will also give us candidate RNAs to try to test whether LGP2, PKR, MDA5, and ZBP1 all bind to and are activated by the same ligands in the setting of ADAR1 loss of function.

A better understanding of the identities of the ligands that trigger MDA5, and the other proteins that contribute to cell death and pathology after ADAR1 loss not only would improve our understanding of AGS, but could allow the development of a screening method for ADAR1 dysfunction in patients with possible ADAR1 dysfunction, by looking for loss of editing of particular targets. Also, knowledge of the ligands that activate each effector would aid in design

of something like a immunotherapy adjuvant that, rather than knocking out ADAR1, could mimic the effects of ADAR1 loss in tumors by simultaneously stimulating the same pathways.

Chapter 5: Conclusions and Future Directions

The study of rare genetic immune diseases has guided much of our understanding of regulation of the innate immune sensors. . AGS, which is a disease of overreactive IFN due to a variety of mutations in negative regulators of nucleic acid sensors is one such example. Through the identification of the mutations carried by AGS patients, the essential role of antiviral effectors (Fig 1) in preventing chronic responses to self DNA and RNA have been recognized. By studying how these mutations cause disease a setting where the link between protein dysfunction and disease is very clear, we can understand what to look for in more heterogeneous disease that may have more subtle defects in the same pathways. Here we describe, in chapter two, a new mouse model of AGS due to an ADAR1 mutation, and how we used this model to confirm the roles of proteins that had been implicated in the response to ADAR1 loss, and may represent novel therapeutic targets for immune-mediated disease.

The *Adar P195A/p150-* model adds to the toolbox for understanding ADAR1 regulation of the RNA sensors. It is the first mouse model to be born live, with MDA5-signaling intact. All previous models – *Adar-/-*, *Adar p150-/-,* and *Adar E861A/E861A* exhibit embryonic lethality unless MDA5/MAVS signaling is abrogated. Our model circumvented this issue by targeting the ADAR1 dysfunction to only the p150 isoform, and introducing a mutation that decreases but does not completely eliminate ADAR1 editing. The ability to study where in the entire organism MDA5 activation occurs allows us to narrow down where to look for the factors that drive disease; where there is pathology, there should be loss of ADAR1 editing, relevant ligands, and all proteins that contribute to pathology. Though the localization of disease manifestations in *Adar P195A/p150-* mice have minimal overlap with the symptoms of AGS, we predict that this is a matter of expression of transcripts that have the potential to be MDA5 ligands if unedited, rather than a difference in the mechanics of the response. Given that the Alu family is unique to primates, it is likely that pathology from ADAR1 loss follows the pattern of Alu family insertion.

Single cell sequencing to determine what transcripts are expressed in cells that produce IFN would help illuminate this.

Using the *Adar P195A/p150-* mice we tested targets that likely play a role in the pathogenesis of diseases with decreased ADAR1 function, and we were able to determine which play a role in a whole organism. In doing this, we have added LGP2 as essential to the IFN response downstream of ADAR1 loss, confirmed that IFNAR plays a key role in pathology, and identified PKR as responsible for pathology while not being required for the IFN response. It remains to be determined exactly how knocking out each of these proteins can seemingly equally prevent disease. Further characterization of each rescue – for example, RNASeq to determine, more broadly, what transcriptional responses are interrupted in each knock out. Additionally, many of the approaches outlined below to understand the specific role of each effector will also be informative for understanding their relationships to one another.

Our current working model of how all these effectors work in concert is depicted in figure 19. Failure to edit RNA in a cell expressing transcripts that contain inverted repeats of SINEs results in recognition by MDA5, assisted by LGP2, to induce IFN production. This IFN signals through IFNAR to upregulate MDA5, LGP2, and PKR in both the initial cell and those nearby, which also are deficient in ADAR1 editing. The upregulation of MDA5 and LGP2 causes ongoing and exacerbated IFN production in response to hypoedited self-RNAs. Upregulation of PKR allows PKR activation by unedited RNA, and results in translational arrest, induction of ISR transcripts, and, eventually, cell death leading to the pathology and reduced cellularity we observe histologically.

The Role of LGP2:

We hypothesize that LGP2 is playing a role in the initial detection of RNA because there is no IFN signature in *Adar P195A/p150 Dhx58-/-* mice, such that they resemble *Adar P195A/p150- Ifih1-/-* mice. Given LGP2's suggested role in facilitating MDA5 filamentation and activation on shorter RNAs than MDA5 alone can be activated on[179], recruitment of LGP2 could

explain how MDA5 is activated by ligands that are less than half the required length for MDA5 filamentation (~500bp). However, this remains to be determined by comparisons of what RNA LGP2 is binding, what MDA5 is binding, and what, if anything, MDA5 is binding in the absence of LGP2. It will also be interesting to determine whether *Adar p150-/- Dhx58-/-* mice are rescued in the same way as *Adar p150-/- Ifih1-/-* mice are. If our model is correct, and LGP2 is required for MDA5 filamentation on any inverted repeat SINE, LGP2 knock out rescue of *Adar p150-/-* mice should be just as effective as MDA5 knock out rescue. However, it is also possible that the ZBD is responsible for editing a subset of RNAs for which LGP2 is necessary, and MDA5 activation, lethality, and IFN in *p150-/-* mice will therefore not exhibit the same dependency on LGP2. Alternatively, LGP2 could be modulating MDA5 and IFN signaling entirely independent of RNA binding.

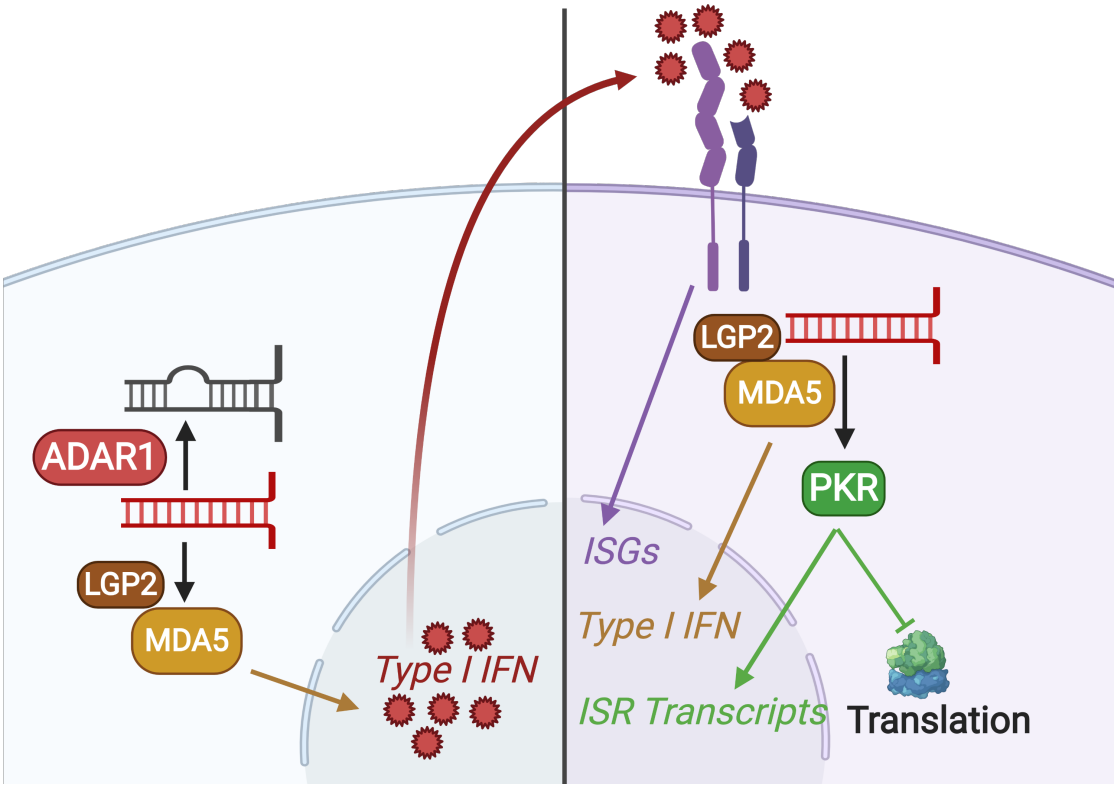

Figure 20: Summary of Endogenous RNA sensing after ADAR1 editing is lost

The Role of PKR:

One of the most important results of this thesis is the demonstration that PKR is essential to the pathology and death that results from ADAR1 loss. This was shown using

rescue *of Adar P195A/p150- Eif2ak2-/-* mice and is the first *in vivo* confirmation of this interaction… The real surprise is the persistence of elevated IFN and ISG response in *P195A/p150- Eif2ak2-/-* mice – the rescued mice have no disease, even in the presence of an aberrant chronic IFN response, which is thought to be the cause of pathology in both mice and patients, and has been the focus of recent trials. [63,180] Clearly, however, chronic IFN alone is not sufficient to drive pathology, and this may explain the incomplete effectiveness of JAK/STAT inhibitors in treating AGS, though it remains to be seen how PKR causes pathology.

Chronic PKR activation has been suggested to cause apoptosis, and it may be this is the cause of the dramatic loss of cellularity in the absence of infiltrate we observed histologically. The *Adar-/-* model has long been thought to have cell death from apoptosis, identified through TUNEL staining of the affected organs/cells[181–183]. However, the method of cell death has not been identified in either *Adar p150-/-,* nor the *Adar P195A/p150-* model, so apoptosis may be a result of p110 loss. The method of cell death in *Adar P195A/p150-* mice, and PKR's role in it, must also be examined in light of data not discussed here: that *Adar P195A/p150-* mice can also be rescued by *ZBP1* knock out. ZBP1 activation can lead to necroptosis, a more inflammatory form of programmed cell death. A comparison of cell death methods by staining for TUNEL in the livers of *Adar P195A/p150-, Adar P195A/p150- Ifihi1-/- (*or other rescue), and *Adar P195A/p150- Zbp1-/-.* Additional crosses of the *Adar P195A/p150-* mice to knock outs of essential effectors of necroptosis, such as RIPK3, will also be informative. We expect if Zbp1 is triggering necroptosis, that RIPK3 knock out will also rescue the mice. However, these crosses will likely be complicated by shunting of cells into different forms of cell death as each pathway is cut off, so an initial characterization of cell death modes in the affected mice would be prudent.

Therapeutic Potential

The role of PKR in ADAR1-associated AGS was also an exciting discovery because many therapeutic tools to inhibit eIF2α phosphorylation downstream of PKR activation already

exist. It is remarkable that chow containing the eIF2B activator, 2BAct, is able to so thoroughly rescue *Adar P195A/p150-* mice, demonstrating the potency of ISR inhibition. It also supports the data from *Eif2ak2-/-* rescued mice - mice rescued by 2BAct treatment, despite the rescue of pathology, runting, and lethality, still have ISGs elevated, confirming by a second method that ISR inhibition can rescue mice without eliminating IFN production. It demonstrates that inhibition of the ISR may be a tractable target for DSH and AGS patients, perhaps in combination with JAK/STAT inhibitors.

The use of a chow to rescue *Adar P195A/p150-* mice also makes asking a number of questions about the relationship between ADAR1, MDA5, and disease more feasible. It remains unclear if AGS is a progressive disease, or one (or a few) distinct decompensation events that result in permanent neurological damage. By putting *Adar P195A/p150-* mice on chow at different times, and by taking them off chow after different periods of time, we can determine whether the lethal dysregulation of the immune response can occur at any time in life, or if there is a window of development in which ADAR1 regulation is especially important.

Ligand Identification

One major unanswered question is whether all the RNA-binding proteins we identified as essential for pathology are binding to the same unedited RNAs. Though we have not confirmed this in *Adar P195A/p150-* mice, it is very likely that MDA5 is binding to unedited inverted repeats of SINEs. PKR has been shown to have the potential to bind to similar elements[102], though not in the setting of ADAR1 editing loss. LGP2 has not been demonstrated to bind to endogenous RNAs, though has the ability to bind to the same RNAs that both MDA5 and RIG-I can[184]. ZBP1 has been suggested to bind to inverted repeats of SINEs and other endogenous retroelement sequences, and to trigger necroptosis when the inhibition imposed by RIPK1 is lost[185]. Determining whether the same is true in the *Adar P195A/p150-* mouse model will be informative for understanding how all the pathways activated downstream of ADAR1 mutation are activated. Additionally, if we can understand whether it is the same ligand, or multiple ligands, this could

inform rational design of an adjuvant that would mimic the effects of ADAR1 loss in tumor cells, without needing genetic modification.

The Role of Stress Granules

Rescue by *Zbp1-/-* mice, the location of the P195A mutation in the p150 ZBD, which is the domain responsible for Adar1 localization to stress granules, and the central role of PKR, upon which SG formation relies in ADAR1 knock out cells[146], also raise the question of whether stress granule formation is central to the observed phenotype. Though we know that Adar P195A retains its localization to the cytosol and responsiveness to IFN (Fig. 6D), we have not tested whether it still localizes appropriately to stress granules. We hypothesize that stress granules may be essential to the Adar *P195A/p150-* phenotype, as a platform from which a positive feedback cycle of IFN is begun, and a location where all the implicated RNA binding proteins encounter unedited RNAs.

We propose the following model: In an undisrupted setting, p150 localizes to SGs, edits the RNAs there, and resolve the SG before other RNA binding proteins accumulate and activate there. This also provokes an interesting model, wherein, perhaps, p150 editing of RNA operates in two different manners; one, mediated by the dsRNA binding domains and intrinsic deaminase domain preference takes place in the nucleus, and the second, mediated by the ZBD, takes place in the cytosol to neutralize SGs. It may be that P195A specifically impairs the ability of p150 to edit RNAs in SGs, and it is the persistence of unedited RNAs and the SGs that form around them that allows other proteins that localize to SG – MDA5 and ZBP1, most critically – to encounter the RNA. SGs have been shown to be essential to IFN production in some viral infections, so may be playing the role in the response to endogenous RNA[186].

To test this, we still need to verify that SGs do form in *Adar P195A/p150-* mice and/or cells, and determine which, if any, of the effectors identified here as essential to mouse death and pathology localize to those SGs, as SG composition has been show to vary depending on the stimulus[187]. We can also begin to indirectly test this model by ascertaining whether SG

formation correlates with the IFN amplification cycle observed in (Fig. 9H), and by knocking out other crucial SG scaffolding proteins, such as G3BP1/2 or TIA-1. If compromising SG formation while leaving PKR intact prevents to IFN response to IFN, this would suggest that it is SG formation that is essential to this phenotype.

The Role of ISR Activation in AGS

Another unresolved question is whether the ISR is activated when mutations are in other proteins that cause AGS – like TREX1, RNaseH2, etc. Since TREX1 degrades DNA, and the lethality of the *Trex1-/-* mouse model is entirely dependent on DNA sensing, it is less clear how PKR activation could result. However, it could be that PKR is activated less directly that we hypothesize it is in *Adar P195A/p150-* and *Adar-/-* settings, or that one of the other three sensors that activate the ISR is activated in *Trex1-/-* mice, as has been suggested in other autoinflammatory diseases[188]. We can easily test this by treating *Trex1-/-* mice with 2BAct to determine if they will be rescued. If 2BAct treatment does succeed, we can then identify which ISR sensor is being activated to drive phosphorylation of eIF2α using mouse knock out crosses as we did with the Adar P195A model.

It is still to be confirmed whether chronic ISR activation is also occurring in AGS patients. Our own attempts to find evidence of elevated ISR – in AGS patient fibroblasts (data not shown), and in reanalysis of published RNASeq data on whole blood from AGS patients[189], did not exhibit any signs of ISR transcript upregulation. This could be because there is none, though given that studies have identified ISR transcripts upregulated after ADAR1 loss,[115] and that cell death is dependent on PKR in human cells[96,97], this seems unlikely. More likely, we are looking in the wrong place. Even in *Adar P195A/p150- mice*, ISR activation is not systemic. The cerebellum has no evidence of ISR activation, perhaps because it is missing key effectors or blocked in some manner. Instead, ISR signatures colocalized with where we saw clear pathology and signs of reduced cellularity, so it stands to reason that the same would be true in AGS patients. To find evidence of ISR activation, we will need to sample the CNS. Additionally,

it will be interesting the determine whether, like IFN, chronic ISR activation is found in all ADAR1 mutation-caused diseases, such as DSH and BSN.

Chronic ISR activation as a driver of immune pathology

Finally, an exciting implication of the PKR/ISR inhibition rescue of *Adar P195A/p150-* mice is that chronic ISR activation may play a role in more common diseases that have chronic aberrant self-RNA sensing. ISR gene expression signatures have been identified in tissue samples from human patients with multiple sclerosis (MS)[190]. Current models of MS envision the ISR as a cytoprotective mechanism that slows disease progression by preventing the loss of myelin-producing oligodendrocytes[190]. However, our findings raise the alternative possibility that the ISR might contribute to disease pathology. Type I diabetes (TID) has been linked to MDA5 sensing. The risk of T1D is elevated in people with hyperactivating mutations in MDA5, and people with hypoactive forms are protected from T1D[191]. Non-obese diabetic (NOD) mice are a common model of T1D which spontaneously develop insulin resistance, and mimics much of pancreatic pathology seen in T1D[192]. Disease in NOD mice has been shown to be MDA5-dependent[193]. It will be interesting to determine whether PKR also plays a role in this model – whether it truly is an RNA-dependent function of PKR, and a self-RNA that is triggering MDA5 in NOD mice can also activate PKR; or if there is another method by which PKR and MDA5 are coactivated to cause disease.

More broadly, we speculate that the link between the ISR and immune pathology might also apply to conditions in which the ISR is activated by distinct mechanisms, including the endoplasmic reticulum stress sensor PERK, the heme sensor HRI, and the nutrient sensor GCN2[107]. All of these kinases share eIF2α as their principal target, and all induce the ISR. In other words, because the ISR contributes to pathology downstream of PKR in this model of ADAR1 mutation, it might also drive inflammation downstream of diverse stresses that are not typically thought of as immune mediated. The coactivation of ISR and the IFN response may also contribute to pathology that results from overly robust responses to RNA viruses, or explain

the increased lethality of virus infection in those with preexisting conditions known to increase ISR signaling, such as obesity[194–196]. Increased phosphorylation of eIF2α is a hallmark of obesity and diabetes-related insulin resistance[197–199], so ISR activation in the context of an IFN response may co-occur more frequently than just after ADAR1 loss, or during infection with RNA viruses that produce long dsRNA. We propose that further study of protective versus pathogenic contributions of the ISR will illuminate new ways to understand and treat human immune diseases.

Chapter 6: Methods

Mice

Adar P195A mutant mice were generated as previously described[200], using the sgRNA target sequence GAAGGGGGAAACCTCCTTTGTGG, and the oligo DNA to replace the sequence, ATCAATCGTATTTTGTACTCCCTGGAAAAGAAGGGAAAGCTGCACAGAGGAAGGGGGAAA CCTGCCTTGTGGAGCCTTGTGCCCTTGAGTCAGGCTTGGACTCAGCCCCCTGGAGTTGTG AATCCAGAT. In brief, C57BL6/J oocytes were microinjected with Cas9 complexed with gRNA for WT *Adar* sequence and ssDNA donor template containing the desired sequence. Oocytes were implanted into a pseudopregnant CD-1 females. Founder pups born were screened by the Surveyor assay. Mice positive by the Surveyor assay were genotyped using TaqMan SNP genotyping, primers: WT: AAACCT**CCT**/ZEN/TTGTGGAGCCTT, Mut: AAACCT**GCC**TTGTGGAGCCTT. Mice positive by SNP genotyping were then sequenced to confirm fidelity of the introduced mutation. Mice were bred to C57BL6/J mice to confirm germline transmission, and *Adar P195A/+* mice were then crossed to one another or to other genetically modified mice.

Adar fl/fl mice[94] were generously provided by Stuart Orkin, and were bred to Cre-expressing mice to generate the *Adar*-null allele as described previously[119]. *Adar p150+/-* gametes[137] were generously provided by Michael Oldstone and made into mice as previously described.[53] *Ifih1-/-* mice[201] were generously provided by Michael Gale, Jr. *Dhx58-/-* mice[202] were generously provided by Michael Gale, Jr. *Ifnar1-/-* mice[203] were backcrossed 14 generations to C57BL/6[204]. *Eif2ak2-/-* mice[205], backcrossed at least 10 generations to C57BL/6J, were generously provided by Gökhan Hotamışlıgil. *Rnasel-/-* mice[206] were generously provided by Robert Silverman. All mice were maintained in a specific pathogen-free (SPF) barrier facility at the University of Washington, and all experiments were done in accordance with the Institutional Animal Care and Use Committee guidelines of the University of Washington. Mouse weights were measured at 23 days of age.

Histology and Pathology

For all histological analyses, matched littermate mice were euthanized in accordance with IACUC protocols by CO_2 asphyxiation followed by cardiac puncture. Mice were washed with PBS and then fixed in 10% neutral-buffered formalin. Tissues were routinely processed, embedded in paraffin, cut into approximately 4 μm sections and hematoxylin and eosin stained. Slides of kidney, liver, and spleen were also stained with periodic acid-Schiff. Additionally, kidney sections were stained with Congo Red and Masson's trichrome.

Tissues were evaluated and scored by a board-certified veterinary pathologist (J.M.S), who was blinded to genotype and experimental manipulation for all groups except for the initial group of mice subjected to phenotyping of multiple organs including decalcified cross section of skull, lungs, heart, kidney, liver, spleen, pancreas, lymph nodes, reproductive tract, stomach, and intestines. These juvenile mice evaluated initially in an unblinded fashion were re-scored blindly prior to manuscript preparation. For subsequent mice, histological analysis was focused on the kidney, liver, and spleen.

For the kidney, expansion of the glomerular mesangial matrix was scored from 0-4, with 0 = normal; 1 = minimal; 2 = mild; 3 = moderate (with accompanying tubular protein); and 4 = severe histological changes. An extent score was also given for the kidney, with 1 representing <10%; 2 = 10-32%; 3 = 33-65%; and 4 representing > 66% of glomeruli affected. For the liver, microvesicular and lesser macrovesicular cytoplasmic vacuolation were scored from 0-5, with 0 = normal; 1 = minimal changes affecting only a small region (< 5%) of the liver; 2 = mild changes throughout the liver but without enlargement of hepatocytes, coalescing lesions, or necrosis; 3 = mild to moderate cytoplasmic vacuolation throughout liver with enlargement of hepatocytes but no necrosis or loss of parenchyma; 4 = moderate, coalescing throughout liver with multifocal mild regions of loss of parenchyma or necrosis; and 5 = severe with moderate multifocal regions of cavitation and necrosis. Liver inflammation was also scored on a 0-5 scale with 0 = fewer than 2 small microgranulomas per section; 1 = minimal scattered inflammation or microgranulomas; 2 =

mild (less than 5% of parenchyma involved); 3 = mild to moderate (11-30%); 4 = moderate (31-60%); and 5 = severe (affecting >60% of parenchyma). Lymphoid depletion of the spleen was scored on a scale of 0-3 with 0 = none; 1 = mild; 2 = moderate; 3 = severe.

Representative images were taken using NIS-Elements BR 3.2 64-bit and plated in Adobe Photoshop Elements. Image white balance, lighting, brightness and contrast were adjusted using auto corrections applied to the entire image. Final magnification is stated.

For measurement of alkaline phosphatase (ALP) and albumin in serum, blood was collected by cardiac puncture from mice at 23 days of age and stored in SST Tubes at 4C until analysis. Samples were run at 2x dilution on a Siemens Atellica 1600 (Siemens Healthineers, Germany).

mRNASeq and differential expression analysis

Total RNA was added directly to lysis buffer from the SMART-Seq v4 Ultra Low Input RNA Kit for Sequencing (Takara), and reverse transcription was performed followed by PCR amplification to generate full-length amplified cDNA. Sequencing libraries were constructed using the NexteraXT DNA sample preparation kit (Illumina) to generate Illumina-compatible barcoded libraries. Libraries were pooled and quantified using a Qubit® Fluorometer (Life Technologies). Dual-index, single-read sequencing of pooled libraries was carried out on a HiSeq2500 sequencer (Illumina) with 58-base reads, using HiSeq v4 Cluster and SBS kits (Illumina) with a target depth of 5 million reads per sample.

Reads were processed using workflows managed on the Galaxy platform. Reads were trimmed by 1 base at the 3' end, and then trimmed from both ends until base calls had a minimum quality score of at least 30 (Galaxy FASTQ Trimmer tool v1.0.0). FastqMcf (v1.1.2) was used to remove any remaining adapter sequence. To align the trimmed reads, we used the STAR aligner (v2.4.2a) with the GRCm38 reference genome and gene annotations from ensembl release 91. Gene counts were generated using HTSeq-count (v0.4.1). Quality metrics were compiled from PICARD (v1.134), FASTQC (v0.11.3), Samtools (v1.2), and HTSeq-count

(v0.4.1). Libraries with less than 2 million mapped reads per sample were not included in the analysis, and analysis was restricted to genes with non-zero counts in all libraries (*n*=8,843 genes). We carried out normalization and tested for differential expression using DESeq2. Gene set enrichment analysis was carried out using fgsea[207], ranking genes by the sorted p values from the differential expression test for each tissue. Gene sets tested included all GO categories, Kegg pathway gene sets, Hallmark gene sets, and Reactome gene sets. We also included the manually curated ISR target gene set as defined previously[160]. In total, 7084 gene sets were evaluated, and multiple testing correction was done using the Benjamini-Hochberg method.

RNASeq and Editing Analysis:

We prepared polyA-enriched mRNA-Seq libraries and used paired-end, 100-base pair sequencing to generate 200 bp reads per molecule. We sequenced to a depth of 184 million reads for the deleted sample and 260 million reads for the control sample. Differential Expression analysis was done as above, and editing analysis was completed using the pipeline published by Defitt et al[208].

Quantitative RT-PCR

Mice were euthanized by CO_2 asphyxiation and cardiac puncture. Organs were immediately immersed in Trizol and frozen at -80C until later processing. To extract RNA, organs were mashed on ice, then resuspended in Trizol by passage through 25G needles. Samples were spun down briefly (5 min at 5000 g), and the supernatant processed by the Direct-zol RNA MiniPrep kit (Genesee Scientific) per the manufacturer's instructions with an additional dry spin after disposing of the final wash to prevent EtOH carryover. Complementary DNA (cDNA) was generated using EcoDry double primed premix (Clontech). Transcript expression was measured using the following ThermoFisher TaqMan Gene expression assays: *Ifi27* (Mm00835449_g1), *Irf7* (Mm00516788_m1), *Oas1a* (Mm00836412_m1), *Asns* (Mm00803785_m1), *Cdkn1a*

(Mm04205640_g1), and *Hmox1* **(**Mm00516005_m1). Samples were assayed in duplicate on a real-time qPCR cycler (CFX96, BioRad).

***In vitro* IFN treatments**

Bone marrow was harvested from age-matched mice and grown/differentiated in RPMI supplemented with 10% fetal calf serum, L-glutamine, penicillin/streptomycin, sodium pyruvate, HEPES, and M-CSF for 7 days. 10^5 BMDM were plated in 12 well plates and rested overnight, then stimulated with 100U/mL recombinant murine IFNb (Sigma, I9032) or equivalent volume of water for 24 hours. Cells were then harvested in Trizol before RNA purification via Directzol kits, and cDNA generation using Ecodry kits as described above. qPCR was performed using iTaq supermix on the Bio-Rad CFX96 Real-Time System, and primers for IFNB (*Ifnb* Fwd 5'-GCACTGGGTGGAATGAGACTATTG-3', *IfnB* Rev 5'-TTCTGAGGCATCAACTGACAGGTC-3') and HPRT (*Hprt* Fwd, 5'-GTT GGATACAGGCCAGACTTTGTTG-3', *Hprt* Rev, 5' -GAGGGTAGGCTGGCCTATAGGCT-3'.

2BAct treatments

Adar P195A/P195A mice were intercrossed with *Adar p150+/-* mice. 48 hours after mating, the breeders were placed on 2BAct chow, formulated to achieve a 2Bact concentration of 300 ppm (300 µg 2BAct/g of meal) as previously described.[160] 2BAct chow was contract manufactured with Envigo. The placebo diet was Teklad 2014 without added compound. Breeders and pups were maintained on 2BAct until termination of survival experiments at 125 days. Mice were weighed at 23 days of age. Littermate mice were harvested for histological and mRNA expression analysis as described above.

EMCV *in vivo*

8-12 week old mice were infected by oral gavage with 10^6 PFU of EMCV, 2x 24 hours apart. Mice were observed twice daily from day 3 - 14 post infection. At each observation, mice were scored by the following criteria: mice that scored 4 or higher twice were euthanized. 0: Healthy mouse (baseline), 1: Lethargic, 2: Ruffled fur, hunched posture, no paresis, 3: Weakness in 1

limb, 4: Moribund. All mice scoring 2 that did not improve at the next monitoring event (mice receiving scores of 2 at two successive checks) will be euthanized according to approved euthanasia procedures. All mice reaching a score of 3 or greater were euthanized immediately and recorded as a death.

***In vitro* stimulations**

BMDM cells were plated at 10^6 per well in a 12-well dish. In the six-well dish format, cells received 4 µg of CT DNA, 10uM cGAMP, 1ug RIG-I Ligand, complexed with 4 µl of Lipofectamine 2000. Control received 4uL of lipofectamine 2000 alone. All cells were harvested 6 hours after stimulations were added. Infections with EMCV were performed the same way, with the indicated MOI of EMCV

4-OHT deletion *in vitro*

BMDM isolated from 6-8 week old *Adar fl/fl Ert2Cre* and control genotype littermates were differentiated as above. 2 x 10^6 BMDM were plated in 6 well plates and treated, after 12 hours rest, with 500uM 4-OHT. MEF were plated in 6 well plates at 2.5 x 10^5 cells per well and treated with 1uM 4OHT after 12 hours rest. BMDM and MEF were both harvested 72 hours after 4-OHT addition in Trizol and processed as above for RNA isolation, cDNA generation, and qRT-PCR assessment.

Western Blot

10^6 BMDM were plated in 6 well plates and rested overnight. BMDM were treated with 100u/mL rIFNb for 6 hours before harvest in 1% Triton X-100 buffer (20 mM Hepes, 150 mM NaCl, 10% glycerol, 1 mM EDTA, and Pierce protease inhibitors). Lysates were vortexed and incubated on ice for 15 min before clearing by centrifugation for 15 min. Proteins were separated on Bolt 4-12% bis-tris gels (Thermo Fisher) in MES buffer for 30 min at 200 V and transferred to Immobilon-FL polyvinylidene difluoride membrane (Sigma). Blots were blocked in 5% bovine serum albumin/Tris-buffered saline with Tween-20 (TBST) for 30 min before incubation at 4°C overnight with primary antibody (CST Rabbit anti MDA5 (D74E4) antibody. Blots were washed

for at least 30 min in TBST before incubation with secondary antibody and image acquisition using a BioRad Chemidoc.

Immunofluorescence

BMDM were seeded onto glass coverslips overnight, then treated with rIFNb for 6 hours. They were then fixed with 4% PFA for 15 minutes at RT. Cells were then washed in PBS and permeabilized with 0.1% Triton X-100 in PBS for 10 minutes at RT. Slides were washed again in PBS, then blocked in 2% FCS in PBS for 1 hour at RT while rocking. Slides were then incubated with primary antibody in block overnight at 4° C. dsRNA was stained for with Scicons Mouse anti J2. HA was stained for with CST Rabbit anti HA C29F4. Cells were washed in PBS and incubated with secondary Ab (anti mouse A568 secondary or goat anti-rabbit a488) at 1:1000for 1 hr at room temperature. Cells were then washed with PBS, stained with DAPI and mounted on glass slides with ProLong Gold Antifade Mountant (Thermo Fisher). Images were captured with a Nikon C2RSi Scanning Laser Microscope.

Tamoxifen deletion *in vivo*

Adar fl/fl Ert2Cre mice were previously described[119]. Tamoxifen-induced deletion was performed according to the protocol available from the Jackson Laboratory. In brief, tamoxifen (Sigma-Aldrich) was dissolved in corn oil (Sigma-Aldrich) at 20 mg/mL overnight at 37°C, filtered through a 0.22 μm Millex GP PES membrane and stored at 4°C. Mice were administered 100 μL of tamoxifen via i.p. injection once a day for three days. Mice were sacrificed at 3.5 days after the first injection, and RNA harvested as above.

Statistical analysis

Quantitative data were visualized and analyzed using GraphPad Prism software. Differences in survival were assessed by the Log-rank (Mantel-Cox) Test. Observed and expected birth rates by genotypes were compared using the Chi-square test. Weights and mRNA expression measured by qPCR were compared between genotypes within each cross using unpaired t-

tests. Significance is indicated as follows in all figures: ns=not significant, *p<0.05, **p<0.01, ***p<0.001, ****p<0.0001.

References:

1. Abedon, S. T. Bacterial 'immunity' against bacteriophages. *Bacteriophage* **2**, (2012).
2. McNab, F., Mayer-Barber, K., Sher, A. & Wack, A. Type I interferons in infectious disease. (2015). doi:10.1038/nri3787
3. Schneider, W. M., Chevillotte, M. D. & Rice, C. M. Interferon-stimulated genes: A complex web of host defenses. *Annual Review of Immunology* **32**, 513–545 (2014).
4. Wong, G. & Qiu, X. G. Type I interferon receptor knockout mice as models for infection of highly pathogenic viruses with outbreak potential. *Zool. Res.* **39**, (2018).
5. Liu, G. Q. & Gack, M. U. Distinct and Orchestrated Functions of RNA Sensors in Innate Immunity. *Immunity* **53**, 26–42 (2020).
6. Ahn, J. & Barber, G. N. STING signaling and host defense against microbial infection. *Experimental and Molecular Medicine* **51**, 1–10 (2019).
7. Pöyhönen, L., Bustamante, J., Casanova, J. L., Jouanguy, E. & Zhang, Q. Life-Threatening Infections Due to Live-Attenuated Vaccines: Early Manifestations of Inborn Errors of Immunity. *Journal of Clinical Immunology* **39**, 376–390 (2019).
8. Casanova, J. L., Holland, S. M. & Notarangelo, L. D. Inborn Errors of Human JAKs and STATs. *Immunity* **36**, 515–528 (2012).
9. O'Shea, J. J., Holland, S. M. & Staudt, L. M. JAKs and STATs in Immunity, Immunodeficiency, and Cancer. *N. Engl. J. Med.* **368**, 161–170 (2013).
10. García-Sastre, A. Ten Strategies of Interferon Evasion by Viruses. *Cell Host and Microbe* **22**, (2017).
11. Iwasaki, A. & Medzhitov, R. Toll-like receptor control of the adaptive immune responses. *Nature Immunology* **5**, 987–995 (2004).
12. Barbalat, R., Ewald, S. E., Mouchess, M. L. & Barton, G. M. Nucleic Acid Recognition by the Innate Immune System. *Annu. Rev. Immunol.* **29**, 185–214 (2011).
13. Ablasser, A. *et al.* CGAS produces a 2′-5′-linked cyclic dinucleotide second messenger that activates STING. *Nature* **498**, 380–384 (2013).
14. Gao, P. *et al.* Cyclic [G(2′,5′)pA(3′,5′)p] is the metazoan second messenger produced by DNA-activated cyclic GMP-AMP synthase. *Cell* **153**, 1094–1107 (2013).
15. Chen, Q., Sun, L. & Chen, Z. J. Regulation and function of the cGAS-STING pathway of cytosolic DNA sensing. *Nat. Immunol.* **17**, 1142–1149 (2016).
16. Barber, G. N. STING-dependent cytosolic DNA sensing pathways. *Trends Immunol.* **35**, 88–93 (2014).
17. Sun, L., Wu, J., Du, F., Chen, X. & Chen, Z. J. Cyclic GMP-AMP Synthase Is a Cytosolic

DNA Sensor That Activates the Type I Interferon Pathway. *Science (80-.).* **339**, 786–791 (2013).

18. Berke, I. C. & Modis, Y. MDA5 cooperatively forms dimers and ATP-sensitive filaments upon binding double-stranded RNA. *EMBO J.* **31**, 1714–26 (2012).
19. Peisley, A., Wu, B., Yao, H., Walz, T. & Hur, S. RIG-I Forms Signaling-Competent Filaments in an ATP-Dependent, Ubiquitin-Independent Manner. *Mol. Cell* **51**, 573–583 (2013).
20. Wu, B. *et al.* Structural Basis for dsRNA Recognition, Filament Formation, and Antiviral Signal Activation by MDA5. *Cell* **152**, 276–289 (2013).
21. Alam, H., Sehgal, L., Kundu, S. T., Dalal, S. N. & Vaidya, M. M. Novel function of keratins 5 and 14 in proliferation and differentiation of stratified epithelial cells. *Mol. Biol. Cell* **22**, 4068–4078 (2011).
22. del Toro Duany, Y., Wu, B. & Hur, S. MDA5 — filament, dynamics and disease. *Curr. Opin. Virol.* **12**, 20–25 (2015).
23. Seth, R. B., Sun, L., Ea, C. K. & Chen, Z. J. Identification and characterization of MAVS, a mitochondrial antiviral signaling protein that activates NF-κB and IRF3. *Cell* **122**, 669–682 (2005).
24. Volkman, H. E., Cambier, S., Gray, E. E. & Stetson, D. B. Tight nuclear tethering of cGAS is essential for preventing autoreactivity. *Elife* **8**, (2019).
25. Liu, H. *et al.* Nuclear cGAS suppresses DNA repair and promotes tumorigenesis. *Nature* **563**, 131–136 (2018).
26. Crowl, J. T., Gray, E. E., Pestal, K., Volkman, H. E. & Stetson, D. B. Intracellular Nucleic Acid Detection in Autoimmunity. *Annu. Rev. Immunol.* **35**, annurev-immunol-051116-052331 (2017).
27. Cao, D., Han, X., Fan, X., Xu, R. M. & Zhang, X. Structural basis for nucleosome-mediated inhibition of cGAS activity. *Cell Res.* **30**, 1088–1097 (2020).
28. Boyer, J. A. *et al.* Structural basis of nucleosome-dependent cGAS inhibition. *Science (80-.).* **370**, 450–454 (2020).
29. Kujirai, T. *et al.* Structural basis for the inhibition of cGAS by nucleosomes. *Science (80-.).* **370**, 455–458 (2020).
30. Zhao, B. *et al.* The molecular basis of tight nuclear tethering and inactivation of cGAS. *Nature* **587**, 673–677 (2020).
31. Michalski, S. *et al.* Structural basis for sequestration and autoinhibition of cGAS by chromatin. *Nature* **587**, 678–682 (2020).

32. Pathare, G. R. *et al.* Structural mechanism of cGAS inhibition by the nucleosome. *Nature* **587**, 668–672 (2020).
33. Kato, H. *et al.* Differential roles of MDA5 and RIG-I helicases in the recognition of RNA viruses. *Nature* **441**, 101–105 (2006).
34. Bruns, A. M. & Horvath, C. M. LGP2 synergy with MDA5 in RLR-mediated RNA recognition and antiviral signaling. *Cytokine* **74**, 198–206 (2015).
35. Keyel, P. A. Dnases in health and disease. *Developmental Biology* **429**, 1–11 (2017).
36. Miyake, K., Shibata, T., Ohto, U. & Shimizu, T. Emerging roles of the processing of nucleic acids and Toll-like receptors in innate immune responses to nucleic acids. *J. Leukoc. Biol.* **101**, 135–142 (2017).
37. Ewald, S. E. *et al.* The ectodomain of Toll-like receptor 9 is cleaved to generate a functional receptor. *Nature* **456**, 658–662 (2008).
38. Stetson, D. B., Ko, J. S., Heidmann, T. & Medzhitov, R. Trex1 Prevents Cell-Intrinsic Initiation of Autoimmunity. *Cell* **134**, 587–598 (2008).
39. Gray, E. E., Treuting, P. M., Woodward, J. J. & Stetson, D. B. Cutting Edge: cGAS Is Required for Lethal Autoimmune Disease in the Trex1-Deficient Mouse Model of Aicardi–Goutières Syndrome. *J. Immunol.* **195**, 1939–1943 (2015).
40. Bhoj, V. G. & Chen, Z. J. Linking retroelements to autoimmunity. *Cell* **134**, 569–571 (2008).
41. Pokatayev, V. *et al.* RNase H2 catalytic core Aicardi-Goutières syndrome-Related mutant invokes cGAS-STING innate immunesensing pathway in mice. *J. Exp. Med.* **213**, 329–336 (2016).
42. Reijns, M. A. *et al.* The structure of the human RNase H2 complex defines key interaction interfaces relevant to enzyme function and human disease. *J Biol Chem* **286**, 10530–10539 (2011).
43. Kretschmer, S. *et al.* SAMHD1 prevents autoimmunity by maintaining genome stability. *Ann. Rheum. Dis.* **74**, e17–e17 (2015).
44. Ayinde, D., Casartelli, N. & Schwartz, O. Restricting HIV the SAMHD1 way: Through nucleotide starvation. *Nat. Rev. Microbiol.* **10**, 675–680 (2012).
45. Kretschmer, S. *et al.* SAMHD1 prevents autoimmunity by maintaining genome stability. *Ann Rheum Dis* (2014). doi:10.1136/annrheumdis-2013-204845
46. Brown, J. T., Bai, X. & Johnson, A. W. The yeast antiviral proteins Ski2p, Ski3p, and Ski8p exist as a complex in vivo. *Rna* **6**, 449–457 (2000).
47. Eckard, S. C. *et al.* The SKIV2L RNA exosome limits activation of the RIG-I-like

receptors. *Nat. Immunol.* **15**, 839–845 (2014).

48. Bass, B. L. & Weintraub, H. *An Unwinding Activity That Covalently Modifies Its Double-Stranded RNA Substrate*. *Cell* **55**, (1988).
49. Nishikura, K. A-to-I editing of coding and non-coding RNAs by ADARs. *Nat. Rev. Mol. Cell Biol.* **17**, 83–96 (2016).
50. Li, Z., Okonski, K. M. & Samuel, C. E. Adenosine Deaminase Acting on RNA 1 (ADAR1) Suppresses the Induction of Interferon by Measles Virus. *J. Virol.* **86**, 3787–3794 (2012).
51. Mannion, N. M. *et al.* The RNA-Editing Enzyme ADAR1 Controls Innate Immune Responses to RNA. *Cell Rep.* **9**, 1482–1494 (2014).
52. Liddicoat, B. J. *et al.* RNA editing by ADAR1 prevents MDA5 sensing of endogenous dsRNA as nonself. *Science (80-.).* **349**, 1115–1120 (2015).
53. Pestal, K. *et al.* Isoforms of RNA-Editing Enzyme ADAR1 Independently Control Nucleic Acid Sensor MDA5-Driven Autoimmunity and Multi-organ Development. *Immunity* **43**, 933–944 (2015).
54. Tolmie, J. L., Shillito, P., Hughes-Benzie, R. & Stephenson, J. B. The Aicardi-Goutières syndrome (familial, early onset encephalopathy with calcifications of the basal ganglia and chronic cerebrospinal fluid lymphocytosis). *J. Med. Genet.* **32**, 881–884 (1995).
55. Crow, Y. J. Aicardi-Goutières syndrome. *Handb. Clin. Neurol.* **113**, 1629–1635 (2013).
56. Rice, G. I. *et al.* Mutations in ADAR1 cause Aicardi-Goutières syndrome associated with a type I interferon signature. *Nat. Genet.* **44**, 1243–1248 (2012).
57. Rice, G. I. *et al.* Gain-of-function mutations in IFIH1 cause a spectrum of human disease phenotypes associated with upregulated type I interferon signaling. *Nat. Genet.* **46**, 503–9 (2014).
58. Crow, Y. J. *et al.* Characterization of Human Disease Phenotypes Associated with Mutations in TREX1, RNASEH2A, RNASEH2B, RNASEH2C, SAMHD1, ADAR, and IFIH1. *Am. J. Med. Genet. A* **0**, 296–312 (2015).
59. Uggenti, C. *et al.* cGAS-mediated induction of type I interferon due to inborn errors of histone pre-mRNA processing. *Nat. Genet.* (2020). doi:10.1038/s41588-020-00737-3
60. Rice, G. I. *et al.* Reverse-Transcriptase Inhibitors in the Aicardi–Goutières Syndrome. *N. Engl. J. Med.* **379**, 2275–2277 (2018).
61. Beck-Engeser, G. B., Eilat, D. & Wabl, M. An autoimmune disease prevented by anti-retroviral drugs. *Retrovirology* **8**, 91 (2011).
62. JAK Inhibition in the Aicardi–Goutières Syndrome. *N. Engl. J. Med.* **383**, 2190–2193 (2020).

63. Vanderver, A. *et al.* Janus Kinase Inhibition in the Aicardi–Goutières Syndrome. *N. Engl. J. Med.* **383**, 986–989 (2020).
64. Rice, G. I. *et al.* Mutations in ADAR1 cause Aicardi-Goutières syndrome associated with a type I interferon signature. *Nat. Genet.* **44**, 1243–8 (2012).
65. Rice, G. I. *et al.* Mutations in ADAR1 cause Aicardi-Goutières syndrome associated with a type I interferon signature. *Nat. Genet.* **44**, 1243–8 (2012).
66. Zhang, J. y. *et al.* The adenosine deaminase acting on RNA 1 p150 isoform is involved in the pathogenesis of dyschromatosis symmetrica hereditaria. *Br. J. Dermatol.* **169**, 637–644 (2013).
67. Rice, G. I. *et al.* Assessment of Type I Interferon Signaling in Pediatric Inflammatory Disease. *J. Clin. Immunol.* 1–10 (2016). doi:10.1007/s10875-016-0359-1
68. Rice, G. *et al.* Genetic, Phenotypic, and Interferon Biomarker Status in ADAR1-Related Neurological Disease. *Neuropediatrics* **48**, 166–184 (2017).
69. Livingston, J. H. *et al.* A type I interferon signature identifies bilateral striatal necrosis due to mutations in ADAR1. *J. Med. Genet.* **51**, 76–82 (2014).
70. Livingston, J. H. & Crow, Y. J. Neurologic phenotypes associated with mutations in TREX1, RNASEH2A, RNASEH2B, RNASEH2C, SAMHD1, ADAR1, and IFIH1: Aicardi-Goutières syndrome and beyond. *Neuropediatrics* **47**, 355–360 (2016).
71. Bass, B. L. & Weintraub, H. A developmentally regulated activity that unwinds RNA duplexes. *Cell* **48**, 607–613 (1987).
72. Saccomanno L and Bass BL (1994), The cytoplasm of Xenopus oocytes contains a fac... - Paper. Available at: http://www.xenbase.org/literature/article.do?method=display&articleId=20964. (Accessed: 4th December 2020)
73. Alon, S. *et al.* The majority of transcripts in the squid nervous system are extensively recoded by A-to-I RNA editing. *Elife* **2015**, (2015).
74. Garrett, S. & Rosenthal, J. J. C. RNA editing underlies temperature adaptation in K+ channels from polar octopuses. *Science (80-.).* **335**, 848–851 (2012).
75. Piechotta, M., Wyler, E., Ohler, U., Landthaler, M. & Dieterich, C. JACUSA: site-specific identification of RNA editing events from replicate sequencing data. *BMC Bioinformatics* **18**, 7 (2017).
76. Higuchi, M. *et al.* Point mutation in an AMPA receptor gene rescues lethality in mice deficient in the RNA-editing enzyme ADAR2. *Nature* **406**, 78–81 (2000).
77. Ivanov, A. *et al.* Analysis of Intron Sequences Reveals Hallmarks of Circular RNA

Biogenesis in Animals. *Cell Rep.* **10**, 170–177 (2015).

78. Shi, L. *et al.* Circular RNA expression is suppressed by androgen receptor (AR)-regulated adenosine deaminase that acts on RNA (ADAR1) in human hepatocellular carcinoma. *Cell Death Dis.* **8**, e3171 (2017).
79. Werry, T. D., Loiacono, R., Sexton, P. M. & Christopoulos, A. RNA editing of the serotonin 5HT2C receptor and its effects on cell signalling, pharmacology and brain function. *Pharmacology and Therapeutics* **119**, 7–23 (2008).
80. Chen, T. *et al.* ADAR1 is required for differentiation and neural induction by regulating microRNA processing in a catalytically independent manner. *Cell Res.* **25**, 459–476 (2015).
81. Ota, H. *et al.* ADAR1 forms a complex with dicer to promote MicroRNA processing and RNA-induced gene silencing. *Cell* **153**, 575–589 (2013).
82. Pfaller, C. K., Donohue, R. C., Nersisyan, S., Brodsky, L. & Cattaneo, R. Extensive editing of cellular and viral double-stranded RNA structures accounts for innate immunity suppression and the proviral activity of ADAR1p150. *PLOS Biol.* **16**, e2006577 (2018).
83. Levanon, E. Y. *et al.* Systematic identification of abundant A-to-I editing sites in the human transcriptome. *Nat. Biotechnol.* **22**, 1001–1005 (2004).
84. Goodier, J. L. & Kazazian Jr., H. H. Retrotransposons Revisited: The Restraint and Rehabilitation of Parasites. *Cell* **135**, 23–35 (2008).
85. Kriegs, J. O., Churakov, G., Jurka, J., Brosius, J. & Schmitz, J. Evolutionary history of 7SL RNA-derived SINEs in Supraprimates. *Trends Genet.* **23**, 158–61 (2007).
86. Chen, L.-L., DeCerbo, J. N. & Carmichael, G. G. Alu element-mediated gene silencing. *EMBO J.* **27**, 1694–705 (2008).
87. Osenberg, S. *et al.* Alu sequences in undifferentiated human embryonic stem cells display high levels of A-to-I RNA editing. *PLoS One* **5**, (2010).
88. Pinto, Y., Cohen, H. Y. & Levanon, E. Y. Mammalian conserved ADAR targets comprise only a small fragment of the human editosome. *Genome Biol.* **15**, R5 (2014).
89. Porath, H. T., Knisbacher, B. A., Eisenberg, E. & Levanon, E. Y. Massive A-to-I RNA editing is common across the Metazoa and correlates with dsRNA abundance. *Genome Biol.* **18**, (2017).
90. Tan, M. H. *et al.* Dynamic landscape and regulation of RNA editing in mammals. *Nature* **550**, 249–254 (2017).
91. Tan, M. H. *et al.* Dynamic landscape and regulation of RNA editing in mammals. *Nature* **550**, 249–254 (2017).

92. Hartner, J. C., Walkley, C. R., Lu, J. & Orkin, S. H. ADAR1 is essential for the maintenance of hematopoiesis and suppression of interferon signaling. *Nat Immunol* **10**, 109–115 (2009).
93. Hartner, J. C. *et al.* Liver Disintegration in the Mouse Embryo Caused by Deficiency in the RNA-editing Enzyme ADAR1. *J. Biol. Chem.* **279**, 4894–4902 (2004).
94. Hartner, J. C., Walkley, C. R., Lu, J. & Orkin, S. H. ADAR1 is essential for the maintenance of hematopoiesis and suppression of interferon signaling. *Nat. Immunol.* **10**, 109–115 (2009).
95. Wang, Q. Requirement of the RNA Editing Deaminase ADAR1 Gene for Embryonic Erythropoiesis. *Science (80-.).* **290**, 1765–1768 (2000).
96. Liu, H. *et al.* Tumor-derived IFN triggers chronic pathway agonism and sensitivity to ADAR loss. *Nat. Med.* **25**, 95–102 (2019).
97. Chung, H. *et al.* Human ADAR1 Prevents Endogenous RNA from Triggering Translational Shutdown. *Cell* **172**, 811-824 e14 (2018).
98. Ahmad, S. *et al.* Breaching Self-Tolerance to Alu Duplex RNA Underlies MDA5-Mediated Inflammation. *Cell* **172**, 797-810.e13 (2018).
99. Mehdipour, P. *et al.* Epigenetic therapy induces transcription of inverted SINEs and ADAR1 dependency. *Nature* **588**, 169 (2020).
100. Kuhen, K. L. & Samuel, C. E. Isolation of the interferon-inducible RNA-dependent protein kinase Pkr promoter and identification of a novel DNA element within the 5'-flanking region of human and mouse Pkr genes. *Virology* **227**, 119–130 (1997).
101. Chang, K. Y. & Ramos, A. The double-stranded RNA-binding motif, a versatile macromolecular docking platform. *FEBS Journal* **272**, (2005).
102. Kim, Y. *et al.* PKR is activated by cellular dsRNAs during mitosis and acts as a mitotic regulator. *Genes Dev.* **28**, (2014).
103. Ishizuka, J. J. *et al.* Loss of ADAR1 in tumours overcomes resistance to immune checkpoint blockade. *Nature* **565**, (2019).
104. Wang, Q. *et al.* Stress-induced apoptosis associated with null mutation of ADAR1 RNA editing deaminase gene. *J Biol Chem* **279**, 4952–4961 (2004).
105. Lemaire, P. A., Anderson, E., Lary, J. & Cole, J. L. Mechanism of PKR Activation by dsRNA. *J. Mol. Biol.* **381**, 351–360 (2008).
106. McKenna, S. A., Kim, I., Liu, C. W. & Puglisi, J. D. Uncoupling of RNA Binding and PKR Kinase Activation by Viral Inhibitor RNAs. *J. Mol. Biol.* **358**, 1270–1285 (2006).
107. Costa-Mattioli, M. & Walter, P. The integrated stress response: From mechanism to

disease. *Science (80-.).* **368**, (2020).

108. Youssef, O. A. *et al.* Potential role for snoRNAs in PKR activation during metabolic stress. *Proc Natl Acad Sci U S A* **112**, 5023–5028 (2015).
109. Pham, A. M. *et al.* PKR Transduces MDA5-Dependent Signals for Type I IFN Induction. *PLOS Pathog.* **12**, e1005489 (2016).
110. Chakrabarti, A., Jha, B. K. & Silverman, R. H. New insights into the role of RNase L in innate immunity. *J Interf. Cytokine Res* **31**, 49–57 (2011).
111. Sadler, A. J. & Williams, B. R. G. Interferon-inducible antiviral effectors. *Nature Reviews Immunology* **8**, 559–568 (2008).
112. Malathi, K., Dong, B., Gale, M. & Silverman, R. H. Small self-RNA generated by RNase L amplifies antiviral innate immunity. *Nature* **448**, 816–819 (2007).
113. Liu, C. X. *et al.* Structure and Degradation of Circular RNAs Regulate PKR Activation in Innate Immunity. *Cell* **177**, 865-880.e21 (2019).
114. Li, Y. *et al.* Ribonuclease L mediates the cell-lethal phenotype of double-stranded RNA editing enzyme ADAR1 deficiency in a human cell line. *Elife* (2017). doi:10.7554/eLife.25687
115. Gannon, H. S. *et al.* Identification of ADAR1 adenosine deaminase dependency in a subset of cancer cells. *Nat. Commun.* **9**, (2018).
116. George, C. X. & Samuel, C. E. Human RNA-specific adenosine deaminase ADAR1 transcripts possess alternative exon 1 structures that initiate from different promoters, one constitutively active and the other interferon inducible. *Proc. Natl. Acad. Sci. U. S. A.* **96**, 4621–4626 (1999).
117. George, C. X., Wagner, M. V & Samuel, C. E. Expression of Interferon-inducible RNA Adenosine Deaminase ADAR1 during Pathogen Infection and Mouse Embryo Development Involves Tissue-selective Promoter Utilization and Alternative Splicing. *J. Biol. Chem.* **280**, 15020–15028 (2005).
118. Schade, M. *et al.* The solution structure of the Zalpha domain of the human RNA editing enzyme ADAR1 reveals a prepositioned binding surface for Z-DNA. *Proc. Natl. Acad. Sci. U. S. A.* **96**, 12465–70 (1999).
119. Pestal, K. *et al.* Isoforms of RNA-Editing Enzyme ADAR1 Independently Control Nucleic Acid Sensor MDA5-Driven Autoimmunity and Multi-organ Development. *Immunity* **43**, 933–944 (2015).
120. Liddicoat, B. J. *et al.* RNA editing by ADAR1 prevents MDA5 sensing of endogenous dsRNA as nonself. *Science (80-.).* **349**, 1–9 (2015).

121. Ravichandran, S., Subramani, V. K. & Kim, K. K. Z-DNA in the genome: from structure to disease. *Biophysical Reviews* **11**, 383 (2019).
122. Schwartz, T., Rould, M. A., Lowenhaupt, K., Herbert, A. & Rich, A. Crystal structure of the Zalpha domain of the human editing enzyme ADAR1 bound to left-handed Z-DNA. *Science (80-.).* **284**, 1841–1845 (1999).
123. Kwon, J. A. & Rich, A. Biological function of the vaccinia virus Z-DNA-binding protein E3L: Gene transactivation and antiapoptotic activity in HeLa cells. *Proc. Natl. Acad. Sci. U. S. A.* **102**, 12759–12764 (2005).
124. Placido, D., Brown, B. A., Lowenhaupt, K., Rich, A. & Athanasiadis, A. A Left-Handed RNA Double Helix Bound by the Zα Domain of the RNA-Editing Enzyme ADAR1. *Structure* **15**, 395–404 (2007).
125. Zhang, T. *et al.* Influenza Virus Z-RNAs Induce ZBP1-Mediated Necroptosis. *Cell* **180**, 1115-1129.e13 (2020).
126. Rich, A., Nordheim, A. & Azorin, F. Stabilization and detection of natural left-handed z-dna. *J. Biomol. Struct. Dyn.* **1**, 01–19 (1983).
127. Athanasiadis, A. Zalpha-domains: At the intersection between RNA editing and innate immunity. *Semin. Cell Dev. Biol.* **23**, 275–280 (2012).
128. Ng, S. K., Weissbach, R., Ronson, G. E. & Scadden, A. D. J. Proteins that contain a functional Z-DNA-binding domain localize to cytoplasmic stress granules. *Nucleic Acids Res.* **41**, 9786–9799 (2013).
129. Feng, Q., Langereis, M. A. & van Kuppeveld, F. J. M. Induction and suppression of innate antiviral responses by picornaviruses. *Cytokine Growth Factor Rev.* **25**, 577–585 (2014).
130. Anderson, P. & Kedersha, N. Stress granules: the Tao of RNA triage. *Trends in Biochemical Sciences* **33**, 141–150 (2008).
131. Anderson, P. & Kedersha, N. RNA granules: Post-transcriptional and epigenetic modulators of gene expression. *Nature Reviews Molecular Cell Biology* **10**, 430–436 (2009).
132. Langereis, M. A., Feng, Q. & van Kuppeveld, F. J. MDA5 Localizes to Stress Granules, but This Localization Is Not Required for the Induction of Type I Interferon. *J. Virol.* **87**, 6314–6325 (2013).
133. Song, C., Sakurai, M., Shiromoto, Y. & Nishikura, K. Functions of the RNA Editing Enzyme ADAR1 and Their Relevance to Human Diseases. *Genes (Basel).* **7**, (2016).
134. Ishizuka, J. J. *et al.* Loss of ADAR1 in tumours overcomes resistance to immune checkpoint blockade. *Nature* **565**, 43–48 (2019).

135. Nemlich, Y. *et al.* ADAR1-mediated regulation of melanoma invasion. *Nat. Commun.* **9**, 2154 (2018).
136. Hayashi, M. & Suzuki, T. Dyschromatosis symmetrica hereditaria. *J Dermatol* **40**, 336–343 (2013).
137. Ward, S. V *et al.* RNA editing enzyme adenosine deaminase is a restriction factor for controlling measles virus replication that also is required for embryogenesis. *Proc Natl Acad Sci U S A* **108**, 331–336 (2011).
138. Ahmad, S. *et al.* Breaching Self-Tolerance to Alu Duplex RNA Underlies MDA5-Mediated Inflammation. *Cell* **172**, 797-810 e13 (2018).
139. Crow, Y. J. Type I interferonopathies: Mendelian type I interferon up-regulation. *Curr. Opin. Immunol.* **32**, 7–12 (2015).
140. Descours, B. *et al.* SAMHD1 restricts HIV-1 reverse transcription in quiescent CD4(+) T-cells. *Retrovirology* **9**, 87 (2012).
141. Uggenti, C., Lepelley, A. & Crow, Y. J. Self-Awareness: Nucleic Acid-Driven Inflammation and the Type I Interferonopathies. *Annu Rev Immunol* **37**, 247–267 (2019).
142. Deddouche, S. *et al.* Identification of an LGP2-associated MDA5 agonist in picornavirus-infected cells. *Elife* **3**, (2014).
143. Bruns, A. M., Leser, G. P., Lamb, R. A. & Horvath, C. M. The innate immune sensor LGP2 activates antiviral signaling by regulating MDA5-RNA interaction and filament assembly. *Mol Cell* **55**, 771–781 (2014).
144. Duic, I. *et al.* Viral RNA recognition by LGP2 and MDA5, and activation of signaling through step-by-step conformational changes. *Nucleic Acids Res* (2020). doi:10.1093/nar/gkaa935
145. Satoh, T. *et al.* LGP2 is a positive regulator of RIG-I- and MDA5-mediated antiviral responses. *Proc Natl Acad Sci U S A* **107**, 1512–1517 (2010).
146. George, C. X., Ramaswami, G., Li, J. B. & Samuel, C. E. Editing of Cellular Self-RNAs by Adenosine Deaminase ADAR1 Suppresses Innate Immune Stress Responses. *J Biol Chem* **291**, 6158–6168 (2016).
147. Li, Z., Wolff, K. C. & Samuel, C. E. RNA adenosine deaminase ADAR1 deficiency leads to increased activation of protein kinase PKR and reduced vesicular stomatitis virus growth following interferon treatment. *Virology* **396**, 316–322 (2010).
148. Pham, A. M. *et al.* PKR Transduces MDA5-Dependent Signals for Type I IFN Induction. *PLoS Pathog* **12**, e1005489 (2016).
149. Schulz, O. *et al.* Protein kinase R contributes to immunity against specific viruses by

regulating interferon mRNA integrity. *Cell Host Microbe* **7**, 354–361 (2010).

150. Kristiansen, H., Gad, H. H., Eskildsen-Larsen, S., Despres, P. & Hartmann, R. The oligoadenylate synthetase family: an ancient protein family with multiple antiviral activities. *J Interf. Cytokine Res* **31**, 41–47 (2011).
151. Zhou, A., Hassel, B. A. & Silverman, R. H. Expression cloning of 2-5A-dependent RNAase: a uniquely regulated mediator of interferon action. *Cell* **72**, 753–765 (1993).
152. Civril, F. *et al.* Structural mechanism of cytosolic DNA sensing by cGAS. *Nature* **498**, 332–337 (2013).
153. Hornung, V., Hartmann, R., Ablasser, A. & Hopfner, K. P. OAS proteins and cGAS: unifying concepts in sensing and responding to cytosolic nucleic acids. *Nat Rev Immunol* **14**, 521–528 (2014).
154. Daou, S. *et al.* A phenolic small molecule inhibitor of RNase L prevents cell death from ADAR1 deficiency. *Proc Natl Acad Sci U S A* **117**, 24802–24812 (2020).
155. Harding, H. P. *et al.* An integrated stress response regulates amino acid metabolism and resistance to oxidative stress. *Mol Cell* **11**, 619–633 (2003).
156. Hinnebusch, A. G. & Lorsch, J. R. The mechanism of eukaryotic translation initiation: new insights and challenges. *Cold Spring Harb Perspect Biol* **4**, (2012).
157. Krishnamoorthy, T., Pavitt, G. D., Zhang, F., Dever, T. E. & Hinnebusch, A. G. Tight binding of the phosphorylated alpha subunit of initiation factor 2 (eIF2alpha) to the regulatory subunits of guanine nucleotide exchange factor eIF2B is required for inhibition of translation initiation. *Mol Cell Biol* **21**, 5018–5030 (2001).
158. Sachs, A. B., Sarnow, P. & Hentze, M. W. Starting at the beginning, middle, and end: translation initiation in eukaryotes. *Cell* **89**, 831–838 (1997).
159. Harding, H. P. *et al.* Regulated translation initiation controls stress-induced gene expression in mammalian cells. *Mol Cell* **6**, 1099–1108 (2000).
160. Wong, Y. L. *et al.* eIF2B activator prevents neurological defects caused by a chronic integrated stress response. *Elife* **8**, (2019).
161. Leegwater, P. A. *et al.* Subunits of the translation initiation factor eIF2B are mutant in leukoencephalopathy with vanishing white matter. *Nat Genet* **29**, 383–388 (2001).
162. Knapp, S., Branger, J. & van der Poll, T. Advances in research of the inflammatory response: the importance of toll-like receptors. *Wien Med Wochenschr* **152**, 552–554 (2002).
163. Sekine, Y. *et al.* Stress responses. Mutations in a translation initiation factor identify the target of a memory-enhancing compound. *Science (80-.).* **348**, 1027–1030 (2015).

164. Bruns, A. M. *et al.* ATP hydrolysis enhances RNA recognition and antiviral signal transduction by the innate immune sensor, laboratory of genetics and physiology 2 (LGP2). *J. Biol. Chem.* **288**, 938–946 (2013).
165. Mannion, N. M. *et al.* The RNA-Editing Enzyme ADAR1 Controls Innate Immune Responses to RNA. *Cell Rep.* **9**, 1482–1494 (2014).
166. Elde, N. C., Child, S. J., Geballe, A. P. & Malik, H. S. Protein kinase R reveals an evolutionary model for defeating viral mimicry. *Nature* **457**, 485–489 (2009).
167. Nejentsev, S., Walker, N., Riches, D., Egholm, M. & Todd, J. a. Rare variants of IFIH1, a gene implicated in antiviral responses, protect against type 1 diabetes. *Science (80-.).* **324**, 387–389 (2009).
168. Robinson, T. *et al.* Autoimmune disease risk variant of IFIH1 is associated with increased sensitivity to IFN-alpha and serologic autoimmunity in lupus patients. *J Immunol* **187**, 1298–1303 (2011).
169. Uyoga, S. *et al.* Glucose-6-phosphate dehydrogenase deficiency and the risk of malaria and other diseases in children in Kenya: A case-control and a cohort study. *Lancet Haematol.* **2**, e437–e444 (2015).
170. Fumagalli, M. *et al.* Correction: Signatures of Environmental Genetic Adaptation Pinpoint Pathogens as the Main Selective Pressure through Human Evolution. *PLoS Genet.* **7**, (2011).
171. Feng, Q. *et al.* MDA5 Detects the Double-Stranded RNA Replicative Form in Picornavirus-Infected Cells. *Cell Rep.* **2**, 1187–1196 (2012).
172. Gorman, J. A. *et al.* The A946T variant of the RNA sensor IFIH1 mediates an interferon program that limits viral infection but increases the risk for autoimmunity. *Nat Immunol* **18**, 744–752 (2017).
173. Toth, A. M., Li, Z., Cattaneo, R. & Samuel, C. E. RNA-specific Adenosine Deaminase ADAR1 Suppresses Measles Virus-induced Apoptosis and Activation of Protein Kinase PKR. *J. Biol. Chem.* **284**, 29350–29356 (2009).
174. Brody, T. *et al.* Flavivirus and Filovirus EvoPrinters: New alignment tools for the comparative analysis of viral evolution. *PLoS Negl. Trop. Dis.* **11**, e0005673 (2017).
175. Whitmer, S. L. M. *et al.* Active Ebola Virus Replication and Heterogeneous Evolutionary Rates in EVD Survivors. *CellReports* **22**, 1159–1168 (2018).
176. Hobert, O. *et al.* The C. elegans neural editome reveals an ADAR target mRNA required for proper chemotaxis. (2017).
177. De Reuver, R. *et al.* ADAR1 interaction with Z-RNA promotes editing of endogenous

double-stranded RNA and prevents MDA5-dependent immune activation. *bioRxiv* 2020.12.04.411702 (2020). doi:10.1101/2020.12.04.411702

178. Tang, Q. *et al.* Recognition of Z-RNA by ADAR1 limits interferon responses. doi:10.1101/2020.12.04.411793
179. Bruns, A. M., Leser, G. P., Lamb, R. A. & Horvath, C. M. The Innate Immune Sensor LGP2 Activates Antiviral Signaling by Regulating MDA5-RNA Interaction and Filament Assembly. *Mol. Cell* **55**, 771–781 (2014).
180. JAK Inhibition in the Aicardi–Goutières Syndrome. *N. Engl. J. Med.* **383**, 2190–2193 (2020).
181. Hartner, J. C., Walkley, C. R., Lu, J. & Orkin, S. H. ADAR1 is essential for the maintenance of hematopoiesis and suppression of interferon signaling. *Nat. Immunol.* **10**, 109–115 (2009).
182. Qiu, W. *et al.* ADAR1 is essential for intestinal homeostasis and stem cell maintenance. *Cell Death Dis.* **4**, e599 (2013).
183. Marcu-Malina, V. *et al.* ADAR1 is vital for B cell lineage development in the mouse bone marrow. *Oncotarget* **7**, 54370–54379 (2016).
184. Childs, K. S., Randall, R. E. & Goodbourn, S. LGP2 Plays a Critical Role in Sensitizing mda-5 to Activation by Double-Stranded RNA. *PLoS One* **8**, (2013).
185. Jiao, H. *et al.* Z-nucleic-acid sensing triggers ZBP1-dependent necroptosis and inflammation. *Nature* **580**, (2020).
186. Manivannan, P., Siddiqui, M. A. & Malathi, K. RNase L Amplifies Interferon Signaling by Inducing Protein Kinase R-Mediated Antiviral Stress Granules. (2020). doi:10.1128/JVI.00205-20
187. Markmiller, S. *et al.* Context-Dependent and Disease-Specific Diversity in Protein Interactions within Stress Granules. *Cell* **172**, 590-604.e13 (2018).
188. Ebstein, F., Poli Harlowe, M. C., Studencka-Turski, M. & Krüger, E. Contribution of the Unfolded Protein Response (UPR) to the Pathogenesis of Proteasome-Associated Autoinflammatory Syndromes (PRAAS). *Frontiers in Immunology* **10**, 2756 (2019).
189. Duncan, C. J. A. *et al.* Severe type I interferonopathy and unrestrained interferon signaling due to a homozygous germline mutation in STAT2. *Sci. Immunol.* **4**, 7501 (2019).
190. Way, S. W. & Popko, B. Harnessing the integrated stress response for the treatment of multiple sclerosis. *Lancet Neurol* **15**, 434–443 (2016).
191. Domsgen, E. *et al.* An IFIH1 gene polymorphism associated with risk for autoimmunity

regulates canonical antiviral defence pathways in Coxsackievirus infected human pancreatic islets. *Sci. Rep.* **6**, 39378 (2016).

192. Chen, Y. G., Mathews, C. E. & Driver, J. P. The role of NOD mice in type 1 diabetes research: Lessons from the past and recommendations for the future. *Front. Endocrinol. (Lausanne).* **9**, 51 (2018).
193. Lincez, P. J., Shanina, I. & Horwitz, M. S. Reduced expression of the MDA5 Gene IFIH1 prevents autoimmune diabetes. *Diabetes* **64**, 2184–2193 (2015).
194. Palaiodimos, L. *et al.* Severe obesity is associated with higher in-hospital mortality in a cohort of patients with COVID-19 in the Bronx, New York. *Metabolism.* **108**, 154262 (2020).
195. Mani, V. R., Kalabin, A., Valdivieso, S. C., Murray-Ramcharan, M. & Donaldson, B. New York inner city hospital COVID-19 experience and current data: Retrospective analysis at the epicenter of the American coronavirus outbreak. *J. Med. Internet Res.* **22**, (2020).
196. Mash, R. J. *et al.* Evaluation of patient characteristics, management and outcomes for COVID-19 at district hospitals in the Western Cape, South Africa: descriptive observational study. *BMJ Open* **11**, e047016 (2021).
197. Nakamura, T. *et al.* Double-Stranded RNA-Dependent Protein Kinase Links Pathogen Sensing with Stress and Metabolic Homeostasis. *Cell* **140**, 338–348 (2010).
198. Nakamura, T. *et al.* A critical role for PKR complexes with TRBP in immunometabolic regulation and eIF2α phosphorylation in obesity. *Cell Rep.* **11**, 295–307 (2015).
199. Carvalho-Filho, M. A. *et al.* Double-Stranded RNA-Activated Protein Kinase Is a Key Modulator of Insulin Sensitivity in Physiological Conditions and in Obesity in Mice. *Endocrinology* **153**, 5261–5274 (2012).
200. Williams, A., Henao-Mejia, J. & Flavell, R. A. Editing the Mouse Genome Using the CRISPR-Cas9 System. *Cold Spring Harb Protoc* **2016**, pdb top087536 (2016).
201. Gitlin, L. *et al.* Essential role of mda-5 in type I IFN responses to polyriboinosinic:polyribocytidylic acid and encephalomyocarditis picornavirus. *Proc. Natl. Acad. Sci.* **103**, 8459–8464 (2006).
202. Suthar, M. S. *et al.* The RIG-I-like receptor LGP2 controls CD8(+) T cell survival and fitness. *Immunity* **37**, 235–248 (2012).
203. Muller, U. *et al.* Functional role of type I and type II interferons in antiviral defense. *Science (80-.).* **264**, 1918–1921 (1994).
204. Kolumam, G. A., Thomas, S., Thompson, L. J., Sprent, J. & Murali-Krishna, K. Type I interferons act directly on CD8 T cells to allow clonal expansion and memory formation in

response to viral infection. *J Exp Med* **202**, 637–650 (2005).

205. Abraham, N. *et al.* Characterization of transgenic mice with targeted disruption of the catalytic domain of the double-stranded RNA-dependent protein kinase, PKR. *J Biol Chem* **274**, 5953–5962 (1999).
206. Prodeus, A. P., Zhou, X., Maurer, M., Galli, S. J. & Carroll, M. C. Impaired mast cell-dependent natural immunity in complement C3-deficient mice. *Nature* **390**, 172–175 (1997).
207. Koretkevich, G., Sukhov, V. & Sergushichev, A. Fast gene set enrichment analysis. *bioRxiv* **10.1101/06**, (2019).
208. Deffit, S. N. *et al.* The C. elegans neural editome reveals an ADAR target mRNA required for proper chemotaxis. *Elife* **6**, (2017).